VOLUME XLII

GEMS & GEMOLOGY

FALL 2006

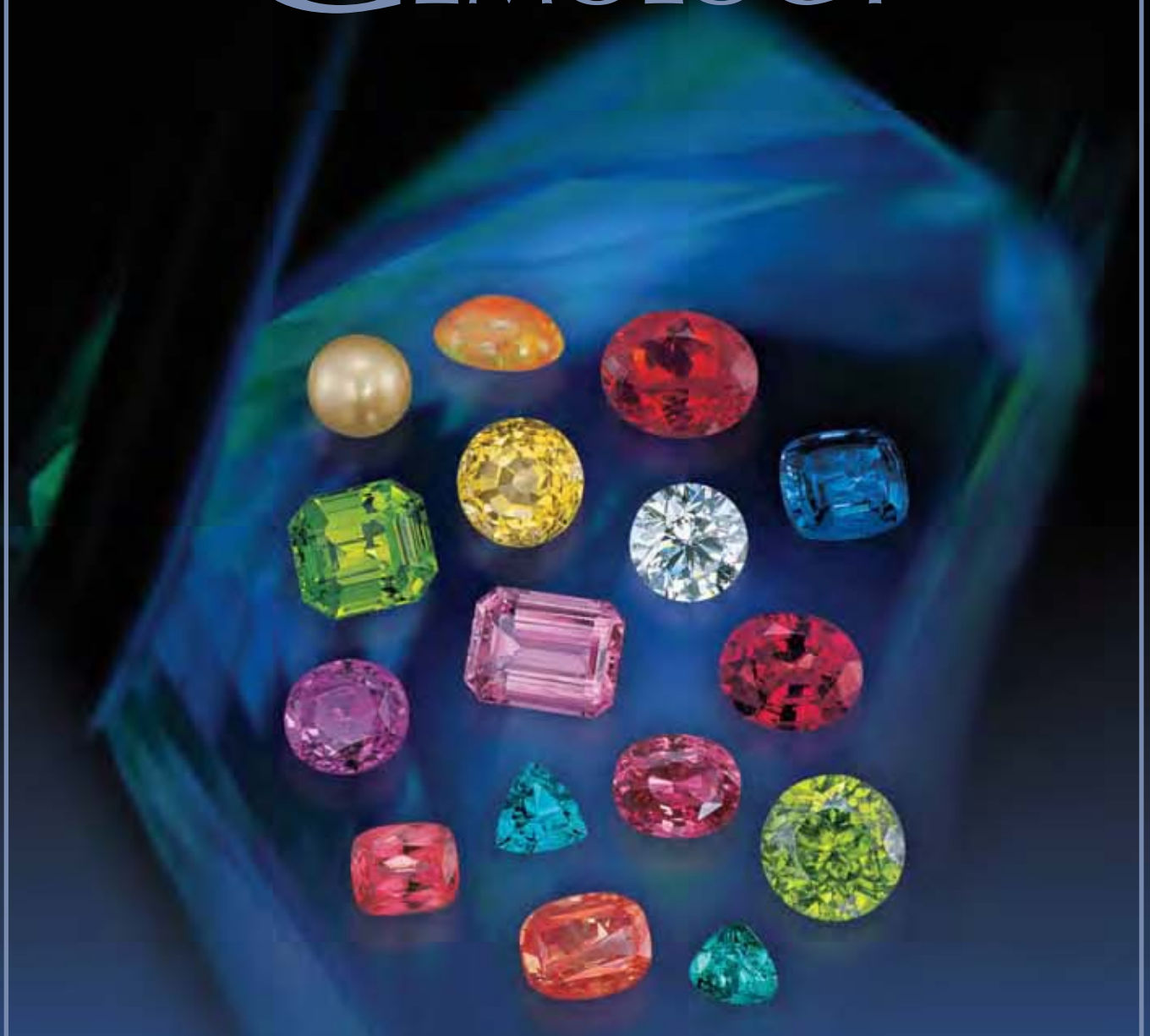

Proceedings of the
4th International Gemological Symposium &
GIA Gemological Research Conference

August 2006 • San Diego, California

THE QUARTERLY JOURNAL OF THE GEMOLOGICAL INSTITUTE OF AMERICA

2006 GIA GEMOLOGICAL RESEARCH CONFERENCE

The identification and characterization of natural, synthetic, and treated gem materials remain essential to ensure continued confidence among consumers. Today, gemological research to address these issues is expanding in many exciting directions that encompass a range of scientific fields. To bring together researchers from these diverse disciplines, as well as a wide variety of participants from academia and the gem and jewelry industry, GIA hosted the **Gemological Research Conference** (GRC) in San Diego on August 26–27, 2006. This conference provided an open forum for scientists and other specialists from around the world to discuss cutting-edge developments in gemology. The program consisted of 60 oral presentations (including 12 invited speakers) and 61 posters, covering the six conference themes. Each abstract was reviewed by selected GRC committee members and edited for clarity. All 121 of these abstracts, plus 28 abstracts from the Symposium Poster Session, are reproduced on the following pages.

More than 700 people registered for the GRC, and two sold-out field trips to the Pala gem-pegmatite district were held before and after the conference. GIA thanks Charles & Colvard Ltd. for their generous financial support of this inaugural event. In addition, several donors supplied funds for GRC travel grants (see inside front cover of this issue). The Pala mine owners, as well as Pala International/The Collector in Fallbrook, are thanked for making their properties available and providing excellent service during the field trips.

Our goal is to hold the Gemological Research Conference on a regular basis. The next GRC is scheduled for the San Diego area in August 2009. We look forward to seeing—and working with—all of you there.

James E. Shigley and Brendan M. Laurs
Co-Chairs, 2006 Gemological Research Conference

Gemological Research Conference 2006 August 26–27

Organizing Committee

The following research scientists and gem dealers are thanked for their help in reviewing abstracts, chairing sessions, and providing advice in shaping the content and form of the 2006 GIA Gemological Research Conference.

Diamond and Corundum Treatments

Alan T. Collins	King's College, London
Filip De Weerdt	HRD Research, Lier, Belgium
Kenneth Scarratt	GIA Thailand, Bangkok

Gem Characterization Techniques

Emmanuel Fritsch	Institut des Matériaux, Nantes, France
Frank Hawthorne	University of Manitoba, Winnipeg, Canada
Franck Notari	GIA GemTechLab, Geneva, Switzerland
George R. Rossman	California Institute of Technology, Pasadena, California
Karl Schmetzer	Petershausen, Germany

General Gemology

Shigeru Akamatsu	K. Mikimoto & Company, Tokyo
Jaroslav Hyršl	Kolin, Czech Republic
Lore Kiefert	AGTA Gemological Testing Center, New York
John M. King	GIA Laboratory, New York
Shane F. McClure	GIA Laboratory, Carlsbad
Russell Shor	GIA, Carlsbad
Christopher P. Smith	GIA Laboratory, New York
Ichiro Sunagawa	Tokyo, Japan
Wuyi Wang	GIA Laboratory, New York

Geology of Gem Deposits

Lee A. Groat	University of British Columbia, Vancouver, Canada
George E. Harlow	American Museum of Natural History, New York
A. J. A. (Bram) Janse	Archon Exploration, Carine, Australia
David London	University of Oklahoma, Norman, Oklahoma
William (Skip) Simmons	University of New Orleans, Louisiana
J. C. (Hanco) Zwaan	National Museum of Natural History, Leiden, The Netherlands

Laboratory Growth of Gem Materials

Vladimir Balitsky	Institute of Experimental Mineralogy, Chernogolovka, Russia
James E. Butler	Naval Research Laboratory, Washington, DC

New Gem Localities

Edward Boehm	JOEB Enterprises, Solana Beach, California
Anthony R. Kampf	Natural History Museum of Los Angeles County, California
Robert E. Kane	Fine Gems International, Helena, Montana

GEMOLOGICAL RESEARCH CONFERENCE

San Diego, August 26–27

People • Places • Events

Top left and top right: GRC co-chairs James Shigley and Brendan Laurs. Middle: Oral presenter Richard Drucker analyzes pricing trends.

Above: Christoph Krahenmann, Mona Lee Nesseth, and Betty Sue King. Near right: Walter Leite and Cristina Baltar with Sergio Costa. Far right: Pornsawat Wathanakul reports on beryllium-treated blue sapphires.

Near right: Poster presenter A.J.A. (Bram) Janse and Poster Session chair Dona Dirlam. Far right: Makhmout Douman's poster presentation.

Top, left to right: Speakers Ahmadjan Abduriyim, Jim Clanin, and Nikolai Sobolev. Above: Saturday lunch. Middle: Lore Kiefert poses a question. Near right: top, attendees visit some of the 93 posters; below, Michael Wise presents his poster on hiddenite deposits.

GRC presenters Elisabeth Strack (far left) and Menahem Sevdermish (second from right) enjoy a break with their colleagues.

Above: Dino DeGhionno and Emmanuel Fritsch. Directly above: the Saturday evening cocktail reception.

Two field trips to the Pala pegmatite district rounded out the GRC. Top left: Elizabeth R mine owner Roland Reed shows specimens to field trip participants. Top right: Israel Eliezri inspects a screening apparatus. Middle, left: Roland and Nata Schluessel stand next to a kunzite-bearing pocket. Below: Pala Chief mine owner Bob Dawson with field trip participants.

Above: Kunzite specimens from the Elizabeth R mine. Right: Stewart mine owner Blue Sheppard guides a group of participants.

ORAL PRESENTATION ABSTRACTS

Gemological Research Conference 2006

August 26–27

Diamond and Corundum Treatments

Identification of Heat-Treated Corundum

Hiroshi Kitawaki (h-kitawaki@gaaj-zenhokyo.co.jp), Ahmadjan Abduriyim, and Makoto Okano

Gemmological Association of All Japan (GAAJ), Tokyo

In accordance with September 2004 revisions to regulations concerning disclosure on gem identification reports, 27 laboratories belonging to the Association of Gemmological Laboratories Japan (AGL) began issuing descriptions of heat treatment in corundum. However, some reports from different gem laboratories were not consistent with the treated status of certain stones (especially between Japanese and overseas laboratories). Here we introduce the methods used in our laboratory for identifying heated and unheated corundum. In addition, we studied the identification characteristics of various kinds of heated synthetic corundum.

Detailed observation of internal features is very important to identify heat-treated corundum. Most crystal inclusions have a lower melting point than the host corundum, and may melt or become discolored by heat treatment. Liquid inclusions are often "healed" by heating, and some substances such as flux can be observed in fractures as residues. Additionally, absorption spectra in the UV-Vis and IR regions may show changes after heating.

Non-basalt-related blue sapphires heated in a reducing atmosphere show absorptions related to O-H bending that are not seen in unheated samples. Similarly, heated Mong-Hsu rubies show absorptions related to O-H bending because of the dehydration of diaspore inclusions. Laser tomography is extremely useful in the identification of heated and unheated corundum, and can clearly detect scattering images of crystal defects such as dislocations, as well as variations in fluorescence.

Synthetic ruby can also be heated, and the resulting alteration of internal features can make these stones more difficult to identify. In the early 1990s, large numbers of heat-treated Verneuil synthetic rubies flooded the gem market in parcels of Vietnamese rubies. Several years later, heat-treated Kashan synthetic rubies appeared on the market. These stones were larger and caused identification challenges in gemological laboratories. Recently, Ramaura synthetic rubies have been heated, and this created new problems in identification. When fused orange flux is observed under magnification, it can provide an indication of a heated Ramaura synthetic ruby. However, minute inclusions, color distribution, and growth zoning should be carefully observed, as they appear quite similar to those of natural ruby.

Treated Diamond: A Physicist's Perspective

Mark E. Newton (m.e.newton@warwick.ac.uk)

Department of Physics, University of Warwick, Coventry, United Kingdom

The technologies for the synthesis of diamond via high pressure, high temperature (HPHT) and chemical vapor deposition (CVD) techniques are becoming more refined. The progress is created by scientists and technologists wishing to exploit the remarkable properties of diamond in a wide variety of applications, as well as producing gem-quality synthetic diamonds. Synthetic diamond can be treated, post synthesis, to modify the as-grown properties and to improve performance in some high-tech devices. Also, treatments can change the color of natural and synthetic gem diamond.

In parallel with the developments in diamond synthesis and treatments, the understanding of the defects (both intrinsic and impurity related) that influence the color of natural and synthetic diamond continues to improve. The physics of diamond defect interactions has been extensively studied over the last 30 years, and observing the defects that are created or destroyed through HPHT annealing, irradiation, and combinations of both has contributed to our present understanding of diamond. From this body of knowledge, we have developed the discrimination techniques that can be used in gem laboratories to identify treated diamonds.

In nature, annealing typically occurs at modest temperatures compared to those used in laboratory HPHT annealing

Editor's note: Underlined author signifies presenter.

treatments. At elevated temperatures, the nitrogen impurity atoms common to most diamonds become mobile and aggregate into defects containing two or more nitrogen atoms. The relatively low temperature allied with geologic time scales ensures that in nature the forward aggregation reaction dominates. However, HPHT treatments (for example to remove brown color) are by necessity carried out over very much shorter time scales (minutes to a few hours), and significantly higher temperatures are required to achieve the desired reaction. The higher temperature also substantially raises the probability of the reverse aggregation reaction (i.e., breaking up nitrogen aggregates). The single substitutional nitrogen defect center (often referred to as the C center) produced in this process is a relatively willing electron donor, and its presence often controls the charge state of other defects. The observation of negatively charged versions of defects (e.g., the negatively charged nitrogen-vacancy defect observed at 637 nm and the negatively charged nitrogen-vacancy-nitrogen defect known as the H2 center) is often key for the identification of treated diamonds. However, it is typically the defect combinations not observed in nature that enable conclusive identification of a treated diamond rather than the spectroscopic identification of a single type of defect.

Role of Beryllium in the Coloration of Fe- and Cr-doped Synthetic Corundum

Visut Pisutha-Arnond (pvisut@gmail.com)[1,2], Tobias Häger[3], Pornsawat Wathanakul[1,4], Wilawan Atichat[1], Jitrin Nattachai[1], Tin Win[5], Chakkaphant Sutthirat[1,2], and Boontawee Sriprasert[1,6]

[1]Gem and Jewelry Institute of Thailand, Bangkok; [2]Department of Geology, Chulalongkorn University, Bangkok; [3]Institute of Gemstone Research, University of Mainz, Germany; [4]Department of Earth Science, Kasetsart University, Bangkok; [5]GEMOC Key Center, Macquarie University, Sydney, Australia; [6]Department of Mineral Resources, Bangkok

X-ray irradiation and Be-diffusion heating experiments were performed on an iron-doped (colorless) synthetic corundum and a chromium-doped (pink) synthetic corundum to evaluate the role of beryllium in causing color in the Be-Fe-Al_2O_3 and Be-Cr-Al_2O_3 systems.

The iron-doped corundum, containing around 140–170 ppm by weight of Fe with negligible concentrations of other trace elements, was irradiated with X-rays (60 kV, 53 mA) for 30 minutes, then the color was faded for one hour with a 100-watt light bulb, and finally the sample was heat treated in a crucible with ground chrysoberyl in an electric furnace at 1780°C in an oxidizing atmosphere for 50 hours. The chromium-doped corundum, containing around 160–210 ppm by weight of Cr with negligible concentrations of other trace elements, was also irradiated with X-rays (80 kV, 4 mA) for 4 hours, then faded for 4 hours with a 100-watt light bulb, and subsequently heat treated with ground chrysoberyl at unspecified conditions by a Thai treater. At each stage of the experiments, the samples were photographed and UV-Vis absorption spectra were recorded.

Both the irradiation and Be-diffusion experiments on the iron-doped synthetic corundum created defect centers that had similar UV-Vis absorption curves and produced yellow coloration. The yellow color was unstable when induced by irradiation, but was stable after Be diffusion.

Experiments on the chromium-doped synthetic corundum produced orange coloration (and similar UV-Vis absorption patterns) by both irradiation and Be-diffusion heating methods. Again, the orange color was unstable when induced by irradiation (and quickly faded to pink), but remained stable after Be diffusion. These results confirm that divalent Be acts as a stabilizer of defect centers or color centers in iron-doped and chromium-doped synthetic corundum. Hence, the spectrum produced by the irradiation of Fe-doped or Cr-doped synthetic corundum was attributed to "metal-related unstable color centers," while that produced in synthetic corundum doped with Be+Fe or Be+Cr was caused by "Be^{2+} + metal-related stable color centers."

The Treatment of Ruby and Sapphire, with Implications for Gem Identification and the Integrity of the Product

Kenneth Scarratt (ken.scarratt@gia.edu)
GIA Research (Thailand), Bangkok

Corundum treatments include impregnating fractures with oils, heating to a variety of temperatures to clarify and change color, sealing fractures through "flux-assisted healing," overgrowing with synthetic corundum, diffusing foreign elements to change color (e.g., Ti for blue and Be for yellow to orange), and the filling of fractures and cavities with glass. While some of these treatments have been carried out in a rudimentary manner for a long time (see figure), in line with advancements in technology they have become highly developed over the last four decades. The latest evolution has resulted in the availability of beryllium-diffused blue sapphires.

With advanced treatment technology, it is now possible to transform large volumes of previously unsalable opaque or

The "blowpipe technique" as originally used in Sri Lanka will slightly alter the color of some corundum. Photo by Kenneth Scarratt.

fractured corundum into transparent stones with distinct and salable colors. These advances have created concern about the integrity of the product, particularly over the last decade because of an increased emphasis on proper treatment disclosure. A combination of technical ability and demand on the mass marketing level has encouraged the production of ruby and sapphire hybrids, where the distinction between natural, treated, and synthetic is becoming increasingly blurred.

Proper treatment disclosures depend on the development and application of effective identification techniques in gemological laboratories. While simple and inexpensive techniques are still effective for detecting many corundum treatments, others such as low-temperature heating and some situations involving beryllium diffusion require a more sophisticated approach. The level of testing sophistication required exceeds the reach of most gemological laboratories, and this is resulting in a situation where only the extremely well-equipped and well-funded laboratories can offer definitive services to support proper treatment disclosure.

It appears likely that the majority of existing gemological laboratories will eventually become limited in their scope and will need to "refer" stones to specialists within the few well-equipped establishments worldwide. If the industry is to receive the proper support, this change will require more cooperation and less competition between gemological laboratories.

Indications of Heating in Corundum from Experimental Results

Chakkaphan Sutthirat (c.sutthirat@gmail.com)[1,2], Krittaya Pattamalai[3], Somruedee Sakkaravej[1], Sureeporn Pumpeng[1], Visut Pisutha-Arnond[1,2], Pornsawat Wathanakul[1,4], Wilawan Atichat[1], and Boontawee Sriprasert[1,3]

[1]Gem and Jewelry Institute of Thailand, Bangkok; [2]Department of Geology, Chulalongkorn University, Bangkok; [3]Department of Mineral Resources, Bangkok; [4]Department of Earth Science, Kasetsart University, Bangkok

Heating experiments were conducted to improve the color in gem corundum from several deposits. The corundum samples came from both metamorphic-type (e.g., Ilakaka-Sakaraha in Madagascar and Songea in Tanzania) and basaltic-type (e.g., Bo Phloi in Thailand) origins. Experimental heat treatments were performed using electric furnaces, with maximum temperatures ranging from 800°C to 1650°C for durations of 1–3 hours at each peak temperature. Heating in an oxidizing environment was done to remove the blue shade of the purple varieties; however, under this condition a yellow coloration can be developed in some corundum. Heating in a reducing environment was done to intensify the color of the blue sapphires. Physical and chemical properties were investigated before the heating experiments; in addition, color change, absorption spectra, chemical analyses, and alteration of inclusions were carefully observed after each heating step. The experiments clearly revealed that optimal temperatures to reduce blue coloration ranged between 800°C and 1000°C, whereas higher temperatures (at least 1400°C) were more suitable for intensifying the blue component of the corundum.

Among the FTIR absorption peaks found in corundum, the O-H stretching peak at about 3309 cm^{-1} is most crucial for identifying high-temperature treatments, as suggested by many researchers. However, the step-heating experiments yielded ambiguous results on the effect of high-temperature heating (in both oxidizing and reducing environments) on the 3309 cm^{-1} peak. Some samples of both basaltic and metamorphic types contained this O-H stretching peak before heating, and it decreased rapidly or disappeared after the step-heating experiments. However, this OH peak was absent from some unheated stones, and then developed during some stages of heating, but was subsequently destroyed at higher temperatures. A few of the sapphires appeared to have no OH peak before or after heating. Based on this study, FTIR spectra are unlikely to provide conclusive evidence for the high-temperature treatment of corundum.

Physical changes in some inclusions were observed during the step heating. Small healing fractures and tension discs appeared to develop even at the lowest temperature and shortest heating duration (800°C for one hour), and gradually expanded at higher temperatures. Turbidity in tiny zircons was observed at 800°C, whereas large zircon inclusions usually became turbid at temperatures of at least 1400°C. Rutile needles started to dissolve into the host corundum at temperatures as low as 1600°C. Mica inclusions appeared to show some changes at 1000°C. Brown-to-black rutile was altered to reddish brown after heating at 800°C, especially in an oxidizing environment.

HPHT Treatment of Type IaB Brown Diamonds

Jef Van Royen (j.van.royen@wtocd.be), Filip De Weerdt, and Olivier De Gryse

Hoge Raad voor Diamant (HRD) Research, Lier, Belgium

The transformation of brown diamonds to colorless using high pressure, high temperature (HPHT) processing has become one of the most important diamond treatments. The common candidates for this treatment are type IIa brown stones. However, type IaB brown diamonds also can be turned (near) colorless by HPHT treatment. The properties of HPHT-treated type IIa diamonds have been studied extensively, but relatively little information is available about the changes in type IaB material as a consequence of this treatment. Therefore, we studied the characteristics of 10 type IaB brown diamonds before and after HPHT processing.

The rough diamonds were fashioned into rounded single-cut stones ranging from 0.20 to 0.53 ct. These diamonds were characterized with UV-Vis and IR absorption spectroscopy, and with Raman photoluminescence spectroscopy. Visual and instrumental color grading were performed, and clarity grades were determined. Moreover, every stone was examined with a DiamondView fluorescence imaging instrument and a D-Screen diamond screening device.

After characterization, the diamonds were subjected to HPHT treatment. Five samples were heated to 2200°C for 10 minutes, and five stones were subjected to 2300°C for 3 minutes, at stable conditions for diamond. Subsequently, the samples were polished to round brilliants with weights ranging from 0.16 to 0.41 ct, and the same characterization methods were applied.

The diamonds originally showed B-center concentrations between 5 and 50 ppm. After treatment, the brown color disappeared. They showed color grades ranging from G to O, with the more intense colors associated with the higher-temperature treatment. This is related to the production of isolated nitrogen impurities (C centers). When examined with the D-Screen, all samples showed an orange light indication, identifying them as diamonds that should be further tested for HPHT treatment.

In conclusion, type IaB diamonds can be made (near) colorless with HPHT treatment at relatively low temperatures. Gemological laboratories should systematically test near-colorless diamonds—not only type IIa, but also type IaB—for HPHT treatment.

Beryllium-Assisted Heat Treatment Experiments on Blue Sapphires

Pornsawat Wathanakul (pwathanakul@gmail.com)[1,2], Tobias Häger[3], Wilawan Atichat[2], Visut Pisutha-Arnond[2,4], Tin Win[5], Pantaree Lomthong[1], Boontawee Sriprasert[2,6], and Chakkaphant Sutthirat[2,4]

[1]Department of Earth Science, Kasetsart University, Bangkok; [2]Gem and Jewelry Institute of Thailand, Bangkok; [3]Institute of Gemstone Research, University of Mainz, Germany; [4]Department of Geology, Chulalongkorn University, Bangkok; [5]GEMOC Key Centre, Macquarie University, Sydney, Australia; [5]Department of Mineral Resources, Bangkok

Beryllium has been used extensively in corundum heat-treatment processes since at least 2000. Corundum samples of metamorphic origins from Madagascar and Sri Lanka with specific internal features (milky, silky, or silky-milky) were heat treated for this study, with and without Be, by blue-sapphire experts in Thailand. Prior to the heating experiments, the samples contained a moderate amount of fine inclusions; the milky ones were translucent and were near colorless to very light blue. The samples with silky inclusions were also translucent, and were colorless to a pastel light blue color; they were commonly zoned with internal silvery reflections. The silky-milky category contained a mixture of these two types.

Each sample was cut into 3–4 pieces, and an untreated portion from each group was retained. The samples were studied using electron microscopy, FTIR and UV-Vis-NIR absorption spectroscopy, and LA-ICP-MS; the latter three techniques were utilized after each step of the heating experiments. SEM-EDS investigations showed that the milky stones contained what were probably very fine particles of rutile and ilmenite, whereas the silky corundum contained rutile and possibly members of the ilmenite-geikielite series.

The corundum samples were heated (without Be) in a fuel furnace to about 1650°C for 70 hours in a reducing atmosphere. The milky type mostly turned transparent blue, whereas the silky and silky-milky sapphires became blue but had a turbid appearance. These turbid samples were then reheated with Be in an electric furnace at 1650°C for 70 hours in an oxidizing atmosphere. After this process, the sapphires became more transparent and lighter in color. These stones could be further enhanced (color intensified) by reheating at ~1500°C for a few hours in a reducing atmosphere.

To explain these phenomena, we postulate an increase of Ti^{4+} solubility by building clusters/nanoclusters of $BeTiO_3$. The solubility of titanium can be explained by charge compensation of the Ti^{4+} with the Be^{2+} replacing two Al^{3+} in the corundum structure. In addition to $MgTiO_3$ and $FeTiO_3$ clusters, $BeTiO_3$ would also readily be incorporated into the corundum. However, the beryllium in the corundum structure could possibly be situated in both octahedral and/or tetrahedral sites. Further experiments and analyses are still being carried out to confirm the incorporation of beryllium into blue sapphires.

Gem Characterization Techniques

Applications of LA-ICP-MS (Laser Ablation–Inductively Coupled Plasma–Mass Spectrometry) to the Gemological Field

Ahmadjan Abduriyim (ahmadjan@gaaj-zenhokyo.co.jp) and Hiroshi Kitawaki

Gemmological Association of All Japan (GAAJ), Tokyo

In recent years, gemological laboratories have been faced with diverse gem identification issues that are difficult to solve and have caused confusion for many gemologists. Chemical analysis by LA-ICP-MS has been successfully applied to certain gemological problems that in some cases were not solvable by the other techniques that are routinely available in gemological laboratories.

For example, high-temperature Be-diffusion treatment of corundum has become widespread, but this element cannot be detected by most analytical instruments and only trace amounts of it are necessary to alter corundum color. LA-ICP-MS can perform a local "micro-destructive" (several micrometers to a hundred micrometers) analysis to determine the element composition, and can detect the presence of Be at the parts-per-million level.

There is demand for geographic origin determination for high-value colored stones such as ruby, sapphire, emerald, and Cu-bearing tourmaline. Without high-quality, detailed analytical data, indications of origin may sometimes be unreliable, even when based on the experience of laboratory gemologists and data uniquely collected by that laboratory. To move away from subjective opinion, a more sophisticated scientific basis is needed for geographic origin determination, such as chemical fingerprinting using quantitative chemical data. For example, diagrams for the following elements are helpful for determining geographic origin: Cr_2O_3/Ga_2O_3 versus Fe_2O_3/TiO_2 for corundum, Cs_2O+K_2O versus Na_2O+MgO and Ga-Zn-Li for emerald, and Ga+Pb versus CuO+MnO and CuO+MnO versus Pb/Be for Cu-bearing tourmaline.

Identifying the parent oyster species of cultured pearls is another challenge for gemologists. Recently white-lip cultured pearls of relatively small size (about 8 mm in diameter) have appeared on the market. Conversely, a few Akoya cultured pearls of 10 mm or larger are also on the market, and

they command a much higher price than white-lip cultured pearls of the same size. Therefore, it is important to distinguish these two materials despite their similar appearances.

Shell beads manufactured from the freshwater *Anodonta* mussel have been used for bead nuclei in cultured pearls. Depletion of this mussel has resulted in the use of nuclei made of shell from the saltwater mollusk *Tridacna squamosa*. Due to the lower durability of this substitute, and the requirement under the Washington Convention that export of *Tridacna* products take place only with official permission, the identification of shell-bead nuclei in cultured pearls is becoming a requirement for the pearl industry. Using a laser beam diameter of only 30 µm to drill a hole through a sample, the concentration of trace elements such as Li, Si, Ti, Mn, Fe, Ga, Sr, Ag, Sn, and Ba can be used to identify the bead material.

High-Energy Ultraviolet Luminescence Imaging: Applications of the DTC DiamondView for Gem Identification

Christopher M. Breeding (christopher.breeding@gia.edu)[1], Wuyi Wang[2], Andy H. Shen[1], Shane F. McClure[1], James E. Shigley[1], and Dino DeGhionno[1]

[1]GIA Laboratory, Carlsbad; [2]GIA Laboratory, New York

The use of UV fluorescence and phosphorescence for the identification of diamonds and colored stones is not new. Gemologists have known for decades that natural and laboratory-grown gems often have distinctive reactions to UV radiation. Treatments commonly cause changes in fluorescence reactions as well. While standard handheld UV lamps are excellent for the observation of bulk fluorescence colors and distribution patterns, they are not very effective in revealing weak and/or highly detailed patterns. The Diamond Trading Company's DiamondView instrument uses very high-energy ultra-short-wave (<230 nm) UV radiation to induce fluorescence in diamond and reveal growth patterns that facilitate the separation of natural from synthetic stones. The instrument incorporates a high-resolution camera along with aperture and exposure adjustment features to digitally capture even the faintest luminescence. When combined with gemological observations and/or high-tech spectroscopic analysis (such as laser-induced photoluminescence), the high-energy UV imaging capability of the DiamondView has applications that extend far beyond synthetic diamond identification. For example, the occurrence and localized distribution of many defect centers such as H3 in diamond can be clearly resolved even when there is no other gemological evidence for their presence. In many cases, it is possible to detect HPHT treatment of type IIb blue diamonds through the presence or absence of particular luminescence features such as dislocation networks and red phosphorescence (see figure). High-energy UV fluorescence imaging is also useful for colored stone identification. For example, subtle curved growth zoning in lightly colored or high-clarity synthetic sapphires can often be detected using this technique. Various types of fracture-filling materials commonly used in ruby, sapphire, and emerald can also be seen with the instrument. The DiamondView's ability to capture high-resolution images of very weak or highly detailed fluorescence patterns in diamonds and colored stones establishes it as another important tool for gemological research and future identification challenges.

Imaging Spectroscopy: A Developing Frontier for Gem Analysis

Nicholas Del Re (nickd@eglusa.com)

EGL USA, New York

Visual and optical cues are highly valuable for identifying and characterizing gems. In the past 25 years, increasingly sophisticated treatments and enhancements have impacted the gem trade. In response, measurements of gems have been evolving from qualitative to more quantitative analysis. Advanced instrumentation such as UV-Vis-IR and Raman spectroscopy, XRF, SEM, SIMS, and LIBS are now used by gemological laboratories. These methods are highly beneficial, but they have shown limitations in sampling and detection when performing compositional and spatial analyses. For example, an instrument will sample a specimen for a selected number of times after it has been positioned in the sample chamber. Often, expected results are not observed, which may initiate additional testing that requires reorientation of the specimen in the chamber and significant time consumption. As the data are typically obtained from a small area, they provide limited results in most cases.

Imaging spectroscopy (i.e., hyperspectral or chemical

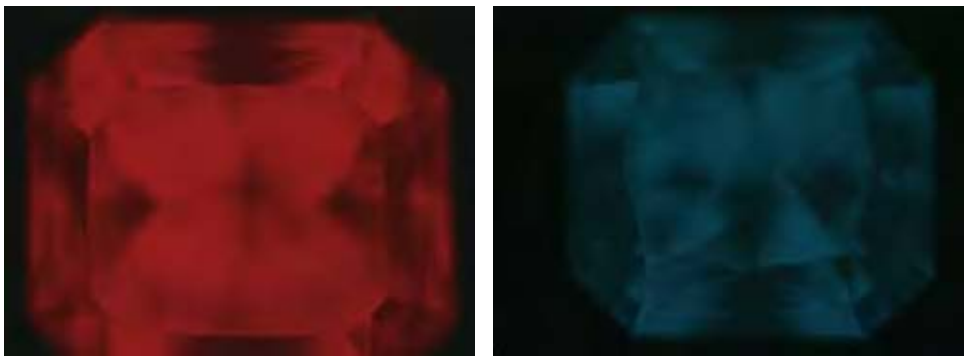

Phosphorescence images from a 1.14 ct type IIb diamond before and after HPHT treatment (repolished to 1.07 ct) are shown with the DTC DiamondView. HPHT treatment caused the disappearance of the distinctive red phosphorescence. Prior to treatment, the diamond was graded Fancy gray. After treatment, the color was Fancy Intense blue.

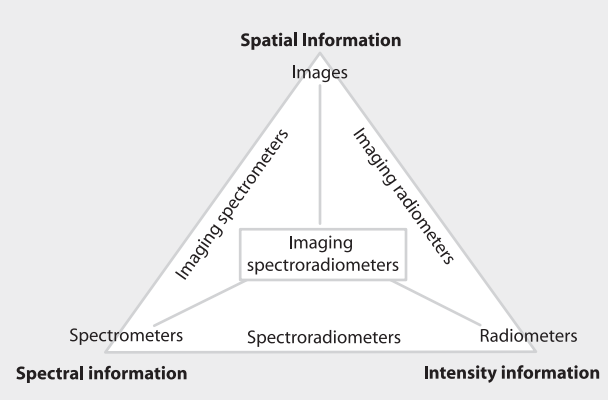

This diagram illustrates the different types of information sought, and the type of sensor used to acquire it, in a hyperspectral imaging system. After Elachi (2006); courtesy of Opto-Knowledge Systems.

imaging), although not entirely new to the field of gemology, has only been used sporadically. With recent advances, however, it merits a closer look. A triangle (see figure) can be used to depict the cornerstones of a hyperspectral imaging system. These are spectrometers, imagers, and radiometers. Respectively, these components capture spectral, spatial, and intensity information. The information from each of these components is comprised of several dimensions. For example, there are numerous spectral bands in the volume sampled. This allows for analysis to be taken to an "nth" dimension. The concept of n-dimensional space, also known as hyperspace, is used when dealing with multidimensional systems. Hyperspace is the logical extension of three-dimensional space for examining more complex multivariable situations. These situations can be handled by multivariate image analysis and chemometrics, which is the application of mathematical or statistical methods to chemical data. Chemometrics can be applied to a gem as it is mapped, so that spatial, chemical, structural, functional, and possibly temporal data can be acquired simultaneously. This methodology can offer more complete solutions for today's difficult gemological problems. Various applications are being explored for specific problems such as detecting HPHT treatment in diamond, natural versus treated coloration for lavender jadeite and "golden" pearls, natural versus synthetic quartz, Be-diffusion treatment of sapphires, and the color grading of gems.

REFERENCE
Elachi C. (2006) *Introduction to the Physics and Techniques of Remote Sensing*. Wiley Interscience, New York.

The Present and Future Potential of Raman Spectroscopy in the Characterization of Gems and Minerals

M. Bonner Denton (mbdenton@u.arizona.edu)[1] and Robert T. Downs[2]
[1]Department of Chemistry, University of Arizona, Tucson; [2]Geosciences Department, University of Arizona, Tucson

A number of important breakthroughs have occurred in recent years that allow Raman spectroscopy to be considered as a routine but powerful analytical tool for identifying and characterizing natural crystalline compounds. The long-standing limitation in sensitivity and the detection limit capabilities of conventional Raman have now dropped to the levels of parts per million and lower. These developments have resulted from a combination of technological advances in optical components, sources, and detector technology.

Advanced technologies developed for fiber-optic telecommunication are now being applied to implement an entirely new generation of miniature spectrometers. Optical systems for entire spectrometers can be built in volumes of cubic millimeters. New approaches for optical component fabrication, mounting, and alignment have been developed that yield highly robust systems capable of providing exceedingly high levels of performance. Performance considerations and design "tradeoffs" include resolution, excitation, wavelength, sensitivity, size, and weight. A new generation of handheld Raman spectroscopic instrumentation is currently being introduced that will find application in diverse fields such as process control, product quality control, medical diagnostics, and environmental analysis, as well as in the analysis of gems and minerals.

The use of Raman spectra to assist in the nondestructive identification of gems, however, requires a credible database as well as appropriate search algorithms. Such a database is currently being developed by the RRUFF project as a public domain asset (http://rruff.info), sponsored by Mike Scott.

Report on the Progress of the RRUFF Project: An Integrated Database of Raman Spectra, X-ray Diffraction, and Chemical Data for Minerals

Robert T. Downs (rdowns@u.arizona.edu)[1] and M. Bonner Denton[2]
[1]Geosciences Department, University of Arizona, Tucson; [2]Department of Chemistry, University of Arizona, Tucson

Recent advances in the miniaturization and optimization of Raman spectroscopic techniques provide the promise of handheld instruments that can be used to quickly and routinely identify and characterize naturally occurring crystalline compounds. For these reasons, we are building a database of Raman spectra that may be used to identify and characterize minerals and inorganic gem materials. The RRUFF project is the largest, most comprehensive research study of minerals ever undertaken. Samples of all known minerals are being subjected to X-ray diffraction to obtain cell parameters, constrain the symmetry, and provide identification. When required, crystal structures are also being determined. This is especially necessary when variations in site occupancies can affect the Raman spectral behavior. Electron-microprobe analysis is being conducted on each sample to obtain an empirical formula. Fragments of the characterized samples are oriented for Raman spectroscopy in the directions necessary to measure symmetry effects of orientation. These fragments are glued onto titanium pins and polished to ensure the highest-quality spectra.

The Raman spectrum of a mineral is analogous to its diffraction pattern, inasmuch as it provides a unique "fingerprint" of

the mineral, influenced by the crystal structure and the bond strengths of the constituent arrangement of atoms. Therefore, a complete library of spectra is essential to the accurate identification of unknown samples. Also under investigation is how well a mature Raman database can be used to estimate chemical composition, site occupancy, and order-disorder, as well as to determine the orientation of the sample. At the time of writing this abstract, the database contains about 1,700 minerals in various stages of examination. Most of the major rock-forming minerals are present. About 25 samples are being added to the project each week. The data are freely available via the Internet at http://rruff.info.

Gem Characterization: A Forecast of Important Techniques in the Coming Decade

Emmanuel Fritsch (emmanuel.fritsch@cnrs-imn.fr)
Institut des Matériaux Jean Rouxel, Nantes, France

Such a "crystal ball" subject is by nature difficult, as no one can pretend to truly predict the future. Nevertheless, trends can be identified, some that have been extremely robust over dozens of years, while others are newer, more subjective, and tentative. Gemologists look for a technique that will make it possible to perform a certain identification task for which existing techniques fail. This is called an enabling technology, and new techniques important in the coming decade will belong to this category.

Let us not forget that the foundation of good gemological work is observation supported by some simple tools and a good binocular microscope, the so-called "classical gemology." This approach will remain the most useful and often the only necessary step. It is too often occulted by hyped "high-tech" instruments. Also, it is clear that some classical physics techniques, already routine in gemology, will continue to play an important role. These include UV-Vis and IR absorption spectroscopy, Raman scattering, and EDXRF chemical analysis.

There are three domains in which useful progress can be predicted, as they all look at more subtle parameters than those commonly explored so far. The first is luminescence. Emission spectra proved to be an enabling technology for the detection of HPHT-treated diamonds. But there are many more possibilities, in particular the use of excitation spectra and of time-resolved luminescence, which offer an almost infinite range of nondestructive possibilities to analyze gem materials.

Second, trace-element analysis is certainly not new to gemology, but it is likely to develop considerably in the coming decade. Advances will be motivated by identification and geographic origin issues. LIBS, LA-ICP-MS, and of course EDXRF can be useful. They each present different advantages and drawbacks in terms of sample damage, accuracy, cost, and detection of light elements.

Third, isotopic studies appear promising, as they have moved into the realm of nearly nondestructive techniques, with SIMS and other ion probes. They have been applied successfully using ^{18}O alone to determine the origin of emeralds, and extensive work on corundum should lead to useful results. Many other isotopes are under study, for example, in diamond.

It is difficult to conceive that developing all these new, typically costly technologies will be achieved successfully by isolated institutions. The building of well-documented, useful databases will likely foster more collaboration between gemological, academic, and industrial labs.

Autoradiographic Investigations of Impurity Distributions in Diamond

Delara S. Khamrayeva (delaras@rambler.ru)[1] and Yulia P. Solodova[2]
[1]Institute of Nuclear Physics of Academy of Sciences, Ulugbek, Tashkent, Uzbekistan; [2]Moscow State Geological Prospecting University, Moscow, Russia

Note: The senior author was unable to deliver the presentation due to a travel delay, and it could not be rescheduled.

This work aims to understand the influence of Co, Ni, Ti, Cr, Mn, and Cu impurities on the quality, microstructure, and morphology of type I natural diamond using the autoradiographic technique. The first step in our study was the determination of the trace-element composition of the diamonds using instrumental neutron activation analysis (INAA) and instrumental gamma activation analysis (IGAA). The diamond specimens were irradiated by neutrons in a nuclear reactor, and for INAA the radionuclides were identified by their energy lines in a gamma spectrum and by their half-life periods. Quantitative trace-element contents were measured by comparing the radionuclide activity of the element in the diamond to that of a standard. For IGAA, the gamma spectra of irradiated samples were measured by means of a Ge(Li) detector and multi-channel pulse analyzer.

The second step involved a study of the spatial distribution of trace elements in the diamonds by activation radiography. This method is based on the registration of secondary beta radiation. After irradiation, the radioactive samples are placed on photographic emulsion, which is used as a detector. The sensitivity of this technique was 108 beta particles/cm^2, and the spatial resolution of the radiograph was about 200–300 μm. A selective autoradiograph was obtained for each trace element, based on the assessment of the nuclear physical parameters, the concentration of radionuclides, and the range of travel of the beta particles. The exposure varied from one hour for short-lived radionuclides to 10 days for long-lived radionuclides.

Using INAA, we found the following trace elements (0.001–200 ppm) in 156 diamonds from Siberia (0.04–1.6 ct): Mg, Ca, Sc, Ti, Mn, Ni, Co, Cr, Cu, Zn, Fe, Sr, Y, Zr, Ru, Sb, Ba, Ce, Eu, Ir, Au, and U. For the autoradiographic study, we selected 12 cubic, four octahedral, and two rounded rhombododecahedral diamond crystals that did not contain any eye-visible inclusions. The selected crystals were sliced into plates oriented parallel to {100}, {110}, or {111}. The plates ranged from 3 to 5 mm, and their thickness was 200–300 μm. Traces of Co (0.01–1 ppm) were detected in all samples. The Co autoradiograph showed lamellar, zonal, micro-zonal distributions of this

element in the octahedral and rhombo-dodecahedral crystals. Traces of Cu (0.1–10 ppm) were concentrated in the central part of the cubic crystals, or in fibrous portions of the other cubic crystals. Similar concentrations of Cu also were found in a cross-like distribution in the rhombo-dodecahedral crystals. Traces of Ti (1–80 ppm) were noted in cubic diamonds having a fibrous structure. Traces of Mn (0.1–1 ppm) were uniformly distributed in the octahedral and rhombo-dodecahedral crystals, but were concentrated in the central or fibrous portions of the cubic crystals.

Automating the Infrared and Raman Spectral Analysis of Gemstones

Steve Lowry (steve.lowry@thermo.com) and Jerry Workman
Thermo Electron Corporation, Madison, Wisconsin

In many gemological laboratories, FTIR and Raman spectroscopy are considered advanced analysis techniques requiring a knowledgeable scientist to visually examine the spectrum to provide a reliable assessment. However in many industries, multivariate statistical analysis techniques are frequently employed to automatically extract valuable information from FTIR and Raman spectra. These techniques treat the spectra as vectors and apply sophisticated mathematical algorithms to compute a result based on the sample vector and a set of reference spectra of fully characterized samples. Most of these techniques have a quality index or standard error value that can be used as a threshold for passing the sample or referring it to a technician for further review. Here we provide examples of how these automated analysis techniques might be applied to problems described in the recent gemological literature.

1. *Sample identification by infrared spectral searching*: A correlation or similarity value is calculated between the spectrum of a sample and each reference spectrum in a "library." The reference spectra that are most similar to the sample are identified and reported with a match value. Our example identifies a green stone as a hydrothermally grown synthetic emerald.
2. *Material verification*: The QC Compare algorithm can be used to verify the composition of a stone. For diamond verification, you might include spectra from all types of diamonds in the diamond class, but for diamond typing you would create separate classes for each type of diamond.
3. *Confirming the presence (or absence) of an important peak*: The presence or absence of small peaks in the spectrum due to trace-level "impurities" may indicate that a stone is synthetic or treated. Classical least-squares techniques (see figure) determine the amount of each reference spectrum that is required to minimize the difference between the sample spectrum and a linear combination of the reference spectra. Our example measures the small hydroxyl peak at 3310 cm^{-1} that is generally present in the spectrum of a natural ruby or sapphire, but disappears when the stone has been beryllium-diffusion treated.
4. *Quantitative analysis of trace components*: The intensity of a peak in the infrared spectrum is proportional to the concentration of the component and the path length of the infrared beam. An example of this is calculating the concentration of the various nitrogen types in a diamond.

Automated workflows can be created that combine these computational techniques with instrument setup and spectral preprocessing to provide an easy, reliable technique for analyzing gemstones.

This example shows a classical least-squares method to automatically verify the presence of small peaks in a diamond's infrared spectrum based on standard error.

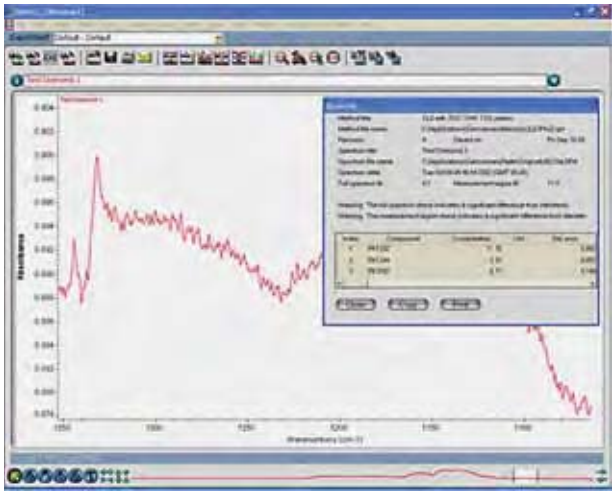

X-ray Diffraction Using Area Detectors for Mineral and Gem Characterization

Jeffrey E. Post (postj@si.edu)
National Museum of Natural History, Smithsonian Institution, Washington, DC

X-ray diffraction is the fundamental method for determining crystal structures and for identifying crystalline phases. A powder X-ray diffraction pattern provides a "fingerprint" that identifies a gem, mineral, or other crystalline material. During the past decade, technological advances in detectors have revolutionized the use of X-ray diffraction for a variety of crystallographic applications. Area CCD (charge-coupled device) and imaging plate detectors are orders of magnitude more sensitive to X-rays than traditional films and scintillation or solid-state detectors. New-generation diffractometers and microdiffractometers fitted with area detectors and conventional X-ray tubes make it possible to routinely collect high-quality X-ray diffraction patterns from a broad variety of samples using typical exposure times of 5–10 minutes. The area detectors permit collection and integration of the full set of Debye-Scherrer diffraction rings, providing improved counting statistics and reduced preferred orientation effects. The combination of the large-area detector, full pattern

integration, and sample oscillation/rotation permits the nondestructive collection of "powder" diffraction patterns from single crystals, including faceted gemstones. Because in most cases it is possible to collect patterns that do not have preferred orientation, the success rate for identification using search-match software and the International Centre for Diffraction Data database is extremely high. The method is particularly useful to gemologists for quick and accurate identification of rare and unusual, or new, gems; for example, we recently identified the first reported wadeite gemstone, for which diagnostic information is not included in standard gemological databases. Area detector diffractometers also provide information about the crystallographic orientation of gemstones. Numerous examples are available of X-ray diffraction studies using a Rigaku D/MAX Rapid microdiffractometer with an imaging plate detector for a variety of samples, including powders, single crystals, and mounted and unset gems.

Characterization of Nanofeatures in Gem Materials

George R. Rossman (grr@gps.caltech.edu)
California Institute of Technology, Pasadena

The inclusions in gem minerals that are commonly observed with an optical microscope occur at a scale of a micrometer or larger. In addition to these inclusions, there are also a multitude of inclusions and features that are larger than the individual atoms that cause color in common gems, but are so small that they cannot be clearly resolved with optical methods. These features can be nearly 1,000 times smaller than features seen with optical microscopes, and are measured in nanometers. Such features can cause iridescence, opalescence, asterism, and turbidity in gem materials. High-resolution scanning electron microscopy allows us to image features on the nano-scale. When images are combined with chemical analysis and electron diffraction patterns, a whole world of previously inaccessible mineralogy becomes available for investigation.

Opals are a classic example of a gem that contains nanoscale features that are the origin of color. A microscopic journey into opals will demonstrate the spectacular differences that occur when the nanofeatures (silica spheres) are arranged either in ordered or disordered patterns. Iridescence in garnets, feldspars, and several ornamental stones is also due to submicrometer-sized features. Star phenomena in stones occur because of oriented inclusions. Both the bodycolor and asterism in rose quartz arise from inclusions of an aluminoborosilicate phase related to dumortierite that are a few hundred nanometers in width. Stars, and particularly turbidity, in sapphire and ruby have been long attributed to myriad minute rutile inclusions. Rarely have these inclusions been identified by direct analysis. High-resolution imaging of the submicroscopic inclusions often fails to find rutile, but instead finds an aluminum oxide phase with a stoichiometry that is consistent with diaspore.

An additional observation frequently made during high-resolution imaging is that the surface quality of stones varies widely. Sub-micrometer-scale surface features from the polishing process are often observed at high magnification and illustrate that there is a wide range of variation in the quality of surface finish.

Infrared Spectra of Gem Corundum

Christopher P. Smith (christopher.smith@gia.edu) and Carolyn van der Bogert
GIA Laboratory, New York

Hydrogen may be incorporated into corundum, forming structurally bonded OH groups. These create a variety of charge-compensation mechanisms that result in specific bands or series of bands in the mid-infrared region of the absorption spectrum. OH groups may occur naturally, or they may be induced or removed through heating.

Commonly, OH absorptions occur as a series of peaks, even though the individual peaks may or may not relate to a singular charge-compensation mechanism. For example, a common OH peak positioned at 3309 cm^{-1} is often associated with additional peaks at 3295 (shoulder), 3265, 3232, and 3186 cm^{-1}. A number of other such correlations have been made, and a naming convention was developed to facilitate rapid reference. These include the 3309-series, 3161-series, 4230-series, 3394-series and 3060-series, as well as others. The association of these series with certain color varieties of corundum and various geologic environments was studied, as well as their application toward identifying the unheated or heated condition of a stone.

Past researchers have attributed the 3161 cm^{-1} band (3161-series; see figure) to OH groups involved in charge-compensa-

The 3161 cm^{-1} mid-infrared spectral feature in this natural-color yellow sapphire from Sri Lanka actually consists of at least six bands. Observations of the occurrence and removal of these absorptions during heating experiments, combined with LA-ICP-MS quantitative chemical analyses, strongly suggest that the 3161-series is related to structurally bonded OH associated with Mg^{2+}.

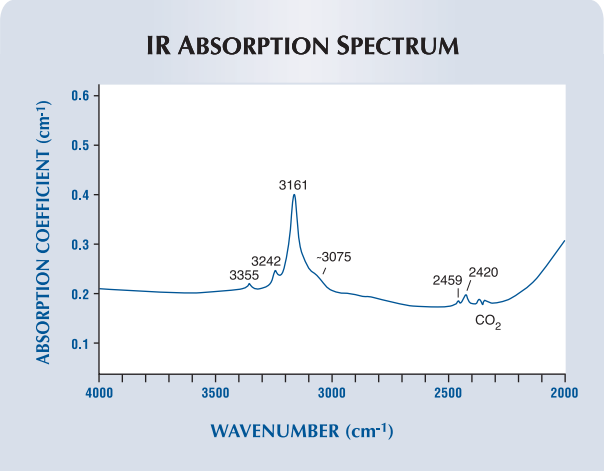

tion with Si^{4+}. However, empirical testing of natural corundum has found that the 3161-series occurs most commonly in natural-color yellow-to-orange and padparadscha sapphires from low-iron metamorphic environments, which owe their color partially or wholly to trapped-hole centers. LA-ICP-MS chemical data and heating experiments suggest that the 3161-series is actually due to structurally bonded OH associated with Mg^{2+}.

The authors have also accumulated an IR spectral reference library of mineral inclusions in corundum. When the spectra of the foreign minerals are superimposed on the IR spectrum of corundum, they may be positively identified. Such minerals include apatite, boehmite, calcite, diaspore, gibbsite, goethite, kaolinite, mica, monazite, and sphene.

Investigation by Synchrotron X-ray Diffraction Topography of the Crystal Structure Defects in Colored Diamonds (Natural, Synthetic, and Treated)

Joe C.C. Yuan (joeyuan@solstargd.21cn.com), Ming-sheng Peng, and Yu-fei Meng
Institute of Gems and Minerals Material, Sun Yat-sen University, Guangzhou, China

Diamonds are not only important for jewelry, but also have a variety of industrial applications. The presence of defects can often produce desirable properties in diamond. For example, plastic deformation may cause diamonds to appear pink or red.

In addition to spectroscopic methods and transmission electron microscopy, we have recently used synchrotron "white-beam" X-ray diffraction topography to observe the microstructures and defects in diamonds. The use of synchrotron X-ray radiation has the advantages of high intensity, polarization, and collimation, along with a small beam size and an adjustable energy level. This nondestructive method provides an ideal and effective way to detect crystal structure defects. Compared to conventional X-ray topography, it requires much less exposure time and provides higher resolution. However, it involves complex equipment that is not easy to operate.

We used the "white beam" of 4W1A X-ray synchrotron radiation in Beijing, China, to investigate crystal structure defects and obtain diffraction patterns of 34 faceted colored diamonds (six natural-color diamonds, three HPHT-grown synthetic colored diamonds, six HPHT-treated colorless and colored diamonds, ten irradiated colored diamonds, and nine fixed-orientation polished colorless or brown natural diamond films). We calculated and defined the index of each diffraction spot on the Laue pattern for each sample. The diffraction spots varied from even, oval, and stretched, to fragmented shapes that corresponded to an increase in the degree of deformation of the diamonds. Various crystal structure defects, such as dislocations, twins, and numerous inclusions, were also located in the samples.

From this study, the extent of defect deformation could be classified as very weak, weak, moderate, and strong (see table in the *G&G* Data Depository at www.gia.edu/gemsandgemology). All of the brown diamonds had strong defect deformation. Diamonds with impurities such as nitrogen, boron, and hydrogen (as determined by spectroscopic methods) had weak-to-moderate degrees of defect deformation. Most of the irradiated natural diamonds showed weak-to-moderate degrees of defect deformation. Colorless and yellowish green diamonds that were HPHT treated from natural brown starting material showed moderate-to-strong degrees of defect deformation. HPHT-grown synthetic diamonds showed a moderate degree of defect deformation.

General Gemology

Color Quantification: A Spectrographic Imaging Approach

Donna Beaton (dbeaton@eglusa.com)
EGL USA, New York

The colored stone market would benefit from a universally accepted color classification system developed from gemstone-specific analytical methods. In the corundum family, it is important to accurately categorize ruby, sapphire, and fancy sapphire colors such as pink, violet, orange, and the highly prized "padparadscha." Apart from defining tolerances, as in corundum, a well-designed system should also evaluate the extent of change-of-color, matching, or metamerism. This report focuses on developing methods to evaluate gemstone color and define color ranges, using padparadscha sapphire as the case study and incorporating a previously accepted definition for that gemstone (i.e., orangy pink or pinkish orange, of medium-to-light tone, and low-to-intense saturation; see, e.g., Crowningshield, 1983).

Aside from the difficulty of correlating the *perception* of color to the physical properties that scientists are able to measure, there are additional problems of assessing the color of transparent, faceted, crystalline materials that are not encountered by most industries that exercise color standards. With gemstones one must consider not only the light that is reflected off the surface, but also light that is transmitted through the stone, and light that has traveled through the stone and is reflected off facets internally. The doubly refractive nature of many gemstones also influences the nature of light that is returned to the eye. So, in choosing a technique/instrument for this study, it was important to find one able to accommodate the nature of the gemstone as well as its interaction with a light source.

Quantitative color information was gathered using a GemSpec digital imaging spectrophotometer manufactured by GemEx Systems. This instrument uses a high-intensity xenon light source to measure the spectral response of the entire unmounted stone in a face-up position. Data for specific lighting conditions and CIE-defined standard light types are obtained through algorithms utilizing spectral responses. In this study, a standard CIE illuminant, a standard 2° observer configuration, and suffuse lighting conditions were used. These conditions were chosen to best represent the majority of gem-buying environments, in which artificial "full-spectrum"

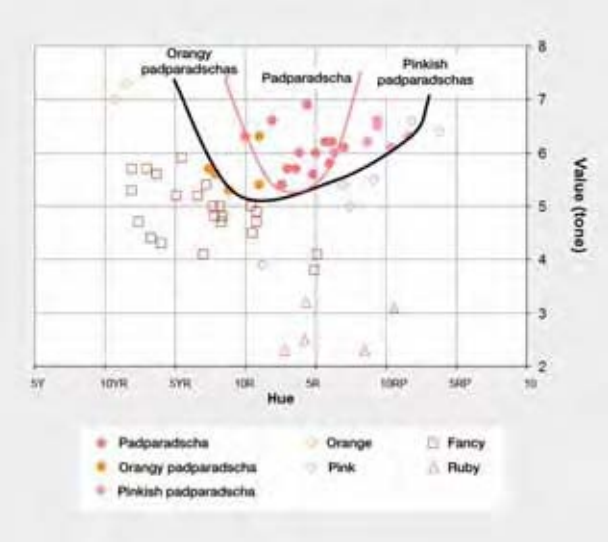

This two-dimensional "slice" of Munsell color space is shown for a chroma (saturation) level of 5–7. The "padparadscha" space in this view is shaped like a tapered parabola.

lighting is used. The data were analyzed in Munsell Notation, CIE xyY, and CIELAB color models. For the Munsell system, a physical model was built, with data points that represent the average overall color of each stone from each subgroup: ruby, pink sapphire, fancy sapphire, orange sapphire, orangy padparadscha, padparadscha, and pinkish padparadscha. For the CIE color spaces, the data were plotted on graphs (see, e.g., figure). The results of this study indicate that a three-dimensional color space could indeed be defined that correlates with a person's perception of what color a padparadscha sapphire should be, and could serve as a criterion to evaluate future padparadscha candidates.

REFERENCE
Crowningshield R. (1983) Padparadscha: What's in a name? *Gems & Gemology*, Vol. 19, No. 1, pp. 30–36.

Rare Reverse Color Change in a Blue Zircon from Myanmar (Burma)

George Bosshart (george.bosshart@swissonline.ch)[1] and Walter A. Balmer[2]
[1]Horgen-Zurich, Switzerland; [2]Bangkok, Thailand

A 6.45 ct round brilliant-cut zircon originating from Mogok exhibited an exceptional color change. The gemstone appeared violetish blue in daylight and bluish green in incandescent light. Identical reactions were observed with the daylight-equivalent illuminant D65 and the incandescent illuminant A in a Gretag-MacBeth light booth (for method and terminology, see Liu et al., 1999). This phenomenon is opposite to the color change of alexandrite, which displays green hues in daylight and purple hues in incandescent light. CIELAB color analysis of this zircon with a Zeiss MCS 311 multichannel color spectrometer revealed a 75° change in hue angle when recorded in a direction parallel to the optic axis (approximately parallel to the table facet; see figure). In a direction perpendicular to the optic axis, the change in hue angle was 65°.

Besides the main constituents of zircon (Zr and Si), qualitative chemical analysis by EDXRF showed evidence of hafnium as a minor element and traces of uranium. The latter identification was supported by radiation spectroscopy. Additional minor EDXRF peaks correlated to erbium and holmium; however, the presence of either element was not fully confirmed. Gaft et al. (2005) listed ytterbium, erbium, and dysprosium as the predominant rare-earth elements (REEs) in natural zircons.

The reverse alexandrite effect of this zircon is due to uncommon and strongly polarized absorption features in the visible region of the spectrum. They consisted of at least 10 multiband absorption maxima dispersed across the entire 400–700 nm range (and of another eight groups of bands up to 1800 nm in the near-infrared region). The absorption peaks located at 656/661, 590, and 683/691 nm (in order of decreasing amplitude) were due to U^{4+}. All other bands were due to traces of REE (George R. Rossman, pers. comm., 2006).

No indications of thermal treatment, such as altered inclusions, were detected in this zircon. The only microscopic features were indistinct growth planes and one mirror-like fracture. Raman spectra did not deviate from those of nonheated zir-

This chromaticity diagram of the uniform CIELAB color space shows the 75° change in hue angle exhibited by the 6.45 ct zircon between daylight-equivalent illuminant D65 and incandescent illuminant A. The diameter of the circle represents a saturation of 10%. It is rare for zircon to show any color change, and even rarer for color-change gemstones to exhibit an incandescent illumination color in the green range, far outside the red region.

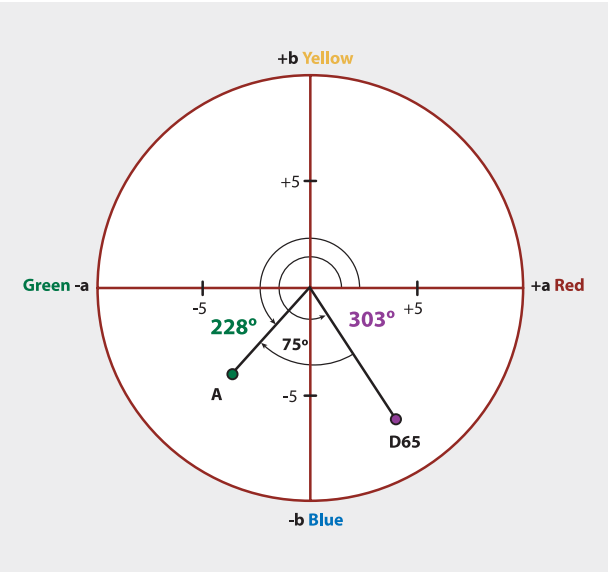

cons. Low-temperature heat treatment, nevertheless, cannot be ruled out completely.

A reverse REE-related color change has not been previously documented in zircon or any other gemstone. The exact mechanism of the color change in this blue zircon may be explained by factors such as complex interactions between REEs and transition metal ions (Thomas Pettke, pers. comm., 2006), multiband transmittance, visual response, and chromaticity adaptation to the different types of illumination. However, it is not well understood.

REFERENCES

Gaft M., Reisfeld R., Panczer G. (2005) *Luminescence Spectroscopy of Minerals and Materials*. Springer-Verlag, New York.

Liu Y., Shigley J.E., Fritsch E., Hemphill S. (1999) A colorimetric study of the alexandrite effect in gemstones. *Journal of Gemmology*, Vol. 26, No. 6, pp. 371–385.

Social, Political, Economic, and Gemological Impacts on Pricing Trends

Richard B. Drucker (rdrucker@gemguide.com)

Gemworld International Inc., Northbrook, Illinois

For more than two decades, Gemworld International has been tracking prices of colored stones and diamonds. Historical trends in pricing during this time period have shown fluctuations according to social, political, economic, and gemological factors. A prediction of future trends based on past history will provide insight for buying decisions in the years ahead. A variety of factors influencing gem pricing are reviewed in this presentation.

The introduction of certain treatments caused prices to decline in some gem varieties. In the mid-1990s, industry awareness that fractures in emeralds were being filled with Opticon was disastrous for the emerald market. The treatment caused an immediate scare and a decline in confidence in emeralds. Today, acceptance and proper disclosure of emerald treatments have improved, and the emerald market is rebounding.

A downturn in ruby prices began in the mid-to-late 1990s. Heat-treated rubies (often with glass residues) from Mong Hsu, Myanmar, flooded the market earlier that decade. The large supply of low-cost material, coupled with a decrease in demand, created a severe decline in ruby prices. Prices have plateaued and are expected to rise.

Beryllium diffusion of sapphire and ruby continues to be a problem for the industry. While struggling with their detection, we are now faced with an abundant supply of goods in the $50–$100/ct range. This has negatively impacted the price of traditionally heated sapphires as well as beryllium-treated sapphires. Conversely, prices of untreated gems are going up as demand for these increases.

Terrorism in 2001 that was falsely linked to tanzanite caused a temporary sharp drop in prices for that gem. Political action by the gem trade, combined with a reduction in supply, have caused tanzanite prices to rise.

The new Supplier of Choice system of diamond distribution imposed by the Diamond Trading Company is a major contributor to the large diamond price increases experienced in recent years. Not since the early 1980s has the industry experienced such rapid price hikes. However, the change in distribution channels has effectively created a more efficient system for selling diamonds at all levels, thereby reducing profit margins. So, the full rough price increases have not been carried through from rough to mid-level distribution, to the retailer, and to the consumer.

Luminescence of the Hope Diamond and Other Blue Diamonds

Sally Eaton-Magaña (sally.magana@gia.edu)[1], Jeffrey E. Post[2], Jaime A. Freitas Jr.[1], Paul B. Klein[1], Roy A. Walters[3], Peter J. Heaney[4], and James E. Butler[1]

[1]Naval Research Laboratory, Washington, DC; [2]Department of Mineral Sciences, Smithsonian Institution, Washington, DC; [3]Ocean Optics Inc., Dunedin, Florida; [4]Department of Geosciences, Pennsylvania State University, University Park

A striking feature of the Hope Diamond is its long-lasting orange-red phosphorescence (see, e.g., figure 5 in Crowningshield, 1989). Other than visual and photographic observation, this luminescence has not been studied. Our experiments employed a technique not often used in gemology, phosphorescence spectroscopy, which was performed on 60 natural blue diamonds from the Aurora Butterfly and Aurora Heart collections, in addition to the Hope Diamond and the Blue Heart diamond. The data were collected using an Ocean Optics deuterium lamp, a fiber-optic assembly to transmit the light, and a USB 2000 spectrometer to record the phosphorescence spectra. Because of the risk of damaging these unique gems, we could not perform several scientifically desirable experiments (such as spectroscopy at liquid nitrogen temperatures). Most luminescence measurements were taken at room temperature, so the majority of the spectra showed broad peaks and no sharp lines.

Nearly all spectra of the blue diamonds examined showed a combination of greenish blue (500 nm) and red (660 nm) phosphorescence. The intensities and the half-lives of each luminescence peak differed for each diamond, which would account for the variety of phosphorescence colors (blue to red) reported by previous researchers. The peak shapes were not significantly different between diamonds, and the peak maxima did not shift with time after the first second.

Blue diamonds are typically type IIb and contain boron impurities. For comparison, we tested four blue HPHT-grown, type IIb synthetic diamonds. These stones exhibited a phosphorescence peak at 500 nm (and also at 575 nm in one diamond), but not at 660 nm.

Prior research has demonstrated that donor-acceptor pair recombination is a likely cause of several bands observed by laser-induced photoluminescence and phosphorescence in synthetic diamonds (see, e.g., Watanabe et al., 1997). In this scenario, holes that are trapped on acceptors (such as boron) and electrons trapped on donors recombine and emit light equivalent to the difference in energy that they possess while separated. This is the first study of natural type IIb diamonds that demonstrates a similar mechanism operating in natural stones.

Acknowledgments: The authors are grateful to Alan Bronstein for his time and for providing access to the Aurora collections, to Thomas Moses and Wuyi Wang of the GIA Laboratory in New York who loaned a DiamondView microscope for this project, and to Russell Feather, Gem Collection manager at the Smithsonian Institution, for his assistance.

REFERENCES

Crowningshield R. (1989) Grading the Hope diamond. *Gems & Gemology*, Vol. 25, No. 2, pp. 91–94.

Watanabe K., Lawson S.C., Isoya J., Kanda H., Sato Y. (1997) Phosphorescence in high-pressure synthetic diamond. *Diamond and Related Materials*, Vol. 6, No. 1, pp. 99–106.

Elbaite from the Himalaya Mine, Mesa Grande, California

Andreas Ertl (andreas.ertl@a1.net)[1], George R. Rossman[2], John M. Hughes[3], Ying Wang[2], Julie O'Leary[2], M. Darby Dyar[4], Stefan Prowatke[5], and Thomas Ludwig[5]

[1]University of Vienna, Austria; [2]Division of Geological and Planetary Sciences, California Institute of Technology, Pasadena; [3]Miami University, Oxford, Ohio; [4]Mount Holyoke College, South Hadley, Massachusetts; [5]University of Heidelberg, Germany

Detailed chemical, Mössbauer, infrared, and structural data were obtained on 12 crystals from gem pockets in the Himalaya mine, San Diego County, California, which is a source for pink and multicolored gem tourmaline. Some of these tourmalines varied strongly in composition. One crystal (sample I, see figure and table) had increasing Ca content (liddicoatite component) and decreasing Zn content (up to ~1 wt.% ZnO) from the Fe-rich core to the Al- and Li-rich rim. The black core (zone 1) was an Al-rich, Mn-bearing schorl. The outer core (zone 2) was a dark yellowish green, Fe- and Mn-bearing elbaite with ~4 wt.% MnO. A yellowish green, intermediate Mn-rich elbaite zone (zone 3) contained a relatively high Mn content of ~6 wt.% MnO. Next there was a light pink elbaite zone (zone 4) with essentially no Fe and <100 ppm Mn^{3+} that was responsible for the color. The near-colorless elbaite rim (zone 5) had the highest Li content and ~1 wt.% MnO. Mössbauer studies of 20 mg samples from the different color zones within this crystal showed that the relative fraction of Fe^{3+} increased continuously from the Fe-rich core to the Fe-poor rim, reflecting the increasing fugacity of oxygen in the pegmatite pocket. Within the core of the crystal, the Si site contained ~0.3 apfu (atoms per formula unit) Al whereas in the rim it contained ~0.2 apfu B, consistent with the average Si-O distances. The intermediate zones contained mixed occupancies of Si, Al, and B.

A near-colorless, late-stage elbaite (sample II) from the Green Cap pocket (extracted in 1998) had ~2 wt.% MnO, ~2 wt.% FeO, and surprisingly ~0.3 wt.% MgO (dravite/uvite component), which is unusual in late-stage elbaite. This sample contained 1.6 wt.% CaO, the highest Ca content of the tourmalines in this study.

A gem-quality, light pink elbaite crystal (sample III) had the highest boron concentration (~0.3 apfu B) at the Si site (which produced a lower Si-O distance) of the three samples; it also contained the highest Al_2O_3 content (~43 wt.%) and essentially no Fe and only small amounts of Mn.

Analysis of water in elbaites is problematic because the crystals often contain fluid inclusions. Thus, conventional methods that extract water from a bulk sample may give erroneous values. Methods such as IR spectroscopy, which allow the distinction between structural OH and fluid inclusions, offer advantages for future tourmaline analyses.

A Close Look at Gemstone Color Grading: Definition of the Key Color

Yulia Grozman (yulia@appraisalplus.biz)
Appraisal Plus, Valley Village, California

Color is the most important factor for determining gemstone quality in colored stones; it is also the most difficult to measure objectively. In colored stones, every facet has a different color (i.e., different hue, saturation, and tone). Despite serious efforts conducted by GIA, there is still some ambiguity in color determination methods. In its *Colored Stone Grading Manual*, GIA formulated the following procedure to assign the color. The tone is an average of all the areas of the stone,

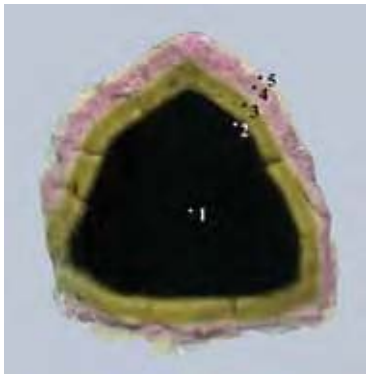

This <4-cm-wide tourmaline slice (sample I) has a schorl core surrounded by elbaite. Photo by A. Wagner.

Colors and chemical compositions of three tourmalines from the Himalaya mine.[1]

Sample no.	Zone no.	Color	Y site	W site
I	1	Black	$Fe^{2+}_{1.1}Al_{1.0}Mn^{2+}_{0.3}Fe^{3+}_{0.3}Li_{0.1}Zn_{0.1}\square_{0.1}$	$(OH)_{0.4}F_{0.4}O_{0.2}$
I	2	Black	$Al_{1.1}Mn^{2+}_{0.5}Li_{0.5}Fe^{2+}_{0.5}Fe^{3+}_{0.1}Zn_{0.1}\square_{0.2}$	$F_{0.7}(OH)_{0.3}$
I	3	Yellowish green	$Al_{1.3}Mn^{2+}_{0.8}Li_{0.7}\square_{0.2}$	$F_{0.8}(OH)_{0.2}$
I	4	Light pink	$Al_{1.8}Li_{1.1}\square_{0.1}$	$F_{0.6}(OH)_{0.2}O_{0.2}$
I	5	Near colorless	$Al_{1.5}Li_{1.2}Mn^{2+}_{0.1}\square_{0.2}$	$F_{0.7}(OH)_{0.3}$
II	–	Near colorless	$Al_{1.3}Li_{0.9}Mn^{2+}_{0.3}Fe^{2+}_{0.2}Mg_{0.1}\square_{0.2}$	$F_{0.8}(OH)_{0.2}$
III	–	Light pink	$Al_{1.7}Li_{1.0}\square_{0.3}$	$(OH)_{0.5}F_{0.5}$

[1]*The Z site was occupied by Al_6, and the V site was occupied by $(OH)_3$, in all the tourmaline samples. The X site was mainly occupied by Na. The T site was mainly occupied by Si with minor Al/B contents. Abbreviation: □ = vacancy.*

while the hue and saturation are based on the "key color." The GIA manual describes key color as "the most representative color that flows through the stone as you rock it." However, the "most representative color" is very different for dark and light stones. In light stones, areas with the highest saturation will be most visible and thus define the key color. In dark stones (e.g., almandine or sapphire), the flashes (or scintillation) produce the strongest perception of color. The present study attempts to advance GIA standards by introducing a new approach for determining the key color and instrumental measurements. The results of the study are color maps with proposed grade borders for gems such as ruby, sapphire, emerald, and others.

More than 300 gemstones were measured using a GemEx imaging spectrophotometer. This measuring system uses an array of photo detectors, instead of the single photo detector typical of other brands, and measures the color of a specific area of a stone. The results are displayed in the Munsell color-order system with the tolerance of ±0.5 units of hue, ±0.5 units of chroma (saturation), and ±0.25 units of value (tone). The resulting maps utilized the existing GIA Colored Stone Grading System that was expanded to 50 hue units (instead of 33), and they used Munsell units for tone and saturation.

The key color was specified manually and quantified using the result of the measurements. These measurements provide the quantitative base for further statistical analysis of the obtained images to develop a formal algorithm for instrumental key color determination. The development of this algorithm will open a way to design an efficient and comprehensive color measurement device for the gem and jewelry industry.

Natural "CO_2-rich" Colored Diamonds

Thomas Hainschwang (thomas.hainschwang@gia.edu)[1], Franck Notari[1], Emmanuel Fritsch[2], Laurent Massi[2], Christopher M. Breeding[3], and Benjamin Rondeau[4]

[1]GIA GemTechLab, Geneva, Switzerland; [2]Institut des Matériaux Jean Rouxel, Nantes, France; [3]GIA Laboratory, Carlsbad; [4]Muséum d'Histoire Naturelle, Paris, France

This study of apparently monocrystalline, so-called CO_2-rich diamonds was performed on several hundred samples that were light to dark brown (appearing black) with various modifying colors, including "olive" (mixtures of green, brown, gray, and yellow), yellow, and almost red. The color was usually heterogeneously distributed in the form of patches or non-deformation-related color banding. Characteristic platelike inclusions were present in nearly all samples. These appeared small, extremely thin, transparent to opaque, and rounded or hexagonal. In general, they were concentrated within certain colored sectors of the diamonds that often exhibited distinct birefringence. The FTIR spectra were characteristic for all samples, with two bands at various positions from 2406 to 2362 cm^{-1} and 658 to 645 cm^{-1}. These bands have been previously interpreted as the ν_3 and ν_2 bands of CO_2 due to inclusions of pressurized solid carbon dioxide (CO_2) in its cubic form (Schrauder and Navon, 1993; Wang et al., 2005). Practically all samples fluoresced a distinct yellow to greenish yellow to long- and short-wave UV radiation, and they showed lasting yellow phosphorescence.

The one-phonon IR absorptions varied dramatically from standard type Ia peaks to very complex bands, which in many cases were inclusion-related. In some diamonds, unknown absorptions dominating the one-, two-, and three-phonon regions were observed, and no satisfactory explanation for their presence could be given. In many samples, the bands observed in the FTIR spectra corresponded to inclusions of carbonates and silicates, notably calcite, mica, and hydrous minerals. Some of the diamonds showed a more-or-less distinct type Ib character.

Our calculations of the theoretical ν_3 and ν_2 band positions at various pressures have caused us to strongly doubt the previous interpretation of the IR bands at 2406–2362 cm^{-1} and 658–645 cm^{-1}. In most cases, the observed absorption positions and shifts (up to 50 cm^{-1}) did not correspond to the calculated values and appeared to be random. Furthermore, the ν_3 and ν_2 bands exhibited highly variable widths (FWHM) and intensity ratios. HPHT-treatment experiments on "CO_2-rich" diamonds also brought unexpected results. A possible reason for this is that the CO_2 molecules are integrated into the structure of the diamonds and that the CO_2 is not present as inclusions.

There are some indications that the hexagonal polymorph of diamond (lonsdaleite) could be present in these diamonds. Further analysis may confirm the identity of the hexagonal platelets as lonsdaleite inclusions, as was previously suggested by Kliya and Milyuvene (1984).

REFERENCES

Kliya M.O., Milyuvene V.A. (1984) Lonsdaleite inclusions as a possible cause of yellow-green fluorescence in diamonds. *Growth of Crystals*, Vol. 12, pp. 308–315.

Schrauder M., Navon O. (1993) Solid carbon dioxide in a natural diamond. *Nature*, Vol. 365, pp. 42–44.

Wang W., Moses T., Moe K.S., Shen A.H.T. (2005) Lab Notes: Large diamond with micro-inclusions of carbonates and solid CO_2. *Gems & Gemology*, Vol. 41, No. 2, pp. 165–167.

Genetic Classification of Mineral Inclusions in Quartz

Jaroslav Hyršl (hyrsl@kuryr.cz)

Prague, Czech Republic

Quartz is a mineral with the highest-known number of different mineral inclusions; over 150 minerals have already been identified in quartz, according to Hyršl and Niedermayr (2003). This book contains a detailed description of inclusions in quartz (including how they were identified), which are listed according to the mineralogical system (elements, sulfides, etc.). For this report, only the most important occurrences are listed according to their genetic type. This approach is important to gemologists working with specimens of an unknown provenance, because it can help with finding a correct locality.

The following genetic types of geologic environments produce the majority of quartz with inclusions:

Alpine fissures

- *Typical localities*: the Alps in Austria and Switzerland, Polar

Urals in Russia, northern Minas Gerais and Bahia in Brazil, Nepal, and Arkansas in the U.S.

- *Typical inclusions*: mica (white muscovite, brown biotite), chlorite (green clinochlore), epidote, actinolite, hematite, ilmenite, rutile, anatase, brookite, titanite, carbonates (calcite, siderite), pyrite, black tourmaline (schorl), cavities after anhydrite, galena, chalcopyrite, fibrous sulfosalts (boulangerite, cosalite, meneghinite, etc.), and monazite

Granitic pegmatites

- *Typical localities*: Minas Gerais in Brazil, Madagascar, and Tongbei in China
- *Typical inclusions*: black or colored tourmaline (elbaite), mica (muscovite and lepidolite), garnet (spessartine and almandine), albite, apatite, columbite, beryl, and microlite

Alkaline pegmatites

- *Typical localities*: Mount Malosa in Malawi, Row Mountain in Russia, and Zegi Mountain in Pakistan
- *Typical inclusions*: aegirine, astrophyllite, epididymite, zircon, and riebeckite

Tungsten deposits

- *Typical localities*: Panasqueira in Portugal, Kara-Oba in Kazakhstan, Yaogangxian in China, Pasto Bueno in Peru, and Kami in Bolivia
- *Typical inclusions*: arsenopyrite, chalcopyrite, pyrrhotite, sphalerite, stannite, helvite, cosalite, carbonates (siderite and rhodochrosite), fluorite, and wolframite

Ore veins

- *Typical localities*: Berezovsk in Russia, Messina in South Africa, and Casapalca in Peru
- *Typical inclusions*: pyrite, galena, sphalerite, chalcopyrite, tetrahedrite, stibnite, molybdenite, cinnabar, gold, and Cu-silicates (ajoite, papagoite, and shattuckite)

Monomineralic quartz veins with amethyst

- *Typical localities*: Mangyshlak in Kazakhstan, Madagascar, and Brazil
- *Typical inclusions*: goethite ("cacoxenite") and hematite ("lepidocrocite" or "beetle legs")

Amethyst geodes in basalts

- *Typical localities*: Rio Grande do Sul in Brazil and northern Uruguay
- *Typical inclusions*: goethite, fluorite, and cristobalite

Dolomitic carbonates

- *Typical localities*: Herkimer in New York, Bahia in Brazil, Sichuan in China, and Baluchistan in Pakistan
- *Typical inclusions*: calcite, pyrite, graphite, hydrocarbons ("anthraxolite"), and natural petroleum oil

REFERENCE
Hyršl J., Niedermayr G. (2003) *Magic World: Inclusions in Quartz*. Bode Verlag, Haltern, Germany.

The Hkamti Jadeite Mines Area, Sagaing Division, Myanmar (Burma)

Robert E. Kane (finegemsintl@msn.com)[1] and George E. Harlow[2]
[1]Fine Gems International, Helena, Montana; [2]American Museum of Natural History, New York

The Hkamti jadeite area, Sagaing Division, northwestern Myanmar, is perhaps the world's most important producer of Imperial jadeite jade. In February 2000, the first group of Westerners visited the jade mines around the mining town of Nansibon (25°51.4'N, 95°51.5'E), 24 km southeast of Sinkaling/Hkamti and ~50 air-km northwest of Hpakan, which is the trading center in Myanmar's Jade Tract (see e.g., Hughes et al., 2000).

The Hkamti region has two mining centers—Nansibon and Natmaw—separated by 32 air-km. At Nansibon, pebbles and boulders of jadeite are hosted in a serpentinite boulder conglomerate, which is steeply inclined at 60°–90°E (Avé Lallemant et al., 2000). The jadeite is concentrated in high-energy, alluvial–fanglomerate channel deposits after being weathered from veins or blocks within serpentinite. The discovery of ancient Chinese mining tools indicates that the Nansibon jadeite area has been mined for centuries. At Natmaw, jadeite has been mined from a primary "dike" as well as recovered as alluvial boulders from the Natmaw River. Based on petrologic and textural interpretations, including cathodoluminescence imaging, Nansibon and other jadeitite formed as vein crystallizations from a hydrous fluid in ultramafic rock (see Harlow and Sorensen, 2005; Sorensen et al., 2006). Nansibon and Natmaw jadeitite is nearly pure jadeitic pyroxene, consisting primarily of jadeite with minor albite; traces of zircon, graphite, and oxidized pyrite(?); abundant fluid inclusions; and rare sodic amphibole selvages. This mineralogy is roughly comparable to jadeitite from the Jade Tract. Glassy albitite is found with the jadeitite, and cobbles in the serpentinite conglomerate include garnet amphibolite, epidote-blueschist, granitic rocks, garnet- or chloritoid-pelitic schists, quartz, and marble. The Hkamti jadeite region appears to be a partially buried, westward branch of the Sagaing fault system that defines the main Jade Tract, suggesting considerable potential for future exploitation.

All mineral mining in the country falls under the control of the Myanma Gem Enterprise (MGE), a subsidiary of the Ministry of Mines, Myanmar. All the jadeite mining concerns in Nansibon are cooperative joint-ventures between the government and private Myanmar companies or individuals. At the time of the authors' visit to the area in 2000, roughly 175 one-acre claims were active. Excavation was mostly carried out by modern open-cut operations; however, jadeite was detected simply by manual inspection of disaggregated conglomerate. During this visit, jadeite samples were collected in a wide range of colors (see figure).

REFERENCES
Avé Lallemant H.G., Harlow G.E., Sorensen S.S., Sisson V.B., Kane R.E., Htun H., Soe M. (2000) The Nansibon jade mines, Myanmar: Structure and tectonics. *American*

This selection of cabochons (0.77–15.58 ct) acquired at Nansibon shows the range of colors in jadeite jade from the area mines. Courtesy of the American Museum of Natural History; photo by D. Finnin.

Geophysical Union Fall Meeting, www.agu.org/meetings/waisfm00.html; search for "T61B-05."

Harlow G.E., Sorensen S.S. (2005) Jade (nephrite and jadeitite) and serpentinite: Metasomatic connections. *International Geology Review*, Vol. 47, No. 2, pp. 113–146.

Hughes R.W., Galibert O., Bosshart G., Ward F., Oo T., Smith M., Sun T.T., Harlow G. (2000) Burmese jade: The inscrutable gem. *Gems & Gemology*, Vol. 36, No. 1, pp. 2–26.

Sorensen S., Harlow G.E., Rumble D. (2006) The origin of jadeitite-forming subduction zone fluids: CL-guided SIMS oxygen-isotope and trace-element evidence. *American Mineralogist*, Vol. 91, No. 7, pp. 979–996.

Identification of Pigments in Freshwater Cultured Pearls with Raman Scattering

Stefanos Karampelas (steka@physics.auth.gr)[1,2], Emmanuel Fritsch[2], Spyros Sklavounos[1], and Triantafyllos Soldatos[1]

[1]Aristotle University of Thessaloniki, Greece; [2]Institut des Matériaux Jean Rouxel, Nantes, France

Understanding the nature of the pigments in natural-color samples can help separate them from their treated equivalents. This study was carried out on more than 30 untreated freshwater cultured pearls from the mollusk *Hyriopsis cumingi* covering their typical range of colors (violet, pink, orange, gray, and white). Raman analysis was performed using four excitation wavelengths in the visible range, three using an argon-ion laser (514.53, 487.98, and 457.94 nm) and one with a krypton-ion laser (647.14 nm). The Raman scattering results were compared with UV-Vis-NIR absorption spectra (obtained in reflectance mode).

All of the colored cultured pearls showed the two major Raman resonance features of polyenic (polyacetylenic) compounds assigned to C-C stretching (~1130 cm^{-1}) and C=C stretching (~1500 cm^{-1}), regardless of their specific hue. These peaks were not detected in the white cultured pearls, and are therefore believed to relate to the coloration. The exact position of the C-C stretching demonstrated the absence of methyl groups attached to the polyenic chains; thus these compounds are not members of the carotenoid family.

With changes in excitation wavelength, we noted variations in the position, shape, and relative intensities of the two most intense bands (see figure). The exact position of the C=C stretching band of polyenic molecules depends strongly on the chain length (i.e., number of C=C bonds). Decomposition with constraints of the broad peak around 1500 cm^{-1} revealed up to nine pigments in the same sample, with a general chemical formula R-(-CH=CH-)$_n$–R′(R and R′ are the end-group pigments, which cannot be detected using Raman scattering) with n = 6–14. All of our samples were colored by a mixture of at least four pigments (n = 8–11), and the different colors were attributable to various pigment mixtures. Raman scattering results paralleled qualitatively those obtained by UV-Vis-NIR diffuse reflectance.

Our preliminary studies on cultured freshwater pearls from the same genus (*Hyriopsis*) but other species (*H. schlegeli* [Biwa pearls] and *H. schlegeli x H. cumingi* [Kasumiga pearls]) have shown that these pigments seem to be characteristic of all cultured pearls originating from this mollusk's genus. Moreover, other organic gem materials such as shell, corals, nonnacreous

The Raman spectra shown here for a grayish purple cultured pearl from H. cumingi *at various excitation wavelengths are characteristic of polyenic compounds. Focusing on the region most "sensitive" to C=C stretching bonds (about 1500 cm^{-1}, see inset), changes in the position, shape, and relative intensities of the peaks are quite apparent. At least five pigments, having a general formula of R-(-CH=CH-)$_n$-R′, can be identified from these peaks: at 1504 (n = 12), 1512 (n = 11), 1522 (n = 10), 1532 (n = 9), and 1543 (n = 8) cm^{-1}. All the peaks are normalized to the main aragonite peak at 1086 cm^{-1}. The spectra are offset vertically for clarity.*

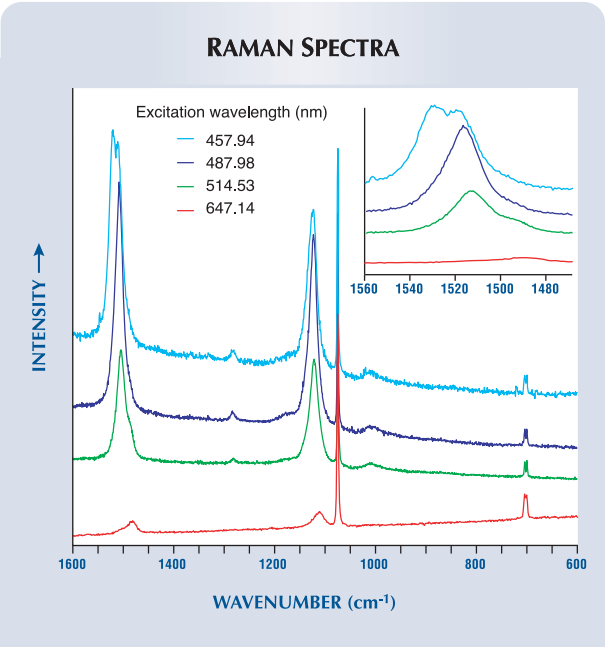

"pearls," etc., appear to have a similar origin of color. Finally, our measurements on some freshwater cultured pearls that were color-treated in different ways prove that the origin of color in the treated freshwater cultured pearls is different, and therefore they can be identified with Raman analysis.

Quantifiable Cut Grade System within an Educational Setting

Courtenay Keenan (ckeenan@auroracollege.nt.ca), Mike Botha, and Robert Ward
Aurora College, Yellowknife, Northwest Territories, Canada

The diamond cutting and polishing industry in Canada's North is unique in that detailed and robust occupational standards were formulated by the Government of the Northwest Territories. Developed with these standards was an innovative Occupational Certification process for workers employed in this industry. This unique situation required the development of a truly quantifiable cut grading system whereby objective, precise feedback relating to the quality of the workmanship is given.

The evaluation for cut quality and finish was first developed to best assess the quality of workmanship of the certification candidates. A demerit system is used whereby each diamond is allotted 100% and demerits are incurred at a rate of 2% per fault in the areas of finish and symmetry. The system describes a fault as any of the following features apparent with 10× magnification:

- Aberrations present on the surface of the diamond as a result of the polishing process (including polish lines, abrasions, and burn marks)
- Faceting errors such as merged facets, open facets, and extra facets

With the advent of computerized proportion scopes (e.g., Sarin Technologies), the cut grade system assumes that the stones under assessment have proportions acceptable to the market.

If properly used by trained graders, this system is scientific, objective, and repeatable. Standardized worksheets (complete with diagnostic diagrams) have been developed to assist the grader and provide an objective paper reference. This system differs from past cut grade systems by offering precise, numerical feedback. Although this system has been applied most often to round brilliants, it is applicable to all diamond cuts.

The Quantifiable Cut Grade System is used by the Aurora College Diamond Cutting and Polishing Program to provide students with objective, numerical, and visual feedback on the quality of their work. Students and staff can reference the worksheets to track skill development and identify potential problem areas. The program exit criteria use this cut grade system by requiring students to achieve at least 70% (≤15 faults) for each diamond polished to be considered suitable for entry into the industry.

Students who successfully complete the training program and enter the diamond polishing industry in the Northwest Territories may apply for Occupational Certification based on these standards after just two years, inclusive of training time. These certification candidates must complete their practical examinations with no stone falling below an 80% grade.

Monochromatic X-Ray Topographic Characterization of Pezzottaite with Synchrotron Radiation

Shang-i Liu (gemedwardliu@yahoo.com.hk), Ming-sheng Peng, and Yu-fei Meng
Institute of Gems and Minerals Material, Sun Yat-sen University, Guangzhou, China

Synchrotron radiation X-ray topography is a nondestructive characterization technique for imaging the defect microstructure of crystalline materials. In this research, monochromatic X-ray surface-reflection topographic images were obtained of gem-quality pezzottaite from Madagascar using synchrotron radiation.

Compared to polychromatic ("white") X-ray topography, the monochromatic technique provides an image of a certain lattice plane instead of a "superimposed" image of a series of atomic planes of the same orientation. It provides a higher resolution image with specific information about the orientation and features of dislocations and strain patterns in the sample. Since surface reflection topography is extremely sensitive to surface microstructure, sample preparation (i.e., polishing) is essential.

X-ray topographic reflection images for (0006), (00012), and (00018) lattice planes at different angular positions along the rocking curve (a curve of the diffraction intensity versus the angular distance from a reference plane) were collected for seven pezzottaite samples. The full width at half maximum (FWHM) and the shape of the diffraction rocking curves reflect the degree of deformation of the sample. The pezzottaite samples exhibited various degrees of crystal perfection. Some crystals showed a mosaic structure containing orientation contrast (a type of X-ray topographic contrast that arises from portions of a sample that are crystallographically misoriented and show variations in diffracted intensity), but with a relatively sharp single-peaked rocking curve, which indicates fairly good crystallinity. However, other samples showed low degrees of crystal perfection, having a fairly wide rocking curve (angles ranging from 300–500 seconds FWHM) with several sharp peaks (see figure).

X-ray topographic images from the imperfect crystals showed large amounts of strain and dislocations with a mosaic structure. Microscopic tubes were observed in the topographs of all seven samples. They were predominantly seen at the boundaries between different domains and along dislocations. We believe that the dislocations are caused by stress and the heterogeneous chemical composition of the material—as revealed by backscattered electron imaging and chemical analysis by electron microprobe and high-resolution inductively coupled plasma–mass spectrometry for Be and Li. Local variations in the crystal structure may cause internal strain resulting in lattice dislocation. This would explain the formation of the "tabby"

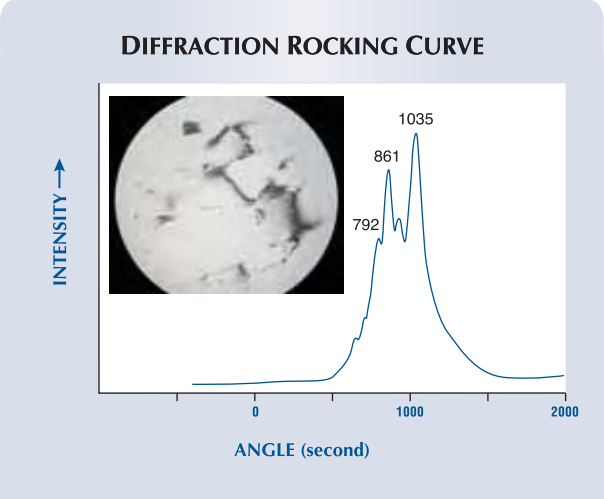

This X-ray topograph (inset) and diffraction rocking curve taken in (00018) reflection show a low degree of crystal perfection with significant lattice dislocation within pezzottaite.

extinction effect and anomalous biaxial character seen in some pezzottaite samples between crossed polarizers.

Universal Color Grading System

Yan Liu (yanliu@liulabs.com)
Liu Research Laboratories, South El Monte, California

A Universal Color Grading System has been developed for accurate color grading of colored stones and colored diamonds. This system is based on the uniform CIELAB color space with 22 hue names, seven lightness levels, and four saturation intensities. The color name grid is optimally designed to use the least number of color samples to represent the maximum number of color names for each hue (i.e., 12 samples to represent 20 color names; see figure). The 22 hues are arranged on a hue circle in CIELAB color space according to a previous study (Sturges and Whitfield, 1995). The hues are divided into cool and warm hues, and their saturation intensities and lightness levels are uniformly distributed according to the Color Name Charts of Kelly and Judd (1976). The significant advantage of this system is that gemstone color can be accurately graded at the fineness of level 6 in the Universal Color Language, and not just approximately estimated as is done by other color grading systems and methods.

Color grades provided by the Universal Color Grading System consist of a color name (arranged in order of saturation, lightness, and hue) and the corresponding CIELAB color coordinates in the form of (C_{ab}*, L*, h_{ab}), which represent chroma, lightness, and hue angle. A sample color grade for ruby is Vivid Medium Red (80.0, 50.0, 26.8). The color name is a verbal description of the color, and the color coordinate is used for accurate color communication.

A computer color imaging system called TrueGemColor has also been developed for color grading of colored stones and colored diamonds using this Universal Color Grading System. The TrueGemColor system is precisely profiled in the CIELAB color space, and more importantly it can be calibrated by users for their individual computer monitors. The TrueGemColor system provides a reference color to match the face-up average color of a gemstone under a standard lighting environment. The reference color can be continuously changed by adjusting the hue, lightness, and saturation values on the screen. The color name and CIELAB coordinates of the matched reference color are automatically assigned as the color grade for the gemstone. Gem laboratories and jewelers will always see the same color if they enter the same color coordinates of the color grade using the TrueGemColor system.

REFERENCES
Kelly K., Judd D. (1976) *Color: Universal Language and Dictionary of Names*. National Bureau of Standards Special Publication 440, U.S. Government Printing Office, Washington, DC.

Sturges J., Whitfield T. (1995) Locating basic colors in the Munsell space. *Color Research & Application*, Vol. 20, No. 6, pp. 364–376.

Chameleon Diamonds: A Proposed Model to Explain Thermochromic and Photochromic Behaviors

Laurent Massi (laurent.massi@cnrs-imn.fr)[1], Emmanuel Fritsch[1], George R. Rossman[2], Thomas Hainschwang[3], Stéphane Jobic[1], and Rémy Dessapt[1]
[1]Institut des Matériaux Jean Rouxel, University of Nantes, France; [2]Division of Geological and Planetary Sciences, California Institute of Technology, Pasadena; [3]GIA GemTechLab, Geneva, Switzerland

Chameleon diamonds are an unusual variety of colored diamond that typically change from grayish green to yellow when heated (thermochromic behavior) or kept in the dark (photochromic behavior). This report is based on a study of more than 40 chameleon diamonds, including the 22.28 ct Green

This name grid of the Universal Color Grading System was developed to use the least number of color samples to represent the maximum number of color names.

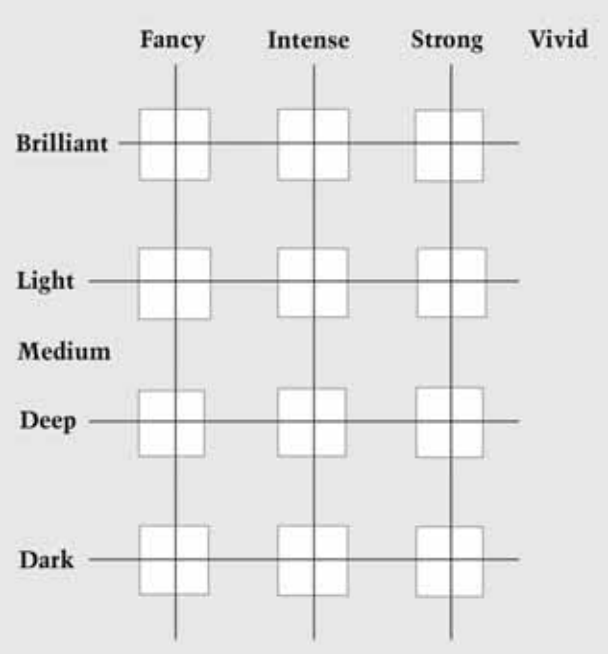

Chameleon and a 31.31 ct oval gem, the largest documented chameleon diamonds known to date.

As described previously for chameleon diamonds, the samples were type IaA, indicating that A aggregates largely dominated the nitrogen speciation. They contained moderate-to-large amounts of hydrogen, in addition to some isolated nitrogen and traces of nickel. Their UV-Vis absorption spectra comprised the continuum typical of type Ib material—even if this character is not detectable with IR spectroscopy—and, in addition, a 480 nm band and a broad band centered at around 800 nm. It is mainly in the red part of the visible spectrum that the color change occurs because when heated or kept in the dark, the essential change in the UV-Vis absorption spectrum is the significant decrease of the very broad band at 800 nm (see figure).

We propose an electronic model that is consistent with all observed color behaviors in chameleon diamonds. The model is based on the premise that, from a physical standpoint, yellow is the stable color whereas green is the metastable one. According to the literature (i.e., Goss et al., 2002), the most plausible model for the hydrogen-related center in diamond is N…H-C (in which the hydrogen atom is located near a bond center between N and C, but closer to C than to N). Since chameleon diamonds are predominantly type IaA, with moderate-to-large amounts of hydrogen, it therefore seems reasonable to suggest that a possible center responsible for the chameleon effect is a nitrogen-hydrogen complex involving the sequence N…H-C.

REFERENCE

Goss J.P., Jones R., Heggie M.I., Ewels C.P., Briddon P.R., Öberg S. (2002) Theory of hydrogen in diamond. *Physical Review B*, Vol. 65, No. 11, pp. 115207-1–115207-13.

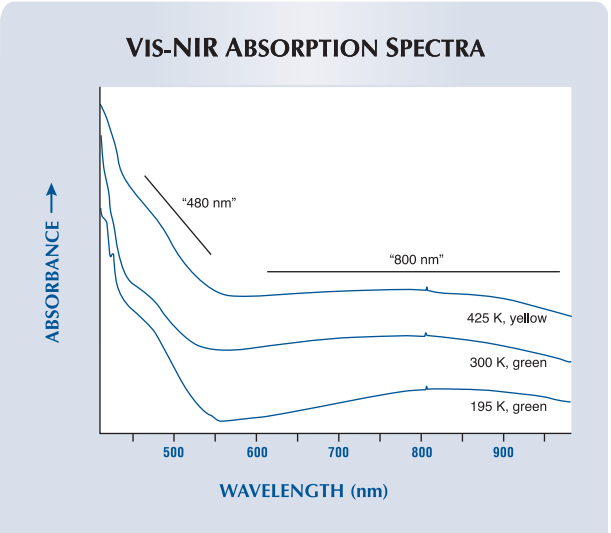

These UV-Vis absorption spectra of a 0.34 ct chameleon diamond at various temperatures show the removal of the very broad band at about 800 nm when the diamond is heated to 425 K, resulting in a change in color from grayish green to yellow.

Source Type Classification of Gem Corundum

Shane F. McClure (smclure@gia.edu)

GIA Laboratory, Carlsbad

The visual characteristics that gemologists and gem traders look for when examining a gemstone—such as hue, tone, saturation, and diaphaneity—are the direct result of the geologic environment in which the stone formed. This environment determines the stone's chemical composition, growth structures, and inclusion suites, all of which affect its overall appearance. These factors are common for all gems, but are particularly significant in corundum.

While many different types of growth environments are possible, for corundum they can be broadly categorized into two main groups: metamorphic and magma-related; the latter will be referred to simply as magmatic in this abstract. The largest distinction between these environments is that the metamorphic corundum formed in the earth's upper crust, whereas the magmatic corundum crystallized much deeper in the earth at mid-crust or lower-crust/mantle levels. Eruptive forces are necessary to transport corundum from the latter group to the earth's surface (typically in an alkali basaltic magma), so it is referred to as magmatic. While these two broad categories of sources for corundum may be readily distinguished by a combination of standard gemological and advanced analytical techniques, they can also commonly be recognized visually by a knowledgeable observer.

Beyond these two broad source designations, there exists a potential to further classify rubies and sapphires of all colors based on their dominant inclusion features and other physical characteristics. These inclusion features may influence the face-up appearance of a ruby or sapphire. For example, "milky" zonal clouds of submicroscopic particles are responsible for the "soft" appearance or "velvety texture" of blue Kashmir sapphires. Other possible features are concentrations of rutile needles, platelets, and particles that are commonly referred to as "silk," which are typical of rubies and sapphires from Mogok, Myanmar (Burma). Such features, although commonly associated with a specific geographic source (e.g., Kashmir or Myanmar), more accurately distinguish a particular "type" of ruby or sapphire. Each corundum type shares other properties—including absorption spectra, chemical trends, and growth structures—which may be encountered in stones from more than one deposit or country.

What is proposed here is a classification for rubies and sapphires using a system that is objective, repeatable, teachable, and relevant. It does not attempt to pinpoint geographic locality or a specific deposit, but it does provide information that directly relates to a stone's appearance and position in the marketplace. The intent is to supply information to the trade that will be useful and consistent in representing their stones, which in turn should benefit the consumer as well.

Color Communication: The Analysis of Color in Gem Materials

Menahem Sevdermish (smenahem@gemewizard.com)

Advanced Quality A.C.C. Ltd., Ramat Gan, Israel

The tremendous growth of Internet-oriented activities, together with the progress made in digital imagery and high-definition computer screens, has prompted this author to explore possibilities in the digital assessment of the color of gems.

This presentation describes the creation of digital images of gemstones in color space, and the subsequent analysis of these images. A sampling, measuring, and recording system was developed to locate the precise position of these images in color space (see figure). This resulted in the incorporation in a database of over 15,000 colors, and over 150,000 images that are combinations of colors and various cutting shapes. Measurements of the color in each image were taken in 400–10,000 spots, each using a specially designed formula. The make-up of these spots can be thought of as the "DNA" of the color, and it is unique to each image.

The accumulated database of these predefined digital images can be used as a visual comparative tool to evaluate the color of actual gemstones. In addition, such a digital analysis and measuring system can be used to perform important tasks in gemological laboratories, research centers, and educational facilities where it is important to quantify gem colors. We are also exploring the possible adaptation of the system to the fashion industry by scanning the designed material and matching a gem color to it. At present, we are using the system to assess the correlation between the colors of colored stones and fancy-color diamonds. We are exploring the creation of an Internet-oriented trading platform based on the digital data of the system, and the possible application of the system as a testing tool for color blindness.

An automatic digital analysis of the color of a gem, which combines the system with a simple digital imaging tool that provides a constant illumination and viewing environment while capturing the gem image, is presently being beta tested. Three fundamental methods that can be used to calibrate a computer monitor—visual calibration, ICC profile-based calibration, and mechanical calibration—are also being evaluated as an important component of this system.

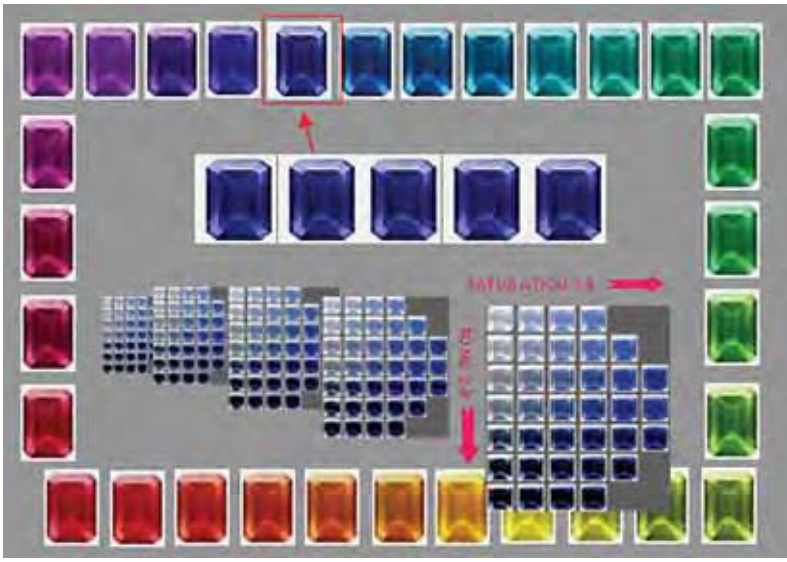

The main screen of this computerized system designed for color communication (Gemewizard software) displays 31 master hues. Tone/saturation grids were developed for each hue, as shown here for blue.

Sapphires from Ban Huai Sai, Laos

Sutas Singbamroong (sssutas@dm.gov.ae)[1], Abdalla Abdelqadir Yousif[1], and Theerapongs Thanasuthipitak[2]

[1]Dubai Gemstone Laboratory, Dubai, United Arab Emirates; [2]Department of Geological Sciences, Chiang Mai University, Chiang Mai, Thailand

Gem corundum from the Ban Huai Sai area, Bokeow Province, northwest Laos, has been mentioned only occasionally in the literature, and limited gemological and spectroscopic data have been published on samples from this area (Johnson and Koivula, 1996; Sutherland et al., 2002). This study presents a more complete characterization of this material.

To date, relatively small amounts of gem corundum have been produced at this locality by mechanized mining as well as primitive extraction methods. Estimates of total corundum production are unavailable. The material is recovered from alluvial deposits derived from basaltic rock. Most of the corundum is blue sapphire, with the crystals typically weighing less than 1 ct.

A total of 306 unheated and 68 heated, gem-quality corundum samples (blue, milky blue, green, and yellow) were obtained from three mining areas near Ban Huai Sai—Huai Ho, Huai Sala, and Huai Kok. These samples were studied using standard gemological and spectroscopic methods (Raman, UV-Vis-NIR, FTIR, EDXRF, and LA-ICP-MS) to identify the inclusions, characterize the spectra, analyze the chemical composition, and investigate the causes of color.

The physical, chemical, and spectral properties of the corundum samples from Ban Huai Sai were consistent with those of other basaltic corundums. They can easily be distinguished from sapphires of other origins on the basis of their absorption spectra and chemical composition, which are both influenced by the comparatively high Fe contents in the basaltic sapphires. Nevertheless, the sapphires investigated here can be separated from material from all other sources by a combination of: (1) the presence of monazite inclusions, which are the most common type of mineral inclusion after feldspar (see figure); (2) the characteristic absorption spectrum with distinctive Fe^{2+}-Ti^{4+} intervalence charge-transfer bands, which are in the range of 520–650 nm and seen in both unheated and heated samples; and (3) significant concentrations of Ti and Fe.

REFERENCES

Johnson M.L., Koivula J.I., Eds. (1996) Gem News: Sapphires and rubies from Laos. *Gems & Gemology*, Vol. 32, No. 1, p. 61.

Sutherland F.L., Bosshart G., Fanning C.M., Hoskin P.W.O., Coenraads R.R. (2002) Sapphire crystallization, age and origin, Ban Huai Sai, Laos: Age based on zircon inclusions. *Journal of Asian Earth Sciences*, Vol. 20, No. 7, pp. 841–849.

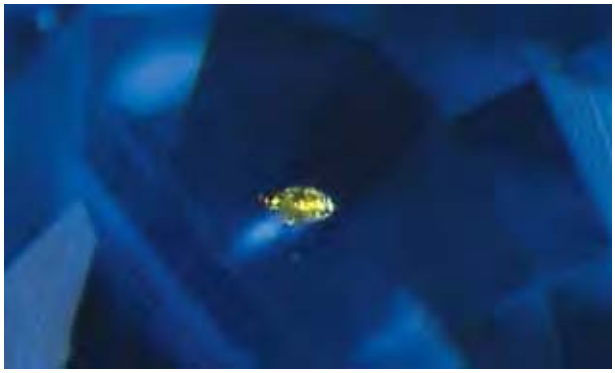

This unheated sapphire from the Ban Huai Sai area, Laos, contains a conspicuous inclusion of yellow monazite. Photomicrograph by S. Singbamroong, ©Dubai Gemstone Laboratory; magnified 25×, oblique illumination.

Fancy-Color Diamonds: Better Color Appearance by Optimizing Cut

Sergey Sivovolenko (serg@next.msu.ru)[1] and Yuri Shelementiev[2]
[1]OctoNus Software, Moscow, Russia; [2]Diamond Design, Moscow, Russia

Considerations for cutting fancy-color diamonds include yield, brightness, saturation, and color distribution. Here we present a system for selecting rough diamonds and determining the optimal shape and proportions during the cutting process.

The color coordinates of a diamond may be calculated based on the absorption coefficient at every wavelength. These coordinates for various thicknesses and hues can be plotted on a saturation vs. brightness diagram (see figure; note that hue can also change with thickness). According to our research, chroma and colorfulness values (Hunt, 2004) may be used to evaluate the potential of a particular rough diamond to achieve a certain color grade when faceted.

Because fancy-color grades depend in part on the path length of light through the cut stone, for every rough diamond with its particular size and spectrum there are restrictions on the possible shapes that can be used to obtain the fancy-color grade.

By using OctoNus ray-tracing software and a computer model of the scanned rough diamond, one can estimate the average light path of any cut from any piece of rough. The few best shapes are optimized based on the diameter, length-to-width ratio, and total depth that correspond to the optimal average light path data. During the optimization process, the cut proportions are varied and the light path length is calculated for every set of cut parameters.

Numerical metrics for dark zones, average saturation, and color distribution enable predictions of the cut stone's color grade. For such calculations, we consider a diamond as a mosaic of small differently colored areas and calculate their color coordinates. A color grade for each proportion set can be determined from a histogram containing information about the total area of each color weighted by its brightness. After the computer calculates color grades for various cut proportions, those with the best color can be determined.

For the best computer-predicted proportions, the color contrast and distribution are checked visually with photorealistic color images of the diamond in different lighting conditions. Using the software, the cutter can compare different faceting plans according to weight, proportions, and color, and will be able to decide which cut diamond has more value. While the proposed technology does not grade the color of a real diamond, both the optimization software and the cutter's expert

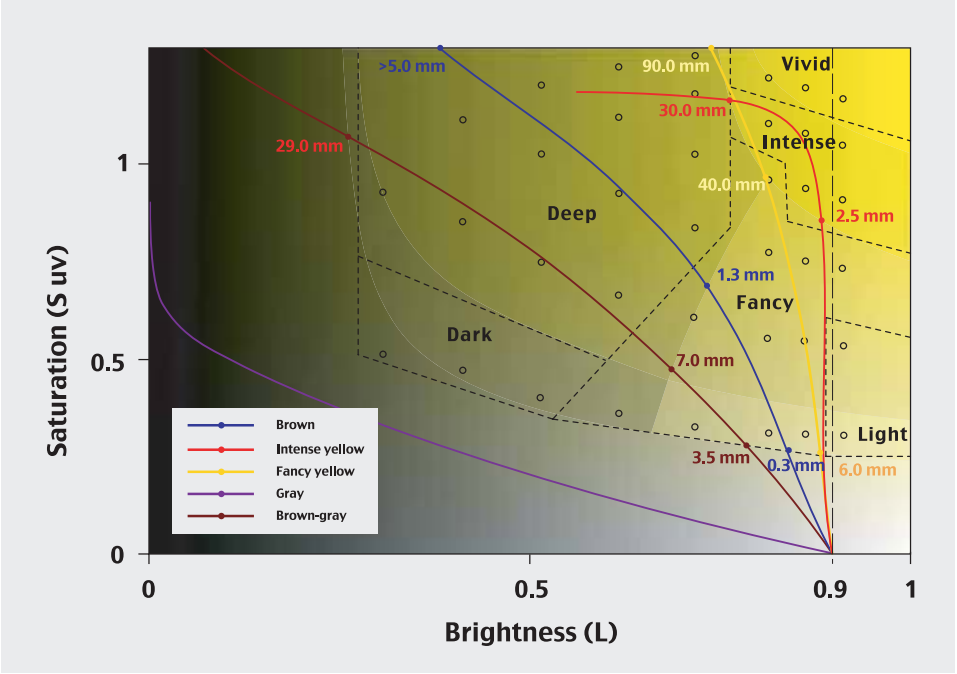

In this diagram, colors in the yellow hue range are plotted according to saturation (S uv) and brightness (L) coordinates. The colored lines show the influence of the stone's thickness on color appearance, according to various diamond colors in this hue range. The black circles are Munsell color coordinates (see, e.g., King et al., 1994).

judgment may enhance colored diamond appearance by increasing both color brightness and saturation while avoiding negative optical effects.

REFERENCES

Hunt R.W.G. (2004) *The Reproduction of Color*, 6th ed. John Wiley & Sons, New York, 702 pp.

King J.M., Moses T.M., Shigley J.E., Liu Y. (1994) Color grading of colored diamonds at the GIA Gem Trade Laboratory. *Gems & Gemology*, Vol. 30, No. 4, pp. 220–242.

European Freshwater Pearls: Origin, Distribution, and Characteristics

Elisabeth Strack (info@strack-gih.de)

Gemological Institute, Hamburg, Germany

European pearls from the freshwater mussel *Margaritifera margaritifera* have been known since Roman times. The mussel prefers rivers and streams in cool, mountainous areas. The shell's length can reach 16 cm. The maximum age is 130 years, and the reproduction cycle is highly specialized, as the glochidiae require a host fish (either trout or salmon) in their first year.

The distribution area stretches from northwestern Spain through France, Belgium, and Luxemburg to central Europe, with a connected area of Germany (Bavaria and Saxony), the Czech Republic, and Austria (Mühlviertel), apart from the northern German Lüneburg Heath (see figure). Western Europe has occurrences in Ireland, England, and mostly in Scotland. The mussel is also found in northern Europe, in Scandinavia and Russia.

The European pearl mussel is listed in the International Union for Conservation of Nature and Natural Resources' *Invertebrate Red Data Book* as "vulnerable," as populations have decreased by 80–90% during the last 100 years. (Fishing for them is now forbidden in all countries.) European freshwater pearls are therefore studied largely for historical interest. For example, the Grüne Gewölbe Museum in Dresden has a necklace with 177 Saxonian pearls.

Fourteen pearls (2.5–8 mm) were examined in detail for this study: two came from Scotland, three from Russia, and nine from Lüneburg Heath. The pearls were provided by a Scottish jeweler, a Russian biology station on the Kola Peninsula, and a family in Lüneburg Heath. The colors included whitish gray, violetish pink, and brown, and their luster was medium to low. They consisted of barrel and egg shapes, baroques, drops, and one "triplet." Their fluorescence to long- and short-wave UV radiation was inert to weak blue and red. Surface structures seen with the optical microscope (20×–40×) consisted of wavy lines and a nail-type pattern; on some pearls no structure was visible.

Computer tomograms revealed concentric growth structures and distinct cores of organic matter. X-radiographs showed no structures or irregular, linear deposits of organic material. Both methods can be used to prove that an inserted nucleus is not present. These European pearls showed a certain resemblance to Chinese and Japanese freshwater cultured pearls, mostly to those of pre-1990 production. A distinctive difference is that none of the 14 pearls examined showed fluorescence to X-rays, which is a characteristic feature of the Asian freshwater cultured pearls.

These European freshwater pearls (4.5–8.5 mm) are from Lüneburg Heath in Germany. Photo by Elisabeth Strack.

Developing Corundum Standards for LA-ICP-MS Trace-Element Analysis

Wuyi Wang (wwang@gia.edu)[1], Matthew Hall[1], Andy H. Shen[2], and Christopher M. Breeding[2]

[1]GIA Laboratory, New York; [2]GIA Laboratory, Carlsbad

The trace-element composition of ruby and sapphire is useful for detecting treatments and for assessing geographic origin. LA-ICP-MS is a powerful chemical analysis technique, but it is prone to problems created by matrix effects between standards and the tested samples. The signal intensity from a given element is determined not only by its concentration, but also by concentrations of coexisting elements, as well as by the structure of the sample. The most reliable method of standardization is to use reference materials with the same major-element composition and crystal structure as the sample being analyzed. For the LA-ICP-MS analysis of gem corundum, it is therefore preferable to develop element-in-corundum standards rather than using NIST glasses, which have very different compositions and structures than corundum.

Synthetic corundum crystals were grown using the Czochralski method with various trace-element dopants, including Mg, Ti, Cr, Fe, V, and Ga. Extensive LA-ICP-MS analysis showed that the relative standard deviations (RSDs) of the doped trace-element concentrations were less than 7% (except for Mg, ~11%). This is comparable to the compositional variations in NIST 612 glass that were measured by the same instrument.

It is technically difficult to grow corundum with a relatively high content of Fe (up to several thousand ppm) using the Czochralski method. Therefore, Fe-rich natural corundum was used instead. The distribution of Fe in many such samples was measured, and a few were shown to be very homogeneous, with an RSD of <5%.

To produce a beryllium-in-corundum standard, high-purity synthetic corundum disks (22.0 mm in diameter and 3.6 mm thick) were coated on both flat surfaces with a thin layer of

BeO in a binder and dried. The disks were heated to 1800°C in an oxygen atmosphere for 100 hours, and then ground on both sides to a depth of 0.3 mm and polished. Extensive LA-ICP-MS analysis showed that the RSD of Be concentrations was ~4% horizontally and ~8% vertically (with depth).

Absolute concentrations of the doped trace elements in the various standards were determined using SIMS analyses, which were calibrated using ion-implanted corundum standards (see table).

LA-ICP-MS analysis was performed on the trace element–doped corundum standards and NIST glasses using the same analytical conditions to evaluate the matrix effects. The NIST glasses were much more easily ablated by the laser, and they also generated significantly higher counts/ppm than the synthetic corundum. As a result, the LA-ICP-MS–measured concentrations of trace elements in corundum would be much lower than the true values when NIST glass standards are used for calibration.

Acknowledgments: The authors are grateful to Q. Chen, J. L. Emmett, S. W. Novak, and G. R. Rossman for helpful discussions.

Trace-element concentrations in corundum standards developed for LA-ICP-MS analysis.

Element	Concentration (ppm by weight)
Be	15.2 ± 0.5
Mg	15.1 ± 2.2
Ti	189 ± 4
V	243 ± 27
Cr	2928 ± 28
Fe	95.1 ± 5.6; 8540 ± 177
Ga	99.4 ± 3.0; 948 ± 43

Geology of Gem Deposits

Garnet Inclusions in Yogo Sapphires

Andrea Cade (acade@eos.ubc.ca) and Lee A. Groat

Department of Earth and Ocean Sciences, University of British Columbia, Vancouver, Canada

Yogo sapphires from central Montana are famous for their natural blue color. Although these stones have been mined intermittently for more than a century, little is understood about the deposit itself. The sapphires are found in an Eocene ultramafic lamprophyre dike on the eastern flank of the Little Belt Mountains. The dike is a member of the Central Montana Alkalic Province, a suite of alkalic rocks intruded from the Late Cretaceous to the Paleocene. The dike is traceable for more than 5 km and ranges in width from more than 7 m to less than 10 cm, pinching out in some places.

At the surface, the dike material weathers quickly and resembles the "yellow ground" of kimberlite. The sapphires are found as macrocrysts within the dike. Several hypotheses have been presented for the origin of the sapphires, including xenocrysts from the crust, crystallization during contact metamorphism of the base of the crust by the lamprophyric magma, crystallization from the magma, and xenocrysts from the mantle. The corroded exterior of the sapphires indicates that they were not in equilibrium with the magma at the time of emplacement, but this does not exclude the possibility that they crystallized from the melt. The purpose of the present research was to study the origin of the sapphires using the composition of mineral inclusions, particularly garnet, within the crystals.

Fourteen garnet inclusions from seven sapphire crystals were examined. The garnet crystals were subhedral to euhedral and pale reddish orange (see figure). Mg, Fe, Ca, Cr, Ti, and Na contents of garnets can be used to distinguish between different parageneses. An electron microprobe was used to collect this preliminary geochemical data. The garnet inclusions were Cr-poor (0.02 wt.%), low in TiO_2 (0.12 wt.%) and NaO (0.02 wt.%), and had values of 10.7, 14.0, and 11.2 wt.% for MgO, FeO_T, and CaO, on average, respectively. This indicates that the garnet inclusions were formed in the mantle in Group II eclogite (B), according to the classification of Schulze (2003), and that the sapphires are xenocrysts in the melt, also originating from the mantle. Although corundum in mantle eclogite is known, this is the only known economic deposit.

REFERENCE

Schulze D. (2003) A classification scheme for mantle-derived garnets in kimberlite: A tool for investigating the mantle and exploring for diamonds. *Lithos*, Vol. 71, No. 2/4, pp. 195–213.

These reddish orange inclusions in a Yogo sapphire are eclogitic garnets. Photomicrograph by A. Cade.

Geology and Mining of Southern Tanzanian Alluvial Gem Deposits

Jim Clanin (jclanin54@aol.com)
JC Mining Inc., Hebron, Maine

Alluvial gem deposits are found throughout southern Tanzania. They are distributed in the Ruvuma region, from Songea in the west to Tunduru in the east and on into the area around Ngurumihiga and Kitowelo in the Liwale region. The deposits are associated with the Kalahari Formation, and consist of unconsolidated eolian sandstone (up to 60 m thick) resting on top of a fluvial basal conglomerate (up to 4.5 m thick). The gems are hosted by the conglomerate, with bigger and better stones generally recovered from the thicker conglomerate layers with the coarser-sized clasts. Many gem varieties are found throughout the region. The most important gems are alexandrite, cat's-eye alexandrite, blue sapphire, ruby, and color-change garnet, spinel, and corundum. Diamonds are occasionally recovered.

Just east of the town of Tunduru lies the Muhuwesi River. There are two types of alluvial deposits along this river. To the north of the bridge on the Tunduru-Masasi road the gems are hosted by Kalahari conglomerates, and to the south of the bridge they are mined from reworked Kalahari sediments in bedrock channels. Gems from the latter area are generally smaller, but there is a greater variety.

In the Liwale region, Kitowelo is the name of a mining village situated along the Nambalapi River; the village is located about 125 km northeast of Tunduru. Here, the Kalahari Formation is also being exploited for alluvial gems. Locally, this formation is called the Mbemburu Sand Series and covers more than 1,300 km^2. There are three areas near Kitowelo where the conglomerate is extensive (e.g., up to 1.75 m thick with cobbles reaching 30 cm across) and such layers have produced gems of 10 g and larger.

In the Tunduru-Liwale region, 17 different gem minerals have been found along the rivers. Altogether, 46 varieties of those species have been described in the literature. There also appears to be a great deal of potential for more alluvial deposits throughout the region, particularly in areas that lie outside of the modern-day river valleys.

Geologic Origin of Opals Deduced from Geochemistry

Eloïse Gaillou (eloise.gaillou@cnrs-imn.fr)[1], Aurélien Delaunay[1], Emmanuel Fritsch[1], and Martine Bouhnik-le-Coz[2]
[1]Institut des Matériaux Jean Rouxel, Nantes, France; [2]Laboratoire de Géochimie, Rennes, France

Seventy-seven opals from 11 countries were characterized and then chemically analyzed by inductively coupled plasma–mass spectrometry (ICP-MS) in order to establish the nature of the impurities, correlate the mode of formation with the physical properties of the opals, and evaluate the use of geochemistry for establishing geographic origin.

The main impurities present were, in order of decreasing concentration, Al, Ca, Fe, K, Na, and Mg (more than 500 ppm). Other noticeable elements in lesser amounts were Ba, Zr, Sr, Rb, U, and Pb. For the first time, a distinction was found between various kinds of opal deposits according to their geochemistry. Compared to those from sedimentary deposits, volcanic opals were characterized by relative anomalies in Eu and Ce in their rare-earth element (REE) patterns. Opals from each volcanic deposit could be distinguished mostly according to their Ca content (or, if necessary, using Mg, Al, K, or Nb). For example, volcanic opals from Ethiopia could be separated by a high Ca content, the presence of Nb, and a positive Ce anomaly in their REE patterns. The opals could also be separated according to their Ba content; sedimentary opals had Ba concentrations higher than 110 ppm, while volcanic opals were generally poor in Ba (see figure). The restricted range of all element concentrations for play-of-color opals around the world indicates that they must have very specific conditions of formation compared to those of common opals.

An initial interpretation of the "crystallochemistry" of this amorphous material looked at the crystallographic site of certain impurities as well as their substitutions. The main replacement is the exchange of Si^{4+} by Al^{3+} and Fe^{3+}. This modification involves a charge imbalance neutralized by the presence of additional cations (mainly Ca^{2+}, Mg^{2+}, Mn^{2+}, Ba^{2+}, K^{+}, and Na^{+}). It was also shown for the first time that the chemistry of an opal influences its physical properties. For example, greater concentrations of iron correlated to darker colors (from yellow to "chocolate brown"). This element inhibits luminescence, too, whereas only trace amounts of U (1 ppm, sometimes less) induce a green luminescence.

Host rocks from Mexico and Brazil were analyzed to understand the conditions of opal genesis and the mobilization of elements during the weathering process. The geochemistry of an opal depends mostly on the host rock, although it may be modified by processes of dissolution during the weathering.

Diamond Occurrence and Evolution in the Mantle

Jeff Harris (j.harris@ges.gla.ac.uk)
Department of Geographical and Earth Sciences, University of Glasgow, United Kingdom

The types and chemical compositions of syngenetic minerals included in diamonds indicate that diamond formation within the earth extends over the depth range from 700 km (some 30 km below the upper/lower mantle boundary) to about 150 km. The presence of ferropericlase with Mg- and Ca-perovskite-structured silicates in the same diamond help define the lower-mantle origin. Diamonds from the transition zone (660 to 410 km) are identified by rare occurrences of spinel in orthorhombic olivine inclusions. Diamond formation, not only within the transition zone, but also in the asthenosphere and lithosphere (410 to 200–150 km), is identified by a systematic variation in the composition of a garnet inclusion called majorite. Trace-element patterns within the majorites indicate that the carbon forming these diamonds may have a

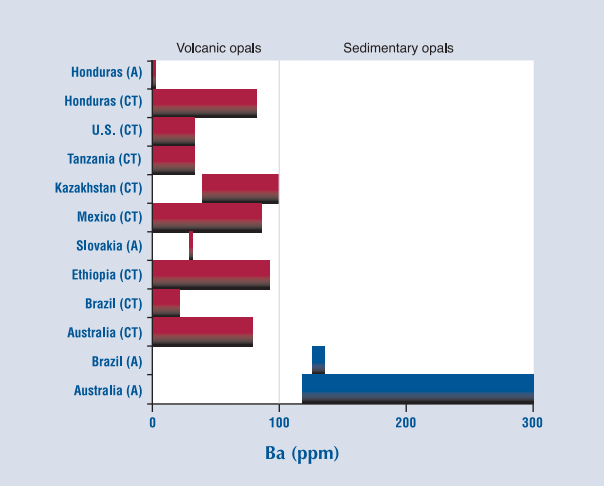

Opals from volcanic and sedimentary origins can be separated on the basis of their barium (Ba) concentrations, regardless of whether they are amorphous (opal-A) or poorly crystallized (opal-CT).

crustal component that is best explained by diamond formation in a subducting slab.

The above mineral assemblages are rare relative to those trapped in diamonds that form at the base of cratons at depths of 180–150 km. These inclusions identify two principal growth environments for diamond: peridotitic (olivine, orthopyroxene, Cr-pyrope garnet, chromite, and rare clinopyroxene, with Ni-Fe sulfides) and eclogitic (jadeitic clinopyroxene and pyrope-almandine garnet, with rutile, kyanite, and Ni-Fe sulfides). Study of these inclusions provides information on the temperature and pressure of diamond formation (950 to 1250°C, and generally between 5 and 6 GPa—the latter equivalent to 150 to 180 km depth), as well as the genesis ages of the diamonds (between 1 and 3.5 billion years old). The age of the earth is 4.5 billion years.

Studies of the carbon isotopes and the total nitrogen contents in the host diamond can be linked to the geochemical information obtained from the inclusions. For all lower-mantle diamonds, the carbon isotopic ratio ($\delta^{13}C$) is that of the mantle at −5‰ with nitrogen contents of zero (type II diamonds). For diamonds in the transition zone and asthenosphere, $\delta^{13}C$ ratios vary widely (−3.5‰ to −24‰), but again the diamonds are invariably type II. Peridotitic diamonds formed beneath cratons have a narrow $\delta^{13}C$ signature centered around −5‰ with nitrogen contents averaging 200 ppm. For eclogitic diamonds, there is also a major $\delta^{13}C$ peak at −5‰, but with tails to more depleted values of −30‰ and enrichments of up to +5‰. Nitrogen contents average 300 ppm.

Diamond genesis may occur either as a direct conversion from graphite, or through chemical reactions involving mantle carbonates or methane. Because of resorption and plastic deformation (the latter causing diamond to become brown), the shape and color of deep diamonds are not good. With shallower diamonds, there is a broader color range and resorption processes are more clearly defined, with octahedral diamonds changing to rounded dodecahedrons, for example. Such shape changes probably occur during kimberlite genesis and emplacement.

Geochemical Cycles of Gem-Forming Elements: What It Takes to Make Tourmaline, Beryl, Topaz, Spodumene, and other Pegmatitic Gems

David London (dlondon@ou.edu)
School of Geology and Geophysics, University of Oklahoma, Norman

Granitic pegmatites are the principal or sole sources of important colored gems that include varieties of beryl, tourmaline, spodumene, topaz, spessartine, and a few others. In addition to the common constituents of Si, Al, and O, each of these minerals contains an essential structural component (ESC) that is comparatively rare: Li in spodumene, Be in beryl, B in tourmaline, F in topaz, and Mn in spessartine. Therefore, the formation of these potential gem minerals is controlled largely by the geologic abundance of the rare ESC that each contains.

The average abundance of Li, Be, B, F, and Mn (see table) may be grouped according to four categories: (1) in the earth's crust; (2) in rhyolite obsidians that represent the unfractionated igneous precursors to granitic pegmatites; (3) a representative concentration of each ESC in granitic pegmatites that notably contain spodumene, beryl, tourmaline, topaz, or spessartine; and (4) the approximate concentration of each element needed to precipitate its characteristic mineral (i.e., reach saturation) in granitic melts at pressures of ~100–300 MPa and at magmatic temperatures of ~600–650°C.

Most gem-bearing pegmatites evolve from granitic melts, which originate by partial melting of sedimentary and igneous rocks in mountain belts at the margins of continents, and beneath rift zones within the continental interiors. The common rock-forming minerals that participate in melting reactions include quartz, feldspars, micas, amphiboles, clinopyroxene, cordierite, garnet, spinel, and perhaps olivine. If a rare ESC is compatible in one of these minerals (e.g., as is Be in cordierite), then that host mineral may sequester the ESC if the mineral does not participate in the melting reaction, or it may provide a source of the rare ESC if that host mineral is a major contributor to the formation of the granitic melt. For the rare elements Li, Be, F, and Mn, the micas—biotite and muscovite—are the most important minerals for determining the rare-element enrichment in the granitic melt at source. Micas and metamorphic tourmaline also contribute most of the B.

Two important observations emerge from the data in the table. First, the formation of minerals with rare ESCs requires an extraordinary degree of chemical refinement via crystal fractionation. In general, these rare minerals become saturated in pegmatite melts only after >95% of the original granitic melt has solidified. Though this evolutionary relationship from granite to pegmatite has long been assumed, it has not previously been demonstrated, and contradictory models have

persisted in the scientific arena. Second, the pegmatites do not always appear to contain sufficient ESCs to form these gem minerals at magmatic temperatures. There are several possible explanations for this conundrum, including the likely case that the ESCs of some gem minerals only become sufficiently concentrated to produce gem crystals after extended fractional crystallization of the pegmatite magmas themselves. As temperature falls, lower concentrations of rare ESCs are needed to crystallize the gem-forming minerals. Recent modeling suggests that pegmatite dikes—miarolitic gem pegmatites in particular—solidify ~200°C below the temperatures expected of granitic magmas. At these lower temperatures, near ~400–450°C, the "saturation" and "pegmatite" concentrations of the ESCs converge to similar values.

Elemental abundance of rare elements that form essential structural components in pegmatitic gem minerals (in ppm).

	Li	Be	B	F	Mn
Crust[1]	20	3	20	625	950
Obsidian[2]	57	4	30	900	700
Pegmatite	3000[3]	550[4]	1900[5]	6400[6]	1200[6]
Saturation	7000[3]	150[7]	6000[8]	30000[9]	10000[10]

[1] *Mason B., Moore C.B. (1982)* Principles of Geochemistry, *4th ed. John Wiley & Sons, New York, 344 pp.*

[2] *Macdonald R., Smith R.L., Thomas J.E. (1992)* Chemistry of the Subalkalic Silicic Obsidians. *U.S. Geological Survey Professional Paper 1523, 214 pp.*

[3] *Stewart D.B. (1978) Petrogenesis of lithium-rich pegmatites.* American Mineralogist, *Vol. 63, pp. 970–980.*

[4] *London D., Evensen J.M. (2003) Beryllium in silicic magmas and the origin of beryl-bearing pegmatites. In E.S. Grew, Ed.,* Beryllium: Mineralogy, Petrology, and Geochemistry, *Mineralogical Society of America Reviews in Mineralogy & Geochemistry, Vol. 50, pp. 445–486.*

[5] *London D., Morgan G.B. VI, Wolf M.B. (1996) Boron in granitic rocks and their contact aureoles. In E.S. Grew and L. Anovitz, Eds.,* Boron: Mineralogy, Petrology, and Geochemistry of Boron in the Earth's Crust, *Mineralogical Society of America Reviews in Mineralogy, Vol. 33, pp. 299–330.*

[6] *Černý P. (2005) The Tanco rare-element pegmatite deposit, Manitoba: Regional context, internal anatomy, and global comparisons. In R. Linnen and I. Sampson, Eds.,* Rare-element Geochemistry of Ore Deposits, *Geological Association of Canada Short Course Handbook 17, pp. 127–158.*

[7] *Evensen J.M., London D., Wendlandt R.F. (1999) Solubility and stability of beryl in granitic melts.* American Mineralogist, *Vol. 84, pp. 733–745.*

[8] *Wolf M.B., London D. (1997) Boron in granitic magmas: Stability of tourmaline in equilibrium with biotite and cordierite.* Contributions to Mineralogy and Petrology, *Vol. 130, pp. 12–30.*

[9] *London D., Morgan G.B. VI, Wolf M.B. (2001) Amblygonite-montebrasite solid solutions as monitors of fluorine in evolved granitic and pegmatitic melts.* American Mineralogist, *Vol. 86, pp. 225–233.*

[10] *London D., Evensen J.M., Fritz E., Icenhower J.P., Morgan G.B. VI, Wolf M.B. (2001) Enrichment and accommodation of manganese in granite-pegmatite systems.* 11th Annual Goldschmidt Conference, *Abstract 3369, Lunar Planetary Institute Contribution 1088, Lunar Planetary Institute, Houston, Texas (CD-ROM).*

The Miarolitic Stage in Granitic Pegmatites: How Mother Nature Makes Big, Clear Crystals

David London (dlondon@ou.edu)

School of Geology and Geophysics, University of Oklahoma, Norman

Gem material is rare for three reasons: (1) many gem-forming minerals are uncommon in nature, (2) the potential gem crystals need to be large enough for jewelry applications, and (3) the crystals must possess a high degree of transparency. One environment in which a variety of minerals achieve large, clear crystal perfection is clay-filled cavities or "pockets" within granitic pegmatites. These cavities, also termed miaroles, are the final portions of granitic pegmatites to solidify.

Industrial mineralogists can create large, clear single crystals of normally insoluble oxides and silicates by growth in high-temperature fluxed melts. These fluxes, which include H_2O, excess alkalis, B, P, and sometimes F, promote the growth of large, clear crystals in two ways. First, the fluxes decrease the viscosity of melts and, as a result, enhance diffusive mass transport of nutrients from the melt to the growing crystal surface. Second and more important, the fluxes interfere with the nucleation of crystals from the melt, such that when a crystal does nucleate, it can grow to a large size. When a flux-rich melt is in contact with silicate crystals, it can dissolve other silicate solids or liquids along the crystal surface, leaving the crystal inclusion-free, and hence transparent.

Nature appears to use the same process in the growth of gem crystals within miarolitic pegmatites. The pegmatite-forming process creates the necessary fluxes by concentrating alkalis, H_2O, B, P, and F in the melt along the boundary interfaces of growing crystals. While the crystal growth rate remains high, these fluxed boundary layers of melt can concentrate rare elements and dissolve solid phases. The transition from ordinary pegmatite to that enriched in rare elements and gem-quality crystals denotes a change in the medium of crystallization from the bulk pegmatite melt (which contains some flux but is typical of granitic compositions) to the fluxed boundary liquid itself. The fluxed medium may exist at low temperatures, and once the fluxes are removed by crystallization or lost to surrounding rocks, then the remainder of the silicate material solidifies into fine-grained aluminosilicate clays. Together with the flux-rich crystalline phases like tourmaline (enriched in B), topaz (F), montebrasite (P) and other rare minerals, the primary pocket clays may constitute the last remains of the original gel-like fluxed boundary medium. The excess, soluble components of the fluxes are lost to the surrounding rocks. Localized reactions between the pocket fluids and the pegmatite host rocks may be useful for the indirect discovery of gem-bearing cavities.

Some Open Questions on Diamond Morphology

Benjamin Rondeau (rondeau@mnhn.fr)[1] and Emmanuel Fritsch[2]

[1]Muséum National d'Histoire Naturelle, Paris, France; [2]Institut des Matériaux Jean Rouxel, Nantes, France

The geologic conditions of natural diamond formation can sometimes be inferred from diamond morphology. For

example, the observation of micromorphology helps establish the mode of growth that derives from the driving force (a combination of all parameters that affect crystal growth such as saturation, temperature, and pressure; see Sunagawa, 1981). Nonetheless, the geologic significance of the many diamond morphologies remains unclear. For example, a high hydrogen content is apparently needed for cuboid growth (Rondeau et al., 2004). However, the exact conditions triggering such growth are still a matter of speculation, as cuboid diamond has never been reproduced by synthesis. Fibrous diamond develops under very high driving force (very favorable growth conditions), much higher than layered, octahedral growth (Sunagawa, 1981). Coated diamonds, showing a fibrous overgrowth on an octahedron, are thought to have developed during kimberlite eruption (Boyd et al., 1994) when pressure diminishes dramatically (and hence, driving force increases) by the overgrowth of fibrous rims on preexisting octahedra. This model is contradictory to the general observation that diamond crystals are very often partially dissolved, as this dissolution is believed to occur in the kimberlite magma as the diamonds are transported to the surface. So, what are the geologic conditions in which fibrous growth may occur?

Moreover, a diamond showing a fibrous core embedded inside a layered, octahedral rim (see figure) may signify that slow octahedral growth can occur after a stage of rapid fibrous growth. Does this signal an abrupt change of growth conditions? And what kind of geologic event could cause such an abrupt transition?

Also, thermodynamic diagrams predict that, generally, the hopper morphology (with hollow, step-like faces and straight edges) develops under intermediate conditions of driving force, between the two above-mentioned growth modes. Nonetheless, hopper morphology has never been observed in natural diamond (even if the term *hopper* has been misused on occasion for skeletal cuboid or mixed-habit natural diamonds; see Koivula et al., 2004). There is no theoretical reason to believe that hopper growth is not possible in natural diamond, since it is observed in certain synthetic diamonds, but why is it not observed in nature? Does this mean that natural diamond grows under conditions for which fibrous growth immediately follows layered growth by increasing driving force?

To answer these questions requires future cooperation between various fields of science (thermodynamics, crystal growth, spectroscopy, petrology, geochemistry, etc.). Also, experimentation is needed to further support certain hypotheses on the formation of unusual diamonds.

REFERENCES

Boyd S.R., Pineau F., Javoy M. (1994) Modeling the growth of natural diamonds. *Chemical Geology*, Vol. 116, No. 1/2, pp. 29–42.

Koivula J.I., Tannous M., Breeding C.M. (2004) Luminescent "hopper" diamond. *Gems & Gemology*, Vol. 40, No. 4, p. 324.

Rondeau B., Fritsch E., Guiraud M., Chalain J.-P., Notari F. (2004) Three historical "asteriated" hydrogen-rich diamonds: Growth history and sector-dependent impurity incorporation. *Diamond & Related Materials*, Vol. 13, No. 9, pp. 1658–1673.

Sunagawa I. (1981) Characteristics of crystal growth in nature as seen from morphology of mineral crystals. *Bulletin de Minéralogie*, Vol. 104, pp. 81–87.

The Gel Model for the Formation of Gem-bearing Pockets within Granitic Pegmatites, and Implications for Gem Synthesis

Matthew C. Taylor (taylor@sci.muni.cz)

Institute of Geological Sciences, Masaryk University, Brno, Czech Republic

Previous theories describing the crystallization of gem "pockets" (cavities) within granitic pegmatites have focused on three origins: (1) supercritical aqueous solutions (water-rich fluids) exsolved from silicate melts; (2) water-rich melts that contain significant amounts of additional fluxes (e.g., boron, phosphorus, fluorine); and (3) dissolution or "solution" cavities that formed by the hydrothermal alteration of preexisting minerals (London, 2003). Evidence now suggests another possible origin for pegmatites and their associated gem pockets: crystallization from supercritical silicic gels (Taylor, 2005). Aqueous-phase and fluxed-melt techniques of crystal growth have been extensively exploited to create many kinds of facetable synthetics, but some gem varieties still elude researchers. Given the hypothesis described below for pegmatite pocket formation, basic growth

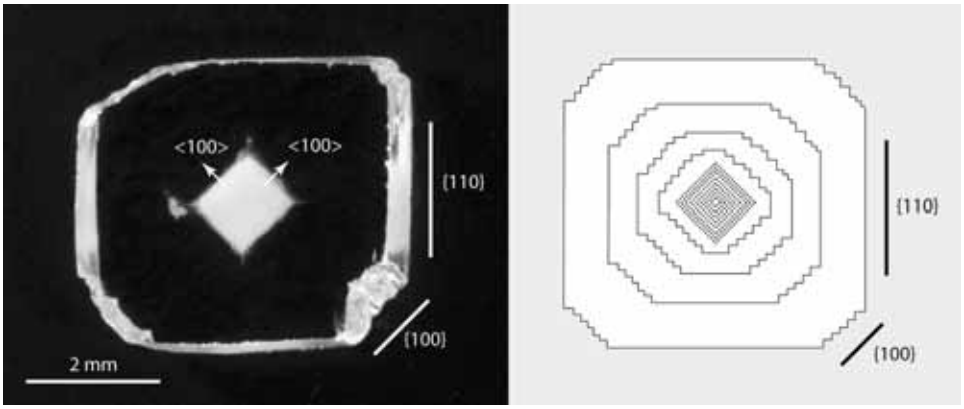

This unusual diamond (prepared as a 1-mm-thick plate) shows a fibrous core surrounded by an octahedral rim; photo by B. Rondeau. The schematic diagram shows the inferred growth layers and their crystallographic orientations.

procedures in subcritical gels (Henisch, 1970) might be adapted to supercritical gels that are dispersed after crystal growth and provide a future direction for gem synthesis, particularly for tourmaline.

The crystallization of granitic pegmatites is now thought to occur mostly below 400°C but in what are still considered magmatic conditions (Sirbescu and Nabelek, 2003). The transition from massive pegmatite into pockets typically starts with blocky crystals of K- and/or Na-feldspar, followed by gem minerals such as spodumene, tourmaline, and beryl (aquamarine), and accompanied by bladed albite ("cleavelandite"). Some gem minerals may also appear late, as shown by beryl (morganite) and topaz that grew on cleavelandite. All of these minerals, however, predate ubiquitous massive quartz as well as quartz crystals in pockets. Pegmatitic tourmaline may exhibit evidence of periodic precipitation (i.e., Liesegang rings) and oscillatory compositional zoning that are not found in a melt or aqueous liquid/vapor where convection can occur, but these features have been described in gels. These phenomena suggest that gem crystal growth in pegmatites is occurring at supercritical aqueous conditions within a dense silicic gel.

The gel model of pegmatite crystallization can be used to explain the formation of gem-bearing pockets through the release of fluids that accompany cooling and crystallization of silicic gels. When consolidating pegmatites cool through the critical temperature of their pore fluids (e.g., steam condensing to liquid water), depending on pore diameters, gels may order into crystalline solids (i.e., massive quartz) or disperse into colloidal solutions (sols). These sols then precipitate as quartz crystals within pockets, along with zeolites, clays, and/or opal below the critical temperature. The release and ultimate accumulation of fluids from silicic gels give rise to pockets in pegmatites and, at times, an abundance of loose gem crystals within the cavities.

REFERENCES

Henisch H.K. (1970) *Crystal Growth in Gels*. Pennsylvania State University Press, University Park, Pennsylvania.

London D. (2003) Gems and minerals from pegmatites—II. Miarolitic pegmatites. *Sooner Rockologist*, May, p. 9, www.geocities.com/oklahomamgs/London/Pegmatite2.

Sirbescu M.-L.C., Nabelek P.I. (2003) Crustal melts below 400°C. *Geology*, Vol. 31, No. 8, pp. 685–688.

Taylor M.C. (2005) The sol-gel nature of pegmatites. *Abstracts of the Elba 2005 International Meeting on Crystallization Processes in Granitic Pegmatites*, Elba, Italy, May 23–30, www.elba-pegmatites.org/Abstracts.doc.

The Sandawana Model of Emerald Formation

J. C. (Hanco) Zwaan (zwaanj@naturalis.nl)

National Museum of Natural History, Netherlands Gemmological Laboratory, Leiden

Sandawana emeralds formed at the contact between greenstones of the Mweza Greenstone Belt and rare-element granitic pegmatites, which were intruded during the main deformation event that occurred 2.6 billion years ago at the southern border of the Zimbabwe craton. Subsequently, a Na-rich fluid was injected along shear zones, causing albitization of the pegmatite and phlogopitization in the greenstone wall-rock. Coeval ductile deformation is indicated by boudinage and folding of pegmatites, by differentiated layering in associated amphibole-phlogopite schist, and by the presence of (micro) shear zones. The synkinematic growth of phlogopite, emerald, fluorapatite, holmquistite, and chromian ilmenorutile indicates enrichment of Na, K, Li, Be, F, P, Rb, Cs, Ta, and Nb in the emerald-bearing shear zone. This suggests that emerald formation is closely related to syntectonic K-Na metasomatism. In this process, microcline, oligoclase, quartz (from the pegmatite), and chlorite (from the greenstones) were consumed, in favor of albite (in the pegmatite), phlogopite, some new actinolite and cummingtonite, holmquistite, fluorapatite, and emerald (at the contact and in the greenstone). Mass balance calculations indicate that a Na- and F-rich hydrous fluid must be involved in these alterations that ultimately caused emerald formation. The presence of small, isolated, highly saline brine inclusions in emerald supports this calculation.

Apatite-phlogopite thermometry gives temperatures of 560–650°C, which is interpreted as the range for emerald formation. These temperatures imply contact metamorphic rather than regional metamorphic conditions. Because of the intimate spatial and temporal relationship with magmatic activity, the pegmatitic/hydrothermal nature of the involved fluid, and the near-magmatic temperatures of phlogopite and apatite formation, a magmatic source for the Na-rich fluids is very likely.

The Sandawana data lead to a new model of emerald formation: It is a product of contact metasomatism between ultramafic rocks and rare-element pegmatites during a deformation event involving late-stage magmatic/hydrothermal activity channeled by shearing. This model does not fit into genetic classification schemes proposed in the literature, and it demonstrates that no single theory can be applied to all schist-type emerald deposits. Gem-quality emeralds can be formed in very different geologic settings, as long as basic conditions are fulfilled: namely, the availability of beryllium and chromium (± vanadium); means of transport to bring the elements together (fluids of magmatic, hydrothermal, metamorphic, or combined origin); conditions in which emerald may form as a stable mineral (temperatures of 300–600°C); and sufficient space to grow transparent and well-formed crystals.

Laboratory Growth of Gem Materials

Growth of CVD Synthetic Diamond

James E. Butler (james.butler@nrl.navy.mil)

Gas/Surface Dynamics Section, Code 6174, Naval Research Laboratory, Washington, DC

Natural diamonds are like snowflakes or graduate students. No two are alike, and many can be gems! Chemical vapor deposition (CVD) of single-crystal synthetic diamond can now exceed the quality and purity of natural diamonds, and it has the technological advantage of reproducibility. For example, various groups have demonstrated growth rates exceeding 100 μm per hour, and produced single crystal plates with lateral dimensions exceeding 10 mm, a rod of over

10 ct, and various colors ranging from colorless ("D") to blue. CVD synthetic diamond will ultimately be most valuable in advancing technologies such as electrical power production and transmission, advanced optics, medical sensors, electronics, and communications, among others.

The technological exploitation of diamond is driven by the extreme and useful material properties of diamond, and it requires repeatability, control, and uniformity unavailable in natural diamonds. The main use (i.e., gem versus industrial) for CVD single-crystal synthetic diamond will depend on the market value of the ultimate device. Significant scientific and technological barriers exist to the growth of single-crystal CVD synthetic diamond. These include substrate quality, preparation, and availability; the CVD growth process; suppression of crystal twin formation; and gas purity and doping.

Growth, Morphology, and Perfection of Single Crystals: Basic Concepts in Discriminating Natural from Synthetic Gemstones

Ichiro Sunagawa (i.sunagawa@nifty.com)
Tachikawa, Tokyo, Japan

Natural gem crystals form under various growth conditions, and may undergo individual growth and post-growth processes that influence their crystal morphology and degree of perfection and homogeneity. In contrast, synthetic crystals are forced to grow within a limited time, with growth usually initiated on a seed, under different conditions from their natural counterparts. Their growth peculiarities are recorded, even in nearly perfect single crystals, through the various forms of imperfections and heterogeneities. These can be visualized even in eye-clean samples if the appropriate methods are applied.

In distinguishing natural from synthetic gemstones, gemologists need to understand how crystals grow, and how their morphology, perfection, and homogeneities are influenced by their growth conditions. Important considerations include:

- The nature of the growth technique employed and the phases involved (melt, solution, or vapor phases)
- The role of driving force for growth (mass transfer and heat transfer; polyhedral, hopper, and spherulitic morphology)
- The structure of the solid-liquid interface (rough and smooth interface, thermodynamic and kinetic roughening transition)
- The growth mechanism (adhesive type on rough interface, two-dimensional nucleation growth, or spiral growth mechanism on smooth interface)
- The origin of lattice defects (dislocations generated from the seed or substrate surface and forming inclusions, element partitioning related to kinetics)
- The methods in which the morphology of crystals and element partitioning are controlled (growth sectors, growth banding, kinetically controlled element partitioning)

These concepts can be used to demonstrate the importance of the science of crystal growth in gemology, as is evident in a comparison of the similarities and differences among natural, HPHT-grown, and CVD-grown synthetic diamonds.

New Gem Localities

Amethyst Mining in Zambia

Bjorn Anckar (bjorn.anckar@geologem.com)
European Union Mining Sector Diversification Programme, Lusaka, Zambia

One of the world's largest producers of amethyst is the Republic of Zambia in south-central Africa. Amethyst mining takes place in several parts of the country, but only three localities have any significance in the gem trade. The most important occurrence is the Mapatizya mining area in the Kalomo District of southern Zambia. Amethyst has been mined here since its discovery in the late 1950s. At present there are about 60 registered mining plots but only about 10 can be considered active producers. Currently, there is one large operator and a few moderate-scale operations. There are also a number of small-scale mining operations as well as an abundance of artisanal miners and illegal diggers. About 5,000 people have settled in the immediate area and depend on amethyst mining for their livelihood. The local climate is very arid, and agriculture is at the subsistence level or lower. The poverty of the area is striking.

Amethyst mining by the large- and moderate-scale operators is accomplished in open pits using bulldozers and excavators. Small-scale operators dig pits and tunnels using only picks and shovels. Processing is very labor intensive, and includes washing, sorting, cobbing, sawing, and final sizing/grading of large amounts of mined material.

Production in Zambia over the last decade averaged about 1,000 tonnes of amethyst annually. The vast majority of this production is low grade and mostly exported to China for carving and bead making. A small portion of the total production constitutes facet grade with a vivid purple "Siberian" hue. Faceted amethyst from Zambia ranges from melee to >50 ct. Heat treatment is not performed, as the material turns an unattractive grayish green. Frequent bush fires and intense sunlight in the area have turned all surface-exposed amethyst veins to this color.

Amethyst mines are also located in central Zambia, in Chief Kaindu's area north-northwest of Mumbwa. The area is most noted for its production of specimens of attractive amethyst druses; some are quite large and weigh several tonnes (see figure). The crystals are generally large, ranging from 2 to 13 cm. One locality, the Lombwa mine, produces material that shows patchy portions of distinct citrine and amethyst, but the two colors tend to blend and the material is difficult to cut into attractive pieces of ametrine.

A vast area with several amethyst mines is located along the border of Zambia and the Democratic Republic of Congo, between Solwezi and Mwinilunga in northwestern Zambia.

The material is often very clear but tends to be pale and is mainly exported to China for carving and bead making. Amethyst from this area responds well to heating, and a large portion of the production is treated to citrine. The Chafukuma mine is considered the producer of the best-quality amethyst in this area.

This large amethyst specimen, shown with Nyambe Nyambe of Jagoda Gems Ltd. in Lusaka, was mined from Chief Kaindu's area in central Zambia. Photo by B. Anckar.

Emerald Mineralization in Northwestern Ontario, Canada

Allison A. Brand (allisonbrand@hotmail.com)[1], Lee A. Groat[1], Mary I. Garland[2], and Robert Linnen[3]

[1]Department of Earth and Ocean Sciences, University of British Columbia, Vancouver, Canada; [2]London, Ontario, Canada; [3]Department of Earth Sciences, University of Waterloo, Ontario, Canada

The Taylor 2 (also known as Ghost Lake) emerald occurrence in northwestern Ontario is associated with a pegmatite of the Mavis Lake Pegmatite Group proximal to the 2,685 million-year-old Ghost Lake Batholith. The Taylor 2 pegmatite consists of three separate limbs that intrude a wide zone of chlorite schist near the eastern end of an altered ultramafic sill. Most of the beryl and emerald occurs in a "zone of mixing" between the southern and central limbs of the pegmatite. The rock in this zone consists of relict orange K-feldspar crystals (<30 cm) in a matrix of anhedral bluish plagioclase, quartz, fine-grained black phlogopite, blue apatite crystals (<1 cm), and black tourmaline crystals (<2 cm). The beryl occurs as euhedral crystals up to 2.3 × 1.8 cm; most are opaque to translucent and white to pale green in color; about 10% are emerald. Stones weighing up to 0.82 ct have been faceted, but most are not truly transparent. Electron-microprobe analyses of the emeralds showed an average Cr_2O_3 concentration of 0.27 wt.% (maximum 0.46 wt.% Cr_2O_3, or 0.04 Cr atoms per formula unit [apfu]), and a maximum V_2O_3 concentration of 0.05 wt.%. The FeO and MgO concentrations were relatively low, with maximum values of 0.54 and 0.70 wt.% (0.04 Fe and 0.10 Mg apfu), respectively. The saturation of the green color increased with substitution of Mg, Fe, Cr, and V for Al at the Y-site. The emeralds showed average Na_2O and Cs_2O contents of 0.81 and 0.13 wt.% (0.15 Na and 0.01 Cs apfu), respectively, but a white beryl from the central limb of the pegmatite contained 1.38 wt.% Na_2O and 1.10 wt.% Cs_2O.

Whole-rock compositions were obtained for eight different rock units in the detailed map area. Relative to Be crustal abundance (<5 ppm) and the normal range of granites (2–20 ppm), the compositions showed high concentrations of Be (89 ppm) in the Taylor 2 pegmatite and elevated Cr in the chlorite schist (2610 ppm) and the altered ultramafic sill (3050 ppm). Geochemical similarities support the hypothesis that the chlorite schist is the faulted analogue of the altered ultramafic sill. The absence of beryl in the latter unit may be due to lower amounts of fluid and/or F concentrations (~150 ppm versus ~1300 ppm for the chlorite schist).

The Taylor 2 emeralds most likely formed through metasomatism driven by granitic magmatism. However, the presence of a displaced wall zone, boudins in the pegmatite, and ductile deformation of both the pegmatite and wall zone suggest that some degree of shearing was involved. This occurrence is unique among Canadian emerald localities, as emerald occurs proximal to the intrusion, whereas at Lened in the Northwest Territories and Tsa da Glisza in the Yukon Territory, emerald occurs distal to the intrusion within quartz veins. Therefore, this study may provide new insights for emerald exploration.

Sapphires from New Zealand

Lore Kiefert (lkiefert@agta-gtc.org)[1], Michael S. Krzemnicki[2], Garry Du Toit[1], Riccardo Befi[1], and Karl Schmetzer[3]

[1]AGTA Gemological Testing Center, New York; [2]SSEF Swiss Gemmological Institute, Basel, Switzerland; [3]Petershausen, Germany

The authors recently examined gem corundum from an alluvial deposit on the South Island of New Zealand. The waterworn pebbles (see figure) were found close to Dunedin, during the reworking of an old gold mining area. Thirty samples were studied, ranging from approximately 3 to 8 mm. The 26 rough samples were transparent to translucent pink (18), transparent to translucent orange to orangy pink (5), and translucent blue (3), and the four polished stones were pink (2 faceted), violetish pink (star sapphire cabochon), and pinkish orange (cabochon). All of the stones were examined with a gemological microscope, and selected samples underwent EDXRF and LIBS chemical

analysis and UV-Vis and FTIR spectroscopy. In addition, quantitative electron-microprobe analysis was performed on five of the sapphires.

Using a combination of spectroscopic and chemical data, the sapphires could clearly be divided into two types: basaltic and metamorphic. The basaltic sapphires were semitransparent, with rutile inclusions. They showed intense blue coloration and lacked the bluish green appearance that is typical of other basaltic sapphires. UV-Vis spectra were typical of the basaltic type, with a strong Fe^{3+} component and no indication of Cr. Analysis of trace elements showed high Fe, Ti, and Ga concentrations, with no or low V and Cr.

The metamorphic sapphires were purplish pink to pink and orange, with UV-Vis spectra dominated by Cr^{3+}. The pinkish orange cabochon had spectroscopic features showing Cr^{3+} and an additional color center, similar to Sri Lankan "padparadscha" sapphires. The metamorphic sapphires had low Fe and Ga values and a higher Cr concentration than the basaltic type. The contents of Ti and V were in the same ranges as in the basaltic sapphires.

In addition to the chemical elements mentioned above, various amounts of the trace elements Na, Mg, K, Ca, Si, and Zr were observed when the sapphires were analyzed by LIBS and the electron microprobe.

The characteristics of the sapphires from New Zealand are in agreement with data from Australian corundum found in the Barrington Tops region (New South Wales) and sapphires from Pailin, Cambodia, as described by Sutherland et al. (1998). Both deposits also produce bimodal corundum suites with magmatic and metamorphic origins.

Sapphires from the Dunedin area of New Zealand show a wide range of colors. The blue sample is of basaltic origin, while the pink and orange stones are from a metamorphic source. From left to right, the polished samples weigh 0.88 ct, 4.02 ct, 0.65 ct, and 1.04 ct. Photo by Min Htut.

REFERENCE

Sutherland F.L., Schwarz D., Jobbins E.A., Coenraads R.R., Webb G. (1998) Distinctive gem corundum suites from discrete basalt fields: A comparative study of Barrington, Australia, and West Pailin, Cambodia gemfields. *Journal of Gemmology*, Vol. 26, No. 2, pp. 65–85.

A Fluid Inclusion Study of the Syenite-Hosted "True Blue" Aquamarine Occurrence, Yukon Territory, Canada

Robert L. Linnen (rlinnen@uwaterloo.ca)[1], David Turner[2], and Lee A. Groat[2]

[1]Department of Earth Sciences, University of Waterloo, Ontario, Canada; [2]Department of Earth and Ocean Sciences, University of British Columbia, Vancouver, Canada

Dark blue, gem-quality beryl (also called "True Blue" aquamarine) occurs at a unique locality in the Pelly Mountains in south-central Yukon Territory. The semitransparent-to-translucent aquamarine crystals are contained in tension-gash, crack-seal quartz veins, commonly with siderite/ankerite, fluorite, and allanite as accessory minerals. The veins are hosted by a Be- and REE-rich Mississippian syenite, near the contacts with coeval metavolcanic rocks. The veins also contain fragments of metamorphosed wallrock that are interpreted to be associated with a Jurassic thrusting event.

Fluid inclusions have been observed in several vein minerals (beryl, quartz, fluorite, and carbonate), although most of the microthermometric data in this study are from beryl. Type 1 inclusions are composed of aqueous liquid-vapor phases and are predominantly secondary, with a smaller population of isolated inclusions that are probably primary. Type 2 are liquid-only aqueous inclusions that are either secondary or originated by necking-down. Type 3 are rare, vapor-rich carbonic inclusions that have a poorly constrained origin. Type 4 are liquid-liquid-vapor (aqueous-carbonic) inclusions and have a similar distribution as type 1 inclusions. Types 1 and 4 form a fluid inclusion assemblage that is synchronous with beryl mineralization, but because the crack-seal veins underwent multiple stages of opening, both primary and secondary inclusions were trapped.

The salinities of type 1 inclusions range from ~6 to 24 wt.% $NaCl_{eq}$; they homogenize to a liquid at 139–238°C, and there is an inverse correlation between salinity and homogenization temperature. The initial melting temperature decreases with increasing salinity, to a minimum of −32°C, which suggests the presence of divalent cations such as Ca^{2+} and Fe^{2+}. The Fe content is particularly important since this element is the most likely chromophore in these aquamarines. Type 4 inclusions range in composition from ~5 to 16 wt.% $NaCl_{eq}$, and homogenize to a liquid at 271–338°C. The presence of variable amounts of CO_2 in type 1 inclusions and variable salinity in type 4 inclusions suggests that they have recorded three-component fluid mixing. Based on the geologic setting of an apparent relationship with Jurassic tectonism and the compositions and temperatures of the fluid inclusions, the aquamarine most likely originated through the remobilization of Be and Fe from the syenite by metamorphic fluids. This is quite unlike the origin of typical gem-quality aquamarine, which forms in granitic pegmatites.

Chromium Chalcedony from Turkey and Its Possible Archeological Connections

Cigdem Lule-Whipp (cigdem@gialondon.co.uk)
GIA London, United Kingdom

The ancient Romans used green chalcedony as a seal stone and in jewelry, but the source of the material has remained a mystery. Pliny the Elder (1st century AD) mentioned that it came from India; however, no green chalcedony has been found there during modern times. Several researchers have suggested that the Roman chalcedony more likely originated from chromium mines in Anatolia. In this study, four rough green chalcedony samples from Turkey were characterized and compared to similar Roman seals from various antique collections. The samples came from the only known source of Turkish green chalcedony: Saricakaya, Eskisehir, in Central Anatolia.

The Turkish chalcedony was translucent to opaque, medium dark bluish green, and generally uniform in color. Diaphaneity was variable within the samples, but chromite inclusions were evenly distributed. Polished areas displayed vitreous luster, but the broken edges of rough material appeared waxy due to the granular structure. Drusy quartz was observed as a secondary filling in the fissures and cracks. The R.I. values were between 1.53 and 1.54, and the S.G. (obtained hydrostatically) was 2.58. The polariscope showed a typical aggregate reaction. The absorption spectrum showed chromium emission lines in the red region, indicating that this element was the cause of the green color. The more translucent material appeared red when viewed with a Chelsea filter and transmitted light. The physical and optical properties of the Anatolian material are within the range of other varieties of chalcedony.

The Anatolian samples were analyzed by whole-rock inductively coupled plasma (ICP) and SEM-EDS. The high Cr content and the presence of euhedral chromite inclusions indicated that this material was not chrysoprase. The SEM analyses also showed areas containing thorium. Geologic relationships and the high Cr content suggest that the Anatolian chalcedony formed via the silicification of serpentinite.

Chromium chalcedony from other localities has been studied by other researchers. The first occurrence was discovered in Zimbabwe in 1953, and the variety was named "mtorolite" (Smith, 1967). Another source was discovered more recently in Western Australia (Krosch, 1990; Willing and Stocklmayer, 2003). Other chromium-bearing chalcedonies have been reported from sources such as Bolivia, the Balkans, and the Ural Mountains (Hyršl, 1999).

Chromium chalcedony from Anatolia and the Roman seals from various collections were compared by means of microscopy and SEM analyses. These chalcedonies showed no differences in color, Chelsea filter reaction in transmitted light, contents of Cr and Ni, or the amount and distribution of chromite inclusions in the matrix. In contrast, the significant layering of black inclusions that is characteristic of "mtorolite" was not present in the Roman seals.

References
Hyršl J. (1999) Chrome chalcedony—a review. *Journal of Gemmology*, Vol. 26, No. 6, pp. 364–370.

Krosch N.J. (1990) Queensland chrysoprase. *Australian Gemmologist*, Vol. 17, No. 8, pp. 303–306.

Smith C.C. (1967) A preliminary account of Rhodesia's new gemstone—chrome chalcedony. *Chamber of Mines Journal*, December, pp. 31–34.

Willing M.J., Stocklmayer S.M. (2003) A new chrome chalcedony occurrence from Western Australia. *Journal of Gemmology*, Vol. 28, No. 5, pp. 265–279.

India—Old Sources and New Finds

H. M. Sultan Mohideen (jeweljem@vsnl.com)
Madras Gem Institute, Alwarpet, Chennai, India

Since ancient times, India has been a major source of gems, most significantly diamonds. Famous diamonds such as the Koh-i-noor and the Darya-e-noor were found in central India in the state of Andra Pradesh. However, with subsequent diamond finds in other locations such as Brazil and Africa, the importance of India as a source of gems diminished.

For more than a century, Jaipur has been a center of gem cutting, where most of the gem rough (mainly emerald) imported from Brazil and Africa was processed. Today, Jaipur is a large cutting center for almost all varieties of gems. But with countries like Brazil developing their own cutting and polishing industries, and with competition from other processing centers such as China and Thailand which have skilled and inexpensive work forces, the Indian gem industry has been striving to find its own local sources of rough. This has led to a sudden interest in exploring and exploiting old mining areas and new localities.

The state of Tamil Nadu, near Sri Lanka, produces high-quality aquamarine, moonstone (in all colors), iolite, star ruby, and many other lesser-known gems such as kornerupine, diopside, enstatite, sphene, bytownite, and all known quartz varieties. Karnataka and Andra Pradesh States produce many ornamental stones such as green aventurine, jasper, and chalcedony, and fine gems such as star ruby. In the past decade, large finds of cat's-eye chrysoberyl and alexandrite were discovered. The state of Orissa has diamonds as well as nearly all gem garnet varieties (except green colors), chrysoberyls, beryl (green, yellow, and blue), fluorite, apatite, cat's-eye sillimanite, moonstones, and ruby. The state of Bihar produces very high quality blue moonstone, rose quartz, and garnet (hessonite).

The oldest kimberlite pipes in India are located in the districts of Panna in Madhya Pradesh, Raipur in Chhattisgarh, and Vajrakarūr and Golconda in Andhra Pradesh. Recently many new kimberlite pipes have been located in these areas by the Geological Survey of India.

There is a renewed interest by the government of Kashmir in exploring the old mines and surrounding areas for the famous blue sapphires. New finds of gem-quality colored tourmaline are reported from this area.

Today, with the exception of organized diamond mining at Panna by the state-owned National Mineral Development Corp., all other gems are mined illegally. This is due to strict

environmental laws and no pragmatic gem mining policy. Most Indian gems find their way into the gem markets of Sri Lanka, Thailand, and Hong Kong.

New Gem Localities in Madagascar

Federico Pezzotta (federico.pezzotta@comune.milano.it)
Natural History Museum, Milan, Italy

Madagascar is host to an abundance and variety of gem materials as a result of its long and complex geologic history. The upper Archean to Neoproterozoic crystalline basement of Madagascar experienced locally unusual and even unique geologic conditions during several mountain-building events. Erosion of these rocks occurred during the late to post-tectonic uplift of the basement, and deposited Permian-Mesozoic sediments along the western margin of the Mozambique basin, locally forming immense paleoplacer deposits (e.g., at Ilakaka). More recently, the morphologic and climatic conditions of the island during the past few million years resulted in the formation of abundant secondary residual and alluvial gem deposits.

Even though research and mining of Madagascar's gems has continued for more than a century, many large areas in the island remain poorly explored and have significant potential for the discovery of new deposits. Within the last few years, the country's improved political situation has allowed for important developments in the scientific research, mining, and trading of gems.

Recently, two major gem discoveries occurred in Madagascar, both in Fianarantsoa Province: (1) a series of multicolored tourmaline deposits, of both primary and residual nature, in a large area between the villages of Ambatofitorahana and Ambohimasoa, along the national road connecting the towns of Ambositra and Fianarantsoa; and (2) a multicolored sapphire deposit of residual nature located 17 km south of the village of Ranotsara, southeast of the town of Ihosy.

The tourmaline deposits are related to a large rare-element miarolitic pegmatite field, surprisingly rather undocumented in the available geologic maps, that extends in a northeast-southwest direction for a distance of ~40 km. Initial discoveries of tourmaline in the area were made in 1995–1996 with the mining of the primary and secondary residual deposits of Valozoro, a few kilometers southeast of Ambatofitorahana. No additional significant discoveries were made until August-September 2005 when, in the Anjoma area (located a few kilometers southwest of Ambatofitorahana), an enormous quantity of multicolored tourmaline (weighing several tonnes, but mainly of carving quality) was found close to the surface at Anjomanandihizana (also known as Nandihizana). Soon afterward, additional multicolored tourmaline deposits were discovered south of this area; the most important ones are Fiadanana (a few kilometers south of Valozoro), Ankitsikitsika (about 15 km south of Anjomanandihizana), and Antsengy (northwest of the village of Ambohimahasoa). Local gem dealers refer to this entire area as Camp Robin, from the name of a village in the center of the district in which much of the gem trading occurs.

The new sapphire deposit, named Marosely, was discovered in October 2005. Transparent bipyramidal sapphire crystals, with colors ranging from blue to purple and, rarely, purplish red (ruby), have been recovered mainly in small sizes (less than 0.4 g). Larger crystals of gem quality are rare, but occasionally they exceed 2 g and produce good-size cut stones (see figure). These crystals originated from the high-grade metamorphic bedrock, and were concentrated in near-surface residual deposits through erosion. The total production of sapphire rough from Marosely, through June 2006, is estimated at about 500 kg.

Afghanistan Gem Deposits: Studying Newly Reopened Classics and Looking for New Deposits

Lawrence W. Snee (lsnee@usgs.gov)
Global Gems and Geology and U.S. Geological Survey (retired), Denver, Colorado

As we refine our understanding of the geologic framework of gem deposits, and as we apply new technology to exploration, we improve our chances of finding new deposits—both in new areas and in newly reopened areas. Currently the U.S. Geological Survey (USGS) is assisting with the Afghanistan reconstruction effort. Our involvement includes geologic mapping, mineral resource assessment, airborne geophysics (gravity and magnetics), aerial photography (orthophoto and synthetic aperture radar), and airborne hyperspectral imaging. All data are being analyzed and published in collaboration with the Afghan Geological Survey.

The Afghan government is particularly interested in the careful study and reassessment of their gem deposits. Despite less-than-perfect logistics, between 2004 and early 2006, this author visited the Panjsher emerald mines (see figure), the Jegdalek ruby deposits, and the lapis mines of Badakhshan, as well as other mineral resource areas that contain gold, copper, chromium, and iron. The USGS intends to continue visiting promising areas to examine and document the mines, to collect samples for laboratory analysis, and to conduct limited on-ground geologic mapping. Laboratory studies of the samples are ongoing and include petrographic, geochemical, geochronologic, X-ray diffraction, fluid inclusion, and hyperspectral measurements. Various sources of satellite imagery, as well as the new airborne data, are being used to define the geologic framework and extent of the gem deposits. We are also translating and evaluating existing geologic maps and literature; much of this literature is in Russian and of limited availability, but several dedicated Afghan geologists were able to save copies during the many years of war. Collaboration with other colleagues and governments in south-central Asia will increase our understanding of the regional extent and potential for similar deposits throughout the region.

As Afghanistan regains political stability, additional opportunities will open for exploitation of known gem deposits, and new ones will undoubtedly be found. The Afghans believe that

These sapphires are from a new deposit known as Marosely, located southeast of Ihosy in south-central Madagascar. The largest stone weighs 2.2 ct, and the color of both stones is natural. Photo by Bruno Drera.

of all their mineral resources, the gem deposits have the greatest potential to be easily and quickly developed. However, mining methods and mine safety must be improved to ensure the adequate development of these resources. The Afghan government, USAID, the World Bank, and the Asian Development Bank are currently in the process of contracting experts to help the local Afghan miners develop safe and profitable gem mining in Afghanistan.

The New Komsomolskaya Mine in Yakutia, Russia: Unique Features of its Diamonds

Nikolai V. Sobolev (sobolev@uiggm.nsc.ru)

Institute of Geology and Mineralogy, Siberian Branch of the Russian Academy of Sciences, Novosibirsk, Russia

The Komsomolskaya diamond mine is located in the Daldyn-Alakit diamondiferous kimberlite field in the Sakha region of western Yakutia, Siberia. Its position is 15 km northeast of the Aikhal diamond mine. Its age (358 million years) is within the range of all productive Yakutian diamond mines (344–362 million years). As with other Yakutian diamond mines, Komsomolskaya produces a high proportion of perfect diamond octahedra. Some of these diamonds contain mineral inclusions that are dominated by chromite (about 60%), which is typical of the peridotitic suite of inclusions found in diamonds of the same size fraction from other Yakutian diamond deposits. However, there are several features of the Komsomolskaya diamonds that are unique to this deposit. These include a higher proportion of whole crystals compared to other Yakutian mines, which results in a higher than average price-per-carat of the diamond production. Additionally, there is a much higher proportion (more than 10 times) of diamonds containing eclogitic inclusions as compared to other Yakutian mines. Evidence for a much deeper source of some of the diamonds is provided by the discovery of an inclusion within a microdiamond that consisted of a majoritic garnet containing a pyroxene solid solution. This mine is also unique for containing the highest proportion (on a worldwide basis) of diamond inclusions of extremely Cr-rich pyrope. Therefore, compared to all the well-known Yakutian diamond mines, Komsomolskaya shows a number of unique features.

In-situ Corundum Localities in Sri Lanka: New Occurrences

Saman Tennakoon[1], Mahinda Rupasinghe (mrmahinda@yahoo.com)[1], and Chandra B. Dissanayake[2]

[1]Sabaragamuwa University of Sri Lanka, Buttala; [2]Department of Geology, University of Peradeniya, Sri Lanka

Sri Lanka is famous for fine gemstones, particularly corundum. Most are obtained from alluvial gem gravels that occur as lenses and bands in the riverbeds and stream valleys of Sabaragamuwa Province, particularly in the Ratnapura district. Precambrian metamorphic rocks underlie 90% of the island and are divided into four major lithologic divisions—the Highland, Vijayan, Wanni, and Kadugannawa Complexes. Most of the major gem fields in Sri Lanka

Geologist Abdul Wasay of the Afghan Geological Survey shows the structural attitude of the emerald-bearing zone of one of the many Panjsher emerald mines at Khenj, Afghanistan. Photo by L. W. Snee.

A series of in-situ corundum occurrences have been found in the region around the towns of Wellawaya and Buttala, which are 11 km apart in southeastern Sri Lanka. Geologically, this area lies near the boundary between the Highland and Vijayan Complexes.

lie in the Highland Complex. High-grade Precambrian metamorphic rocks of granulite-facies conditions are characteristic of these gem-bearing source rocks. Although there have been isolated examples of in-situ gem discoveries in Sri Lanka over the past 100 years, the origin of these deposits has not been thoroughly studied.

In 2004, the authors discovered five corundum deposits in the region around the towns of Wellawaga and Buttala, near the boundary between the Highland and Vijayan Complexes in southeastern Sri Lanka (see figure). The first new deposit was located in Gampanguwa, where well-formed, hexagonal, translucent pale blue and gray corundum crystals were found on a mountain top. The crystals varied from 1 to 15 cm (most were 5 cm), and they were hosted by partially weathered rock that was easily breakable. The quantity of corundum at this deposit is unknown.

The second deposit was discovered on a mountain top in Bubulagama, which lies 3 km from the Gampanguwa deposit. Bluish and pinkish corundum crystals were found in the partly weathered source rock. Although these crystals (1 to 3 cm long) were of low gem quality, the deposit contained a greater amount of corundum than at Gampanguwa. Generally the corundum crystals were accompanied by biotite, sillimanite, perthitic potassium feldspar, plagioclase, and accessory spinel.

The other corundum deposits were found in the villages of Galbokka, Makaldeniya, and Gampaha, which are close to the other two deposits. Landslides had occurred earlier in these regions, and gem-quality pale blue corundum and milky-colored "geuda" were found in the overburden.

The Kirindioya River, which flows through this area, contains alluvial deposits with a variety of gem minerals, such as corundum, spinel, garnet, zircon, and tourmaline. The in-situ occurrences mentioned above may be the source of alluvial corundum in this region. Geologically, an important feature of these five corundum localities is that they lie along the boundary between the Highland and Vijayan Complexes.

ABSTRACTS OF POSTER SESSIONS: A MARKETPLACE OF NEW IDEAS

This section contains abstracts of poster presentations that were given at the **Gemological Research Conference** and the **International Gemological Symposium.** The GRC poster abstracts were reviewed by the GRC Committee (see p. 80), and the Symposium posters were reviewed by the Symposium Poster Session Committee:

Shane Elen	GIA Research, Carlsbad
Sheryl Elen	Richard T. Liddicoat Library and Information Center, GIA, Carlsbad
Al Gilbertson	GIA Research, Carlsbad
Caroline Nelms	Richard T. Liddicoat Library and Information Center, GIA, Carlsbad
Thomas W. Overton	*Gems & Gemology,* GIA, Carlsbad
Robert Weldon	Richard T. Liddicoat Library and Information Center, GIA, Carlsbad

All of the poster presenters and committee members are thanked for making the poster session, which was kindly sponsored by Swarovski, such an important and informative part of the GRC and Symposium.

Dona M. Dirlam
Chair of Poster Session Committee

GEMOLOGICAL RESEARCH CONFERENCE

4TH INTERNATIONAL GEMOLOGICAL SYMPOSIUM

POSTER SESSION ABSTRACTS

Gemological Research Conference 2006

August 26–27

Diamond Treatments

High-Pressure, High-Temperature (HPHT) Diamond Processing: What Is this Technology and How Does It Affect Color?

Sonny Pope (spope@sundancediamonds.com)
Sundance Diamonds, Orem, Utah

HPHT processing of gem diamond is actually a simple process to understand. If a diamond is heated to above 750°C in air, it will start to burn. However, if the diamond is under extreme pressure (i.e., similar to natural diamond formation), then even temperatures up to 2000°C will not cause significant degradation. These extreme annealing temperatures create the conditions for diamond to change color.

While the concept is easily understood, many do not fully appreciate the investment and maintenance demanded by this technology. Sundance Diamonds uses a propriety press that was developed for HPHT processing that costs close to $1 million. Providing the extreme conditions necessary for this process creates the need for continual maintenance with costly materials. Sundance Diamonds could not survive without its parent company and their team of scientists and engineers to support and maintain the equipment. Even with continual investment to reduce the risks and optimize the outcome, HPHT treatment remains a volatile process with the possibility of fracture and complete loss of the diamond being treated.

Traditionally, the HPHT process has been used to reduce brown hues in type IIa diamonds to appear colorless or near colorless. Now, through years of research, almost any brown diamond can benefit from HPHT technology. Nitrogen, a common diamond impurity, can be manipulated at high temperatures to yield colors that are rare in nature. Green and intense yellow were the first colors to show promise; with irradiation, pink and purple stones are now possible. With ongoing research we hope to be able to present a whole rainbow of reproducible colors. All of these niche colors offer the potential for additional usability and profit from brown diamonds.

Natural Diamond Enhancement: The Transformation of Intrinsic and Impurity Defects in the Diamond Lattice

Victor G. Vins (evins@academ.org)[1], Alexander P. Yeliseyev[2], Sergei V. Chigrin[1], and Alex G. Grizenko[3]

[1]New Diamonds of Siberia Ltd., Novosibirsk, Russia; [2]Institute of Mineralogy and Petrography, Siberian Branch of the Russian Academy of Science, Novosibirsk; [3]Lucent Diamonds Inc., Lakewood, Colorado

Changes in diamond crystal structure that occur during high-pressure, high-temperature (HPHT) treatment are discussed in this report. About 1,200 type Ia and about 10 type IIa diamonds with varying degrees of brown color associated with plastic deformation were investigated in this study. Two types of changes took place during HPHT treatment at temperatures ranging from 1800 to 2300°C: (1) decrease in plastic deformation, and (2) thermally activated aggregation and dissociation of nitrogen-related defects.

A decrease in plastic deformation occurred at all temperatures of the HPHT treatment and was accompanied by a reduction of dislocation density of at least 1,000 times and, therefore, an almost complete decoloration of the type IIa diamonds. Dislocation movement within the crystal lattice started at temperatures exceeding 1800°C, and this caused the formation of vacancies and interstitials; their concentrations were always higher in diamonds exhibiting greater dislocation density.

In the type Ia diamonds, vacancies were trapped at the main nitrogen aggregates (A and B), which led to the formation of H3 and H4 color centers, respectively. Under HPHT conditions H4 centers were not stable. They dissociated following the model: H4 → H3 + H3. As a result, a large number of H3 centers formed in the diamond lattice, causing an attractive yellow-green color. At temperatures ranging from 2000 to 2100°C, dislocations in the type Ia diamonds destroyed B defects as they moved through the lattice and created simpler nitrogen-related defects, such as N3 and C centers. Absorption spectra of the treated diamonds revealed increased absorption due to N3 centers and a new absorption at wavelengths below 550 nm due to C centers. The formation

of C centers, which are electron donors, was accompanied by a change of the charge state for some H3 centers, leading to the formation of H2 centers ($H3 + e^- \rightarrow H2$). The absorption due to the H2 centers caused an intense green color in the type Ia diamonds.

Thermally activated changes in type Ia diamonds began at temperatures exceeding 2150°C, with A centers dissociating to form two C centers. The formation of additional C centers caused an increase in the concentration of H2 centers to the detriment of H3 centers, which made the type Ia diamonds greener. At temperatures exceeding 2200°C, in addition to the dissociation of A to C centers, there was also aggregation of A defects into B defects. In some samples, an increase in intensity was recorded from B^- carbon aggregates (platelets).

Knowing the above-mentioned regularities, and diamond characteristics such as the nitrogen content in A and B forms and the degree of plastic deformation (based on the saturation of brown color), we can choose HPHT treatment conditions to produce more desirable diamond colors.

Gem Characterization Techniques

The Gemstones of the Shrine of the Three Magi (ca. 1200 AD) in Cologne Cathedral, Germany

Manfred Burianek (manfred.burianek@uni-koeln.de)
Institute of Crystallography, University of Cologne, Germany

Unique medieval works of art like the Shrine of the Three Magi (see figure) are maintained in their religious context and are almost inaccessible for scientific examination. Fortunately, as part of an all-embracing scientific documentation of this famous reliquary, the Building Administration of Cologne Cathedral provided the author with the opportunity to perform the first gemological examination of the gem materials (except the engraved stones) contained in the shrine. The 800-year-old shrine is a unique late Romanesque masterwork from the Rhine-Maas art circle, and is the largest reliquary in the Western world. It is decorated with more than 1,700 stones and 304 cameos from various periods of its complex history. Due to the special location and the large size of the reliquary (110 × 152 × 221 cm), the gemstones could only be examined through direct observation with a loupe. In addition to describing the gemstone inventory in the shrine, this study was undertaken with the following goals in mind:

1. Dating the gemstone polishing by looking for era-typical characteristics (e.g., shape, surface marks, etc.)
2. Determining the original (medieval) gem inventory
3. Determining the possible medieval gem sources
4. Developing statistics and schemes for the scientific documentation of changes in the gem inventory during restoration (especially in 1961–1973)
5. Performing nondestructive identification of any simulants (removed during the 1961–1973 restoration, predominantly glass and assembled stones, ca. 16th–19th century)

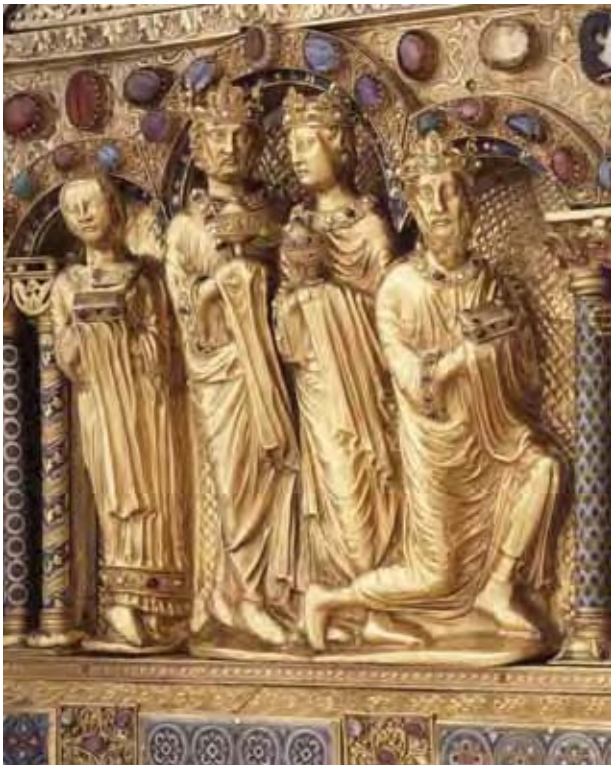

Numerous gems embellish this lower left front section of the Shrine of the three Magi in Cologne Cathedral, Germany. Photo by the Building Administration of Cologne Cathedral.

The gem inventory of the shrine is dominated by sapphire (430 pieces), ruby (60), emerald (141), garnet (525), amethyst (268), and pearls (211). The shrine also contains beryl, rock crystal (including the so-called Large Citrine, ~380 g), chalcedony, some pieces of millefiori, and ancient glass.

The medieval-era gem inventory of the shrine consists of about 200 remarkable sapphires and 50 emeralds. Nearly 100 of the sapphires were drilled for their former usage as beads, which signifies their secondary use in the shrine. The internal features of the sapphires suggest a Sri Lankan origin. For the origin of the medieval emerald inventory, Egyptian sources can be considered.

This contribution demonstrates some techniques and provides results from a gemological characterization of an outstanding reliquary, and also shows the problems and uncertainties that can arise during the analysis of gemstones in ancient works of art in general.

Defects in Single-Crystal CVD Synthetic Diamond Studied by Optical Spectroscopy with the Application of Uniaxial Stress

David Charles (david.charles@kcl.ac.uk)[1], Alan T. Collins[1], Gordon Davies[1], and Philip Martineau[2]
[1]King's College, London, United Kingdom; [2]Diamond Trading Company (DTC) Research Centre, Maidenhead, Berkshire, United Kingdom

It is now possible to grow gem-quality, single-crystal synthetic diamond by chemical vapor deposition (CVD). We can

expect that, at some time in the future, it will become viable to commercially produce this material for the gem trade. It is straightforward for a well-equipped gemological laboratory to differentiate CVD synthetic diamond from natural diamond and from synthetic diamond produced by high-pressure, high-temperature synthesis. Nevertheless, it is important to understand the defects that are characteristic of CVD synthetic diamond. One valuable technique in characterizing defects in diamond is the measurement of optical absorption and luminescence spectra, together with the application of uniaxial stress. Such measurements can determine the symmetry of a given defect. In principle, this knowledge may help to establish an atomic model for the defect. In favorable cases, isotopic substitution can indicate the chemical nature of one or more of the constituents of a defect.

The CVD synthetic diamond samples, shaped as rectangular blocks (approximately 1.25 mm long), were squeezed between two hardened steel anvils that generated stresses up to approximately 2 GPa. Stresses were applied along the [001], [110], and [111] crystal directions; this was typically achieved by using two specimen orientations, one with (001), (110), and $(1\bar{1}0)$ surfaces and the other with (111), $(1\bar{1}0)$, and $(11\bar{2})$ surfaces.

Photoluminescence and cathodoluminescence (CL) spectra from single-crystal CVD synthetic diamond are normally dominated by emission of a zero-phonon line at 575 nm, associated with the nitrogen-vacancy center in its neutral charge state. In addition, such specimens frequently exhibit sharp emission lines at 466.5, 467.0, 496.8, 532.8, and 562.5 nm in the CL spectra. While under uniaxial stress, the 466.5, 496.8, and 562.5 nm centers showed no emission parallel to the [001] growth direction, indicating that a preferential orientation occurred during growth. We found that the symmetries were "rhombic I" for the 466.5 and 496.8 nm defects, and "monoclinic I" for the 562.5 nm center. A plausible structure for the rhombic I centers is V-X-V, where the V are vacancies and X is a carbon atom or an impurity atom.

Comparison of the CL emission line positions in specimens grown with ^{15}N and ^{14}N added to the gas phase showed an isotope shift for the 532.8 nm line. This clearly demonstrates that the defect giving rise to this line involves nitrogen; unfortunately the uniaxial stress measurements indicated that the symmetry of this defect is low. Consequently, determining the detailed structure of this center will present a challenge.

Overview of Dislocation Networks in Natural Type IIa Diamonds

Katrien De Corte (k.de.corte@wtocd.be)[1], Ans Anthonis[1], Jef Van Royen[1], Maxime Blanchaert[1], Julien Barjon[2], and Bert Willems[3]

[1]Hoge Raad voor Diamant (HRD) Research, Lier, Belgium; [2]Groupe d'étude de la Matière Condensée (GEMAC), CNRS—Université de Versailles St Quentin, Meudon Cedex, France; [3]Electron Microscopy for Materials Science (EMAT), University of Antwerp, Belgium

The characteristics of dislocation networks in a representative suite of untreated natural colorless (D to J) type IIa diamonds submitted to the HRD lab are reported here. The majority of these diamonds had dislocation networks that could be observed by cathodoluminescence and the DTC DiamondView instrument. The presence and features of dislocation networks may help in identifying natural diamonds.

Both "elongated" and polygonized dislocation networks that are linked with slip planes were commonly observed in the diamonds. The dislocation nets outlined cells that were mostly 5–50 µm in diameter.

Furthermore, based on the strength of luminescence of the networks compared to that of the surrounding background, the diamonds could be divided into two groups: those with dark networks and those with bright networks (see figure). Most diamonds of the best color grade D belonged to the latter group. The relation between luminescence, dislocations, and other defects is not fully understood.

Natural type IIa diamonds frequently have dislocation networks. These may also be present in natural type IIb and natural type IaB diamonds. So far, dislocation networks have not been reported in the luminescence patterns of high pressure, high temperature (HPHT)–grown synthetic diamonds (which are characterized by cubo-octahedral growth). In general, dislocations in CVD synthetic diamonds are predominantly aligned parallel to the growth direction, whereas in natural diamonds a three-dimensional network is typical. DiamondView images of orange-luminescent CVD diamonds can show striations that result from differential uptake of impurity-related defects on risers and terraces of steps on the growth surface (Martineau et al., 2004). For the rare natural type IIa diamonds that show orange luminescence, dislocations show up as dark networks in DiamondView images, possibly because the dislocations have a local quenching effect on the orange nitrogen-vacancy luminescence (P. M. Martineau, pers. comm., 2006).

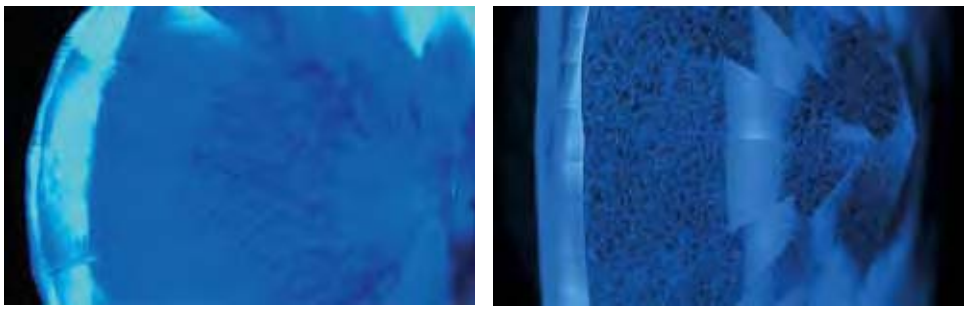

These DiamondView images of natural, colorless type IIa diamonds show dislocations as dark networks (left) and bright networks (right).

REFERENCE
Martineau P.M., Lawson S.C., Taylor A.J., Quinn S.J., Evans D.J.F., Crowder M.J. (2004) Identification of synthetic diamond grown using chemical vapor deposition (CVD). *Gems & Gemology*, Vol. 40, No. 1, pp. 2–25.

Luminescence, Reflected-Infrared, and Reflected-Ultraviolet Digital Photography: Gemological Applications

Shane Elen (selen@gia.edu)[1] and Sheryl Elen[2]

[1]GIA Laboratory, Carlsbad; [2]R.T. Liddicoat Jr. Gemological Library and Information Center, GIA, Carlsbad

Until the advent of relatively inexpensive digital cameras, luminescence photography was a time- and film-consuming process. Reflected infrared and ultraviolet film photography, a process that records the IR or UV light reflected by a sample, was typically beyond the reach of the average photographer. However, digital photography produces near-instantaneous results with no film costs, and also provides an opportunity to visualize features that are subtle or invisible to the human eye.

Visible luminescence can provide visual information that relates directly to a gemstone's history. When properly documented, luminescence images become a valuable identification and teaching tool. However, many luminescence images, particularly of pearls, suffer from poor exposure, lack of detail, and poor color definition. Through the application of the correct lighting and the use of filters, digital photography and image processing can resolve many of these drawbacks, often resulting in fine detail that is normally difficult to observe by eye or capture on film.

The UV and near-IR regions of the spectrum often contain valuable absorption information that may be used to identify natural, synthetic, and treated gem materials. These data beyond the visible range are typically obtained by spectroscopy. However, it is possible to visualize these regions of the spectrum through false-color photography. Fortunately, the charge-coupled devices (CCDs) used in many digital cameras are sensitive to these invisible regions of the spectrum and record them in one, or more, of the visible color channels (red, green, or blue).

In the gemological literature, the authors found only two prior applications of reflected IR photography for cut and polished gem materials (Komatsu and Akamatsu, 1978; Fjordgren, 1986), and none for UV-reflected photography. This may be partially indicative of the difficulties related to these techniques when using 35 mm photographic film.

Possible gemological applications include pre-screening of gem parcels, educational aids, and the identification of natural, synthetic, and treated gem materials, such as pearls (see figure). However, luminescence and reflected UV or IR photography could potentially be applied to any natural gem material in which the synthetic or treated-color counterpart exhibits different luminescence or reflectance properties in the UV or near-IR region of the spectrum. These might include, but are not limited to, identifying natural and treated blue sapphires, identifying diamond types and simulants, and separating blue sapphires of metamorphic and magmatic origin.

REFERENCES
Fjordgren O. (1986) Infrared detective. *Lapidary Journal*, Vol. 39, No. 12, pp. 39–41.

Komatsu H., Akamatsu S. (1978) Differentiation of black pearls. *Gems & Gemology*, Vol. 16, No. 1, pp. 7–15.

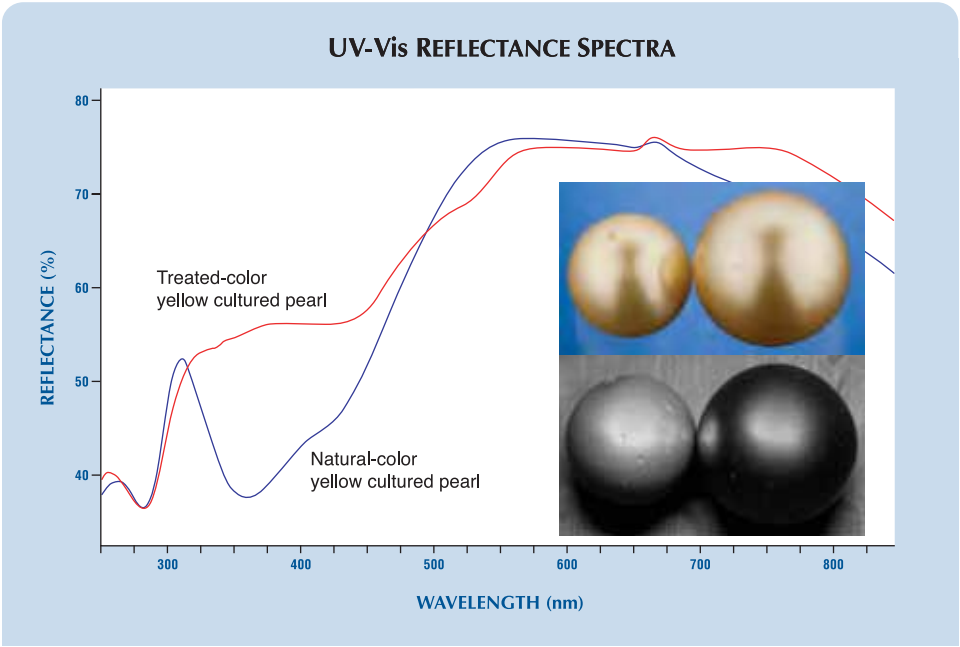

These UV-Vis spectra compare the reflectance of natural- and treated-color "golden" cultured pearls. The natural-color sample (right) exhibits weak reflectance in the UV region of the spectrum because its pigmentation readily absorbs ultraviolet wavelengths. The black-and-white photo (bottom) records UV light reflected from the surface of the cultured pearls. Here, the natural-color sample appears darker than the treated-color one due to its lower ultraviolet reflectance.

Magnetic Separation of Gemstones

Sylvia M. Gumpesberger (sgumpesberger@hotmail.com)
Canadian Gemmological Association, Toronto, Ontario, Canada

Some gems are more magnetic than others, making the magnetic separation of gem materials possible. Historically, this approach was hindered by the low strength of available magnets such as aluminum-nickel-cobalt ("Alnico"). Powerful and focused neodymium-iron-boron (NdFeB) magnets were used by this author to more closely examine the magnetic characteristics of gem materials. A 0.6 × 2.5 cm rod-shaped magnet and a pair of 0.25 × 0.6 cm disk magnets were selected for this study through experimentation.

Initial and key separations were made using three methods of different mechanical advantage:

- Direct method: magnet pulled responsive gems across a low friction surface.
- Pendulum method: responsive gems attracted a magnet suspended from a thread; conversely, the magnet attracted responsive gems suspended in a gem bag.
- Floating method: magnet attracted or repelled responsive floating gems or responsive gems attracted or repelled a floating magnet.

Mathematical formulas were not needed. Hundreds of specimens were tested, including gems in nonmagnetic settings. Quarantined space minimized competing magnetic fields and air currents while using the more sensitive pendulum or floating magnet methods.

Starting with the direct method for loose stones, the gems exhibiting observable magnetic interactions were separated out, which immediately narrowed the range of possible gem identifications. The pendulum and occasionally the floating methods offered greater mechanical advantage or sensitivity for testing larger specimens, as well as those lacking flat faces such as gem rough, those in nonmagnetic settings, and samples requiring detection with very subtle susceptibilities (i.e., diamagnetic or repellant materials, garnet-and-glass doublets topped with a thin slice of garnet, etc.).

The testing showed that gems containing essential Fe and/or Mn tended to respond to varying degrees, with Mn-rich specimens exhibiting a stronger response. The possible influences of element valence and magnetic inclusions were pondered, as were the challenges regarding isomorphous replacement in some gems (e.g., Fe and Mn in tourmaline and garnet). Certain colors of cubic zirconia and all colors of gadolinium gallium garnet (GGG) also responded, the latter relatively strongly. Many useful initial and key separations were made (e.g., see table in the *G&G* Data Depository at http://www.gia.edu/gemsandgemology). Notable separations within the garnet group included spessartine vs. hessonite, demantoid vs. tsavorite (approaching end-member grossular), and almandine vs. pyrope (approaching end member).

A Variation on the Crossed Filters Approach Using Pocket LED Light Sources

Sylvia M. Gumpesberger (sgumpesberger@hotmail.com)
Canadian Gemmological Association, Toronto, Ontario, Canada

Gemologists have widely employed UV radiation to stimulate fluorescence in gem materials. However, the recent commercial availability of pocket-sized, near-monochromatic light emitting diode (LED) units has revived the use of G. G. Stokes' crossed filters approach because LEDs easily substitute for filtered incident light, as previously demonstrated by crossing a blue LED with a red filter (see Lamarre, 2002; Gumpesberger, 2003; Hoover and Williams, 2005). (Note: Crossed filters should not be confused with crossed polarizing filters.)

The author has experimented with variations on the classic crossed filters approach to determine which qualities of light stimulate visible red luminescence in Cr-bearing gems including ruby, red spinel, emerald, and alexandrite. The experiments tested various frequencies of near-monochromatic LED sources including red, yellow, green, blue, and long-wave UV (with peak outputs of 630, 592, 525, 470, and 370 nm, respectively) and a red LED pocket laser (630–680 nm), in combination with gel color filters. The observed effects were compared to those produced by conventional long- and short-wave UV lamps. Short-wave LEDs do not currently exist.

In a dark environment, each LED light source was individually directed at each gem specimen at close range. Single and combined gel filters were selected to absorb various incident wavelengths while transmitting some visible red fluorescence. In the case of the red LED and laser LED pocketlights, care was taken to select a combination that absorbed the visible red incident wavelengths while transmitting the longer visible red fluorescent wavelengths.

In many cases, crossing filters with various visible incident wavelengths stimulated a more evident red fluorescence in these Cr-bearing specimens than conventional long- and short-wave UV incident wavelengths. Visible red incident wavelengths were often surprisingly effective, notably in emerald (i.e., the red luminescence was distinct from the transmission of red incident light).

To simplify potentially complex light/filter combinations, gemologists could benefit from crossing visible blue and visible red LED pocketlights with a Chelsea filter to effectively detect the presence of Cr in gem materials. Further experimentation is continuing with diamonds, which have shown varying results.

REFERENCES

Gumpesberger S. (2003) Pocket LED light sources for gemmologists, Part I. *Canadian Gemmologist*, Vol. 24, No. 3, pp. 94–101.

Hoover D.B., Williams B. (2005) Crossed filters revisited. *Journal of Gemmology*, Vol. 29, No. 7/8, pp. 473–481.

Lamarre C. (2002) Light emitting diodes as light sources in portable gemological instruments. *Journal of Gemmology*, Vol. 8, No. 3, pp. 169–174.

Cathodoluminescence Spectroscopy to Identify Types of Natural Diamond

Hisao Kanda (kanda.hisao@nims.go.jp)
National Institute for Materials Science, Tsukuba, Japan

Natural diamonds are classified into types IaA, IaB, Ib, IIa, and IIb. IR absorption spectroscopy is useful for identifying diamond type. However, this method is limited because it only provides average information from a bulk volume; it is difficult to obtain a spectrum from a microscopic area. Since both type I and type II domains may be found in the same crystal, identifying the distribution of diamond types within microscopic regions of a sample would provide a better understanding of its composition.

Cathodoluminescence (CL) spectra have the potential to identify diamond types on a microscopic (i.e., micrometer) scale. Although a variety of luminescence bands have been reported in diamond (see Zaitsev, 2001), a direct correlation between these bands and diamond type has not been well established.

Thirty natural diamonds were polished along {110} faces. The samples were cooled to about 80 K, and CL spectra were acquired from various points on the polished surfaces and CL images were also taken of the surfaces using a scanning electron microscope fitted with a spectrometer. Micro-FTIR spectra were taken of a small area (0.1 × 0.1 mm) on the polished surfaces.

According to the FTIR measurements, four of the diamonds were type IIa. No type IIb diamonds were encountered. The micro-FTIR spectra showed an inhomogeneous distribution of nitrogen impurities. Nitrogen-free (i.e., type IIa) regions were found even in the type Ia crystals.

The following correlations between the diamond types and CL bands were determined:

1. Type IaA: N9 system with a zero phonon line (ZPL) at 236 nm, and band-A with a maximum at ~415 nm.
2. Type IaB: peaks at 243.5, 246, 248, and 256 nm, and the N3 system with a ZPL at 415 nm.
3. Type IIa: FE system, appearing at 235, 242, and 250 nm.

The CL spectra also provided information on the plastic deformation of the diamonds. The presence of the 2BD system, the band-A line, the 490.7 nm line, the H3 system, or the 575 nm system can each provide evidence of plastic deformation. There are two types of band-A luminescence: in type IaA, it has a maximum at ~415 nm, while diamond containing plastic deformation has a band-A maximum at ~435 nm. The various broad bands were described by Collins (1992).

The CL measurements detected nitrogen impurities more sensitively than the IR spectra, and nitrogen-related peaks were observed in the CL spectra of type IIa diamonds. Despite this inconsistency, CL measurements can provide approximate information on diamond type within a microscopic area.

References
Collins A.T. (1992) The characterization of point defects in diamond by luminescence spectroscopy. *Diamond and Related Materials*, Vol. 1, No. 5/6, pp. 457–469.

Zaitsev A.M. (2001) *Optical Properties of Diamond: A Data Handbook*. Springer-Verlag, Berlin.

The Identification of Gemstones by Photoluminescence: Synthetic and Natural Mg-Al Spinels

Leonardo Maini[1], David Ajò[1], and Sylvana Ehrman (sjehrman@msn.com)[2]
[1]Istituto di Chimica Inorganica e delle Superfici, Consiglio Nazionale delle Ricerche, Padova, Italy; [2] Scientific Methodologies Applied to Cultural Heritage Inc., Silver Spring, Maryland

Spectroscopic properties of transition-metal ions, even at trace levels, allow the use of optical spectroscopy as a nondestructive test for discerning between natural and synthetic gemstones (both loose and mounted). The most important peculiarity of the spinel structure is cation inversion and, for some synthetic crystals, the presence of vacancies arising from an Al:Mg ratio higher than 2. Both cationic disorder and vacancies give rise to a great variety of photoluminescent behaviors of Cr^{3+} in Mg-Al spinels.

Due to the particular interaction between the Cr^{3+} ion and its local environment in the spinel structure, the mere collection of spectral data referring to samples of known origin seems to be inadequate to provide any general predictive criterion for assessing the origin of unknown samples. We propose a multidisciplinary comprehensive approach, based on the synthesis through different methods (Verneuil and flux) of appropriate spinel standards in our laboratories, in order to compare under uniform conditions their spectral features to those of natural spinels (both untreated and heated). Both natural spinels and their synthetic analogues were analyzed by means of electron microprobe and X-ray diffraction to define the composition and structural details of each sample.

Accurate photoluminescence (PL) spectra of 16 of these crystals were then collected at 6, 77, and 298 K, using different laser excitation wavelengths. The careful interpretation of the spectra of this set of samples provided general predictive criteria, and many hints on the conditions under which PL can effectively be used as a probe to identify the origin of chromium-doped spinels. Our criteria focus, among others, on intensity ratios measured under certain excitation wavelengths, as well as on line widths in the region between 680 and 700 nm. A coherent description of the dependence of the spectral features upon the history of each sample was achieved. We proved for the first time that even spinels with the same cation inversion and chemical composition—which are almost identical under extensive X-ray diffraction analysis—can show wide variations in their PL spectral differences that are mainly related to the short-range Cr^{3+} environment.

Fingerprinting Gem Beryl Samples Using Laser-Induced Breakdown Spectroscopy (LIBS) and Portable X-ray Fluorescence (PXRF)

Nancy J. McMillan (nmcmilla@nmsu.edu)[1], Catherine E. McManus[1], Tori L. Gomez[1], Russell S. Harmon[2], Frank C. De Lucia Jr.[3], and Andrzej W. Miziolek[3]

[1]Dept. of Geological Sciences, New Mexico State University, Las Cruces; [2]Environmental Sciences Division, U.S. Army Research Office, Research Triangle Park, North Carolina; [3]Weapons & Material Research Directorate, U.S. Army Research Laboratory, Aberdeen, Maryland

Minimally destructive chemical analysis of gem-quality minerals has many possible applications, including the fingerprinting of single stones, the identification and tracking of stolen or lost stones, and evaluating the provenance of gemstones. The ideal methods for gem analysis should be simple to use, reliable, and minimally destructive. The challenge, however, is that simple and minimally destructive techniques tend to yield results with poorer precision and accuracy than traditional, laboratory-based analytical techniques. As part of a larger study on the chemical fingerprints of beryls, the present authors have obtained data on beryls by four simple, rapid, and portable techniques: LIBS spectra in air, LIBS spectra in argon, PXRF spectra, and PXRF elemental concentrations. LIBS is exceptional in its ability to detect the presence of light elements (e.g., Li, B, Be, and Na), allowing for accurate determination of stoichiometric relationships. PXRF is complementary in that it detects heavy elements well, but in general cannot detect elements lighter than P.

Six gem-quality uncut beryls (aquamarines from Pakistan, Mozambique, India, and China; heliodor from Brazil; morganite from Afghanistan) were analyzed by the four techniques with the goal of uniquely identifying individual specimens. Five LIBS spectra, containing peaks for most elements lighter than La, were collected from different locations on the same crystal face, each after a single cleaning shot. Three PXRF spectra were collected from each sample (15 mm diameter area); elemental concentrations (Ti, Cr, Mn, Fe, Co, Cu, Zn, Rb, Sr, Ag, Ba, and Hg) were then calculated from the spectra by the PXRF software. The LIBS analyses left craters of approximately 100 μm in diameter on the surfaces of the crystals; PXRF analysis was nondestructive.

The following calculations were made to evaluate the parameters by which each stone could be uniquely identified: (1) the ratio of regression of a single-shot LIBS spectrum, single PXRF spectrum, or PXRF concentrations to each of the other spectra or concentrations; and (2) the ratio of the regression of a single LIBS spectrum, single PXRF spectrum, or PXRF concentrations to the average spectrum or concentrations for that specimen. Identification success rates, as defined by the highest correlation coefficients of the linear regressions, are given in the table.

These results will be verified and expanded in two ways: (1) using a larger and more diverse sample set, and (2) testing the double-pulse LIBS technique for this purpose.

Percentage of gem-quality beryl specimens that were successfully fingerprinted using variations of LIBS and PXRF and different calculations.

Method	LIBS in air	LIBS in argon	PXRF concentrations	PXRF spectra
Single shot/ single shot	74.2%	61.7%	61.1%	66.7%
Single shot/ average spectrum	96.7%	90.0%	83.3%	100%

Color Grading of Color-Enhanced Natural Diamonds: A Case Study of Imperial Red Diamonds

Sergei Smirnov[1], Sergei Ananyev[2], Victoria Kalinina[1], Victor Vins (evins@academ.org)[3], and Alex Grizenko[4]

[1]Siberian Gemological Center, Novosibirsk, Russia; [2]Krasnoyarsk State University of Nonferrous Metals and Gold, Krasnoyarsk, Russia; [3]New Diamonds of Siberia Ltd., Novosibirsk; [4]Lucent Diamonds Inc., Lakewood, Colorado

Natural fancy-color diamonds are rare and highly valued by the gem trade. The development of various color enhancement techniques has led to the appearance of commercially available yellow, green, and red color-enhanced natural diamonds. Although the color grading of natural-color diamonds is challenging, it is becoming a routine procedure for producers of color-enhanced diamonds. In the system for natural-color red and pink diamonds presented by King et al. (2002), some grades covered a wide range of tones and saturations of the same hue, and the system required comparison with a collection of reference diamonds (which would be extremely expensive). The lack of generally accepted color grading scales and relatively inexpensive master stones for colored diamonds created the need to develop special scales and color grading procedures for the pink and red color-enhanced diamonds known under the trademark "Imperial Red."

The color scale is based on the standard approach to describing colored gemstones. The GIA GemSet Color Book was used to compare the colors. All diamond samples (more than 200) were observed with a daylight lamp, a GIA DiamondLite, and the overhead daylight lamp of a Gemolite Ultima B gemological microscope. Most of the Imperial Red diamonds were graded as red with an orange or purple modifying color. Some samples were graded as purple with a red modifying color. Based on the color description and the ratio of diamonds of different color grades, a color-grading chart for Imperial Red diamonds was developed (see figure). The most attractive samples within each color grade were determined to have a tone less than 6 and a saturation greater than 4. The least attractive samples showed dark tones (7–8) and low saturations (1–2).

Prices for color-enhanced diamonds were calculated using color coefficients and this color chart. Assuming that the cost of color-enhanced diamonds cannot be lower than enhancement expenses, or higher than the price for colorless

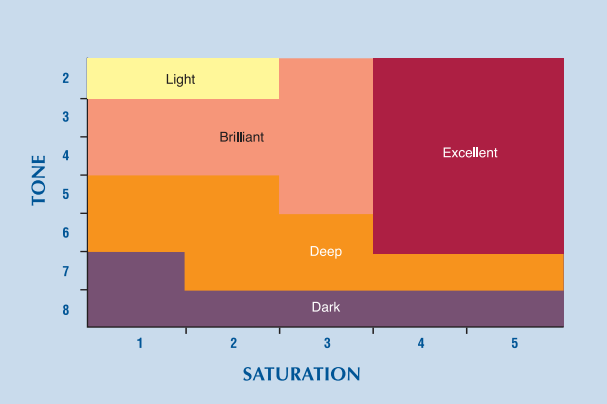

This color chart was developed for color grading Imperial Red diamonds.

diamonds, we determined the coefficients that increase the price of color-enhanced diamonds (from yellow to red). Depending on tone and saturation, the price increase extends diagonally across the chart shown here from left to right and from the bottom to the top. To help customers understand the price differences between different color grades of Imperial Red diamonds, the following terms are used: Dark, Deep, Light, Brilliant, and Excellent. The color-grading chart can be used for all types of color-enhanced diamonds.

REFERENCE
King J.M., Shigley J.E., Guhin S.S., Gelb T.H., Hall M. (2002) Characterization and grading of natural-color pink diamonds. *Gems & Gemology*, Vol. 38, No. 2, pp. 128–147.

Study of the Biaxial Gemstones on the Refractometer

Darko B. Sturman (darkos@rom.on.ca)
Royal Ontario Museum, Toronto, Ontario, Canada

Observations on the refractometer of biaxial gemstones are best shown on diagrams where rotation angles are plotted on the horizontal axis with corresponding refractive indices on the vertical axis. In general, two shadow edges are observed during the rotation. Each shadow edge has one position where β can be determined. The polarizing filter must be used to distinguish between the "true" and "false" β before the optic sign can be determined.

Sometimes, optic sign is insufficient for identifying biaxial gemstones with overlapping refractive indices (e.g., for topaz/danburite or peridot/sinhalite/diopside), and terms such as "strongly negative" or very complex descriptions of the movements of the shadow edges are required. However, these complex descriptions, as well as the use of the polarizing filter, can be avoided in many cases by the simple determinations of the optic angles for both possible "β" readings (one from each shadow edge). It takes only several seconds longer to record these "β" readings at the time when γ and α indices are determined. The procedure for determining the optic angle is as simple as determining the optic sign. Partial birefringences γ-β and β-α are calculated first, and then entered into a diagram where the optic angle is found.

This observation gives two solutions that are compared to the optic angles of gemstones with overlapping refractive indices. In many cases only one match is found. However, on rare occasions when two calculated optic angles match the optic angles of two different gemstones, the only solution is to use the polarizing filter.

Inclusions in White-Gray Diamonds of Cubic Habit from Siberia

Sergey V. Titkov (titkov@igem.ru)[1], Yulia P. Solodova[2], Anatoliy I. Gorshkov[1], Larisa O. Magazina[1], Anatoliy V. Sivtsov[1], Elena A. Sedova[2], Murad D. Gasanov[2], and Georgiy G. Samosorov[2]
[1]Institute of Geology of Ore Deposits, Petrography, Mineralogy, and Geochemistry, Russian Academy of Sciences, Moscow, Russia; [2]Russian State Geological Prospecting University, Moscow

Some kimberlite pipes of the Siberian platform contain unusual semitransparent diamonds of cubic habit that are white-gray or milky gray. In some stones, zones with straight or curved boundaries showing various color intensity (from white and light gray to dark gray) can be observed. The coloration is caused by the presence of numerous fine inclusions. The nature of the inclusions and the cause of the white-gray coloration were examined in this study.

The microinclusions were studied with a JEOL JEM-100C transmission electron microscope (TEM) equipped with a Kevex 5100 energy-dispersive X-ray spectrometer, and with a JEOL JSM-5300 scanning electron microscope equipped with an Oxford LINK ISIS energy-dispersive X-ray spectrometer. Micrometer-sized inclusions were identified by their chemical composition as determined by energy-dispersive spectroscopy and by the structural parameters calculated from TEM electron diffraction patterns. Three white-gray diamond cubes were studied from the Jubileynaya kimberlite pipe.

The diamonds contained abundant microinclusions of calcite, which likely caused their coloration. In addition, they contained various assemblages of microinclusions of native Cu and Fe, Fe-Cr and Fe-Cr-Ni alloys, polydymite, Cu and Fe-Ni sulfides, anhydrite, apatite, and some other minerals. Microinclusions of native metals and sulfides were most abundant in darker zones of the diamonds.

In some early work, carbonate inclusions in diamond were thought to have an epigenetic origin. Later research demonstrated that carbonate inclusions in perfect octahedral diamond crystals actually may have a primary origin (McDade and Harris, 1999; Leost et al., 2003). It therefore may be suggested that in white-gray diamonds, primary inclusions of aragonite or disordered calcite (which are stable at the pressures and temperatures within the diamond stability field; see Suito et al., 2001) later transformed into calcite upon cooling. Alternatively, the diamonds initially may have entrapped carbonate melt or fluids, from which calcite later crystallized, as suggested for various unusual inclusions in cubic diamonds that are not stable at the pressures and temperatures of diamond crystallization (Klein-BenDavid et al., 2006).

Acknowledgments: This work was supported by grant No. 04-05-64606 from the Russian Foundation of Basic Research.

REFERENCES

Klein-BenDavid O., Wirth R., Navon O. (2006) TEM imaging and analysis of microinclusions in diamonds: A close look at diamond-growing fluids. *American Mineralogist*, Vol. 91, No. 2/3, pp. 353–365.

Leost I., Stachel T., Brey G., Harris J.W., Ryabchikov I.D. (2003) Diamond formation and source carbonation: Mineral associations in diamonds from Namibia. *Contributions to Mineralogy and Petrology*, Vol. 145, No. 1, pp. 15–24.

McDade P., Harris J.W. (1999) Syngenetic inclusion bearing diamonds from the Letseng-la-Terai, Lesotho. In J.J. Gurney et al., Eds., *Proceedings of the 7th International Kimberlite Conference*, Vol. 2, Cape Town, South Africa, pp. 557–565.

Suito K., Namba J., Horikawa T., Tanigichi Y., Sakurai N., Kobayashi M., Onodera A., Shimomura O., Kikegawa T. (2001) Phase relations of $CaCO_3$ at high pressure and high temperature. *American Mineralogist*, Vol. 86, No. 9, pp. 997–1002.

General Gemology

Ruby-Sapphire Quality Grading for the Gem Trade

Wilawan Atichat (wilawan@mozart.inet.co.th)[1], Pongchan Chandayot[2], Visut Pisutha-Arnond[1,3], Pornsawat Wathanakul[1,4], Sakda Siripant[1], Sakrapee Saejoo[1], Chotima Kunwisutpan[1], Boontawee Sriprasert[1,5], and Chakkaphant Sutthirat[1,3]

[1]Gem and Jewelry Institute of Thailand, Bangkok; [2]Asian University, Chonburi, Thailand; [3]Geology Dept., Chulalongkorn University, Bangkok; [4]Earth Science Dept., Kasetsart University, Bangkok; [5]Department of Mineral Resources, Bangkok

Grading systems for color, clarity, and cut have been developed by the Gem and Jewelry Institute of Thailand–Gem Testing Laboratory (GIT-GTL) to improve the overall quality grading of ruby and sapphire from various global sources. These quality grading systems are used for communication in the gem and jewelry trades in Thailand and Japan (currently for ruby). This ongoing research has been expanded from the ruby and sapphire grading systems previously established by GIT-GTL.

Ruby and sapphire quality factors were determined from the results of a questionnaire that was given to gem traders in Thailand. These data were then used as a basis to establish eight preliminary sets of master stones that included ruby and various sapphires (blue, orange-pink, purple, pink, orange, yellow, and green). Each set contained 15 stones of varying quality. These master stone sets were then sent to gem traders to solicit opinions. The outcome data were then integrated into the color, clarity, and cut grading systems. Eight final standard (master stone) sets were then developed, composed of 25 oval-shaped, 0.75 ct stones covering five quality grades (Excellent, Very good, Good, Fair, and Poor).

For color grading, the stones were placed 15–25 cm from the standard light source (Macbeth 5000 K with an intensity of 1200 lux), and were visually graded face-up at a distance of 30 cm and viewed perpendicular to the table surface. The hue, tone, and saturation of the stones were considered; dispersion and scintillation were excluded.

For clarity grading, a Dialite Flip light source was positioned to the side of the stones (1 cm away), which were placed on a dark background and graded using a 10× loupe. For confirmation purposes, the clarity of the stones was graded again with the unaided eye at 30 cm distance (and 15–20 cm from the light source) in the face-up position against a white background. The clarity grading was evaluated by using the GIT-GTL scoring system. As for the cut grading, factors for brilliance, face-up proportions, profile proportions, and finish were taken into consideration. The overall quality grading was usually performed by at least three experienced gemologists.

The final evaluation of these corundum standard sets by gem traders in Thailand revealed that they are generally compatible with the quality grading being used in the trade. GIT-GTL is currently using these master stone sets for ruby-sapphire grading for some clients in Thailand and Japan.

Coated Topaz

Riccardo Befi (rbefi@agta-gtc.org), Lore Kiefert, and Min Htut
AGTA Gem Testing Center, New York

Coated topaz has become quite popular, and the material is now available in a wide variety of colors such as pink, orange, blue to green, and with a multicolored effect. Though attractive, most of the coatings are produced using a simple dye or a sputtering method as described by Schmetzer (2006), and are easily scratched off. Some of the coatings (especially pink) initially deceived gemologists because the coatings were applied only to the pavilion. Therefore, EDXRF analysis (normally performed on the table) only detected topaz. When such stones are analyzed from the side, the coating can be detected by its high Ti concentration.

Another type of coating produces green and blue colors, and the manufacturer claims that this process is diffusion-related rather than a simple coating. An examination by the authors showed that the coloring agent is not removed as easily as with other colors of coated topaz, and neither scratching nor exposure to acetone affected it. However, overnight immersion in hydrofluoric acid, which dissolves silica minerals, caused a discoloration (see figure), but no etching of the topaz. Subsequent experiments on green-coated topaz by immersion in hydrochloric acid and hydrofluoric acid for one hour appeared to dissolve the coating just as efficiently. These experiments proved that diffusion of chemical elements into the topaz itself had not occurred. However, some chemical reaction between the topaz and the coating must have taken place to prevent the coating from being easily removed. Analysis with EDXRF spectroscopy revealed Co as the color-giving element, while LIBS analysis showed additional traces of Ca, Na, Li, and K in the top layer.

Schmetzer (2006) described, among others, a process which produces a more durable surface coating, and is the one most likely applied to our samples. This technique is based on heat treatment of faceted gem materials in a transition metal–bearing powder. The transition metal used for blue-to-green colors is Co, the most prominent element found in the coating of our topaz samples.

This 5.57 ct "diffused" (coated) topaz is shown before (left) and after (right) immersion in hydrofluoric acid. Photo by Min Htut.

REFERENCE
Schmetzer K. (2006) Surface coating of gemstones, especially topaz—A review of recent patent literature. *Journal of Gemmology*, Vol. 30, No. 1/2, pp. 83–90.

Three-Dimensional Solid Modeling in Applied Diamond Crystallography

Mike Botha (mbotha@auroracollege.nt.ca), Courtenay Keenan, and Robert Ward

Aurora College, Yellowknife, Northwest Territories, Canada

Aurora College offers a diamond polishing training program in Yellowknife. The curriculum consists of applied mathematics, applied diamond crystallography, diamond history, diamond grading, and three-dimensional solid modeling with a significant practical diamond polishing component. The program is designed to provide students with the cognitive and practical skills to successfully enter the Canadian secondary diamond industry. The program attracts local, national, and international students. Up to 30 students graduate from this program each year.

Since diamond is the hardest known material, we have the dilemma that only diamond is available to cut diamond. Therefore, students need to understand directional hardness and know to avoid cutting facets in octahedral and hexahedral directions. A sound understanding of the crystal structure is imperative if a diamond is to be fashioned cognitively to the highest possible cut grade.

Three-Dimensional Solid Modeling

To enable our students to quickly assimilate the complexities of the diamond crystal, we have developed a course using Autodesk Inventor to demonstrate the following:

- Tetrahedral structure
- Unit cell
- Mathematical cube analysis
- Crystal morphologies
- Assembly of various crystal models relative to coordinates
- Animation of the preceding assembly
- Interrelation of diamond crystal morphologies
- Crystal planes

Diasphere

This is a new concept in applied diamond crystallography and allows the students to correctly identify the hexahedral, octahedral, and dodecahedral planes. It also explains the polishing directions and points of directional transition in relation to the different crystal planes in three dimensions. The purpose of this training model is to enable students to cut and polish diamonds without having to "find the grain" of a diamond. Lower costs are achieved by saving time and equipment.

Application

Once students fully grasp and apply the knowledge, they are able to polish diamonds and avoid the surface anomalies associated with facets being too close to octahedral and hexahedral planes, thus resulting in a higher quality finish.

Characterization of Sapphires from Yogo, Montana

Andrea Cade (acade@eos.ubc.ca)[1], Branko Deljanin[2], Lee Groat[1], and Marina Epelboym[3]

[1]Department of Earth and Ocean Sciences, University of British Columbia, Vancouver, Canada; [2]EGL Gem Lab, Vancouver; [3]EGL USA, New York

Yogo sapphires from central Montana are well known for their natural blue color. They are found as tabular crystals in an Eocene ultramafic lamprophyre dike. The sapphires have been mined intermittently for more than 100 years, but little gemological data are available.

An examination of 12 faceted stones and 20 rough sapphires showed that they were predominantly blue to violet blue, with lesser quantities of purple and pink. Typically they were evenly colored and did not show color zoning. The sapphires were lightly included and often "eye-clean" and transparent. Fluid inclusions were uncommon. The most common mineral inclusions (predominantly identified visually using a gemological microscope) were rutile, sulfides, and garnet (identified by SEM); less commonly observed were biotite, calcite, and analcime. Rutile formed orange-to-brown, subhedral-to-euhedral crystals; no exsolved rutile needles were seen.

The refractive indices were n_o = 1.669–1.770 and n_e = 1.760–1.762, yielding a birefringence of 0.008–0.009. Specific gravity varied from 3.97 to 4.03. Pleochroism was observed as weak-to-medium blue and purple in the blue stones, and as medium-to-strong purple and brownish orange in the purple sapphires. The purple stones exhibited moderate red fluorescence to long-wave UV radiation, while the blue stones showed faint red or no fluorescence.

UV-Vis-NIR spectroscopy was performed on 22 samples using a Varian Cary 50 Scan spectrophotometer. The blue stones had sharp bands at 375, 387, and 450 nm attributed to Fe^{3+} absorption, and broad absorption maxima at 590 and 700 nm attributed to Fe^{2+}-Ti^{4+} charge transfer. Narrow bands

at 400, 560, and 695 nm (attributed to Cr), in combination with the bands observed in the blue stones, were responsible for the color of the purple sapphires. The chemical composition of 50 samples (15 faceted and 35 rough stones weighing 0.05–1.21 ct) was analyzed by EDXRF spectroscopy using a Key Master XRF gun. The EDXRF data confirmed that Fe and Ti were the cause of color in the blue stones, while Cr, Fe, and Ti were the chromophores in the purple sapphires.

Statistical Study of the Performance and Predictive Value of Color Measurement Instruments for Cape-Colored Rough Diamonds

Tom Ceulemans (info@chromascope.be) and Eva Van Looveren
Chromascope, Antwerp, Belgium

The price of rough diamonds is determined by their potential to give polished stones of a certain quality. Besides evaluating the possible size, clarity, and cut of the finished goods, estimating the final color is one of the main problems for the trader. For polished diamonds, one can use master stones to evaluate cape color, but for rough diamonds this method cannot be used. The trader has to rely on his own experience and/or the use of color measurement devices currently available on the market. This study investigated how predictive these instruments are compared to visual inspection by an experienced diamond trader.

More than 300 cape-colored rough diamonds were examined. The stones had various origins, and showed UV fluorescence reactions that varied from inert to very strong. The diamonds had an average weight of 2.43 ct, and while some were makeables, most of them were sawables. All of them were type Ia with colors between D and M. The origin of the yellow cape color was the presence of N3 centers. This center is caused by the grouping of three nitrogen atoms and creates a zero-phonon line at 415.5 nm in the blue region of the visible spectrum.

The color of the stones was visually evaluated before and after cutting by experts, and by using two commercial color measurement instruments: the Yehuda color machine and the Chromascope cape color measurement device. A statistical evaluation was made between: (1) the visual and instrumental color grade estimations, and (2) the color grade results of the rough stones versus the corresponding polished results measured in the different ways. The results showed that no method gives a 100% guaranteed color estimation, but the success rate of the methods varied between 70% and 90% within a one color grade error margin. The exact amount of error depended on the method used (visual, Yehuda, or Chromascope), the intensity of fluorescence, the diamond's origin, and the homogeneity of the color.

"Bahia Gold" Golden Rutilated Quartz, Serra da Mangabeira, Novo Horizonte, Bahia, Brazil

Brian Cook (brian@naturesgeometry.com)
Nature's Geometry, Laguna Beach, California

Golden rutilated quartz deposits are located 400 km west of Salvador, central Bahia, in the Serra da Mangabeira mountain range. The range (16 × 80 km) is oriented in a north-northwest direction, and composed mainly of peralkaline intermediate to felsic volcanic and volcaniclastic rocks of the Rio dos Remedios group (within the Espinhaço supergroup). The volcanism took place in the Middle Proterozoic (1.7–1.2 billion years ago), and was accompanied by pyroclastic and clastic sedimentation (Cordani and Blazekovic, 1970). The rocks have undergone very slight to phyllitic metamorphism, and are situated at the western scarp of the Chapada Diamantina. The Brasiliano thermo-tectonic cycle (Upper Proterozoic) is responsible for gold mineralization and for abundant quartz veining throughout the region. Rutilated, smoky, and colorless quartz crystals are found in pockets and fissures of the quartz veins. The majority of production has been recovered from weathered rock down to 20 m below the surface.

Optical-grade quartz was collected from the surface of the Serra da Mangabeira in the 1940s. Smoky quartz and quartz with golden rutile needles were considered unsuitable for optical use and tossed aside. Eventually the rutilated quartz found its way to the stone centers of Governador Valadares and Teófilo Otoni in Minas Gerais. The broad-bladed golden rutile associated with hematite only occurs within this narrow volcanic range. Rarely, rutile oriented epitaxially on brilliant hexagonal hematite crystals produces "rutile stars." It is thought that the golden-to-copper color of the rutile is related to its iron content.

Electric percussive hammers have increased quartz production in the area by allowing the deposits to be explored to greater depths. In the past, most mining was limited to hand working the weathered layers. Today, hand labor is reaching to 40 m depth with drifts to 25 m. Mechanization, along with higher demand since 2002, has resulted in a rush for the rutilated quartz. Up to 1,000 *garimpeiros* worked the deposits during the dry season (May–November) in 2005, but production figures are difficult to estimate. Thousands of kilograms of quartz may be produced monthly. The quality and size of rutilated quartz varies widely and is very inconsistent. All grades are usable, since there is an established bead and carving grade market. The gem-grade material represents less than 10% of production, and is in strong demand. Production is likely to be more regulated in the future as federal and state agencies are beginning to monitor the area.

REFERENCE
Cordani U.G., Blazekovic A. (1970) Idades radiometricas das rochas vulcanicas dos Abrolhos. *Congresso Brasileiro de Geologia XXIV*, Brasilia, pp. 29–30.

Software for Gemstone Grading and Appraisal Valuation

Richard B. Drucker (rdrucker@gemguide.com)
Gemworld International Inc., Northbrook, Illinois

Since 1982, Gemworld International has published a comprehensive pricing guide for the gem and jewelry industry,

called *The Guide*. In 2000, Gemworld became owner of Guide Appraisal Software, further developing the methods by which appraisers could grade and price gemstones. Integrating the GIA colored stone grading system of hue, tone, and saturation, along with clarity and cut parameters, gem grading and pricing can be entirely produced electronically. By integrating known gemological formulas with researched pricing from *The Guide*, reasonably accurate wholesale valuations can be achieved. Appraiser input then can incorporate extrapolated results into meaningful retail appraisals.

GIA teaches colored stone and diamond evaluation methods. The diamond scale is universally accepted. Colored stones are more diverse and subjective in grading. For this reason, based on clarity, we differentiate between "types" of gems and grade them accordingly. An emerald is typically more included than an aquamarine, so GIA classifies emerald as a "type III" gem and aquamarine as a "type I" gem. Appraisal software can easily classify all gems and adjust for clarity grading. By entering the hue, tone, and saturation based on the GIA system or the Gem*e*wizard system that is now being used by GIA Education, an overall color grade for the gem can be obtained. Finally, cut can be assessed using standard accepted proportion analysis. The GIA course uses the following cut grading categories: excellent, very good, good, fair, and poor. Combining the color, clarity, and cut by weighting each factor appropriately, the grade can then be applied to pricing grids.

Appraisers constantly face the challenge of accurately and consistently assessing gems for grading and valuing. Today, this can be achieved more reliably through technology-based software.

Demantoid from Iran

Garry Du Toit (gdutoit@agta-gtc.org)[1], Wendi Mayerson[2], Carolyn van der Bogert[2], Makhmout Douman[3], Riccardo Befi[1], John I. Koivula[4], and Lore Kiefert[1]

[1]AGTA Gemological Testing Center, New York; [2]GIA Laboratory, New York; [3]Arzawa Mineralogical Inc., New York; [4]AGTA Gemological Testing Center, Carlsbad

Demantoid was first found in Iran in October 2001. The deposit is located in Kerman Province in southeast Iran at 1500 m above sea level. So far, approximately 120 kg of material has been mined, of which 5% was of gem quality. Cat's-eye demantoid is produced rarely (Douman and Dirlam, 2004). Besides the green demantoid variety, light yellow, orange, light orange, and brownish orange andradite are found at the same location. The garnets occur as clusters and as single well-formed crystals that are hosted by regionally metamorphosed asbestiform rocks within serpentine. Associated minerals include chlorite, apatite (large colorless crystals), and an attractive banded opaque material consisting of layers of apatite and calcite. Another associated mineral was identified as an amphibole, probably manganoriebeckite.

Twelve rough and 27 faceted demantoids were analyzed for this study. Sixteen samples were magnetic. The more transparent samples contained "fingerprints" along with straight and curved fibrous needles, consistent with those seen in Russian demantoids. These samples also revealed fractures along growth planes, which were also seen in the cat's-eye samples examined earlier; such fractures have been observed repeatedly in the Iranian material, and may distinguish them from the Russian material. The R.I. was above 1.81, and the S.G. was determined as 3.82 by the hydrostatic method. Both readings are consistent with the properties of demantoid from Russia. A desk-model spectroscope revealed a strong band at 443 nm and two bands at 622 and 640 nm, indicating Fe^{3+} and Cr^{3+} as the chromophores. These chromophores have also been found in demantoids from Pakistan (Milisenda et al., 2001). EDXRF spectroscopy showed significant chromium in several of the samples.

REFERENCES

Douman M., Dirlam D. (2004) Gem News International: Update on demantoid and cat's-eye demantoid from Iran. *Gems & Gemology*, Vol. 40, No. 1, pp 67–68.

Milisenda C.C., Henn U., Henn J. (2001) Demantoide aus Pakistan. Gemmologie, *Zeitschrift der Deutschen Gemmologischen Gesellschaft*, Vol. 50, No. 1, pp. 51–56.

Fluorescence of Fancy-Color Natural Diamonds

Sally Eaton-Magaña[1], Jeffrey E. Post[2], Roy A. Walters[3], Peter J. Heaney[4], and James E. Butler[1]

[1]Naval Research Laboratory, Washington, DC; [2]Department of Mineral Sciences, Smithsonian Institution, Washington, DC; [3]Ocean Optics Inc., Dunedin, Florida; [4]Dept. of Geosciences, Pennsylvania State University, University Park

Gemological characterizations of diamonds commonly contain descriptions of fluorescence and phosphorescence. Typically, these include the color and relative intensity in response to short-wave (254 nm) and long-wave (365 nm) UV radiation. In addition, the corresponding spectra can be useful for indicating the presence of multiple centers that cannot be visually detected, the location of peak maxima, and peak shape.

The Aurora Butterfly, a collection of 240 loose colored diamonds (total weight of 166.94 ct), was on temporary display at the Smithsonian National Museum of Natural History from January to July 2005. It provided a unique opportunity to study the fluorescence reactions of a wide variety of colored diamonds. The diamonds were exposed to a UV source with wavelength varying from 250 to 425 nm, and the emission spectra were recorded. To avoid the risk of damaging these valuable gems, we could not perform some scientifically desirable experiments (e.g., low-temperature spectroscopy). An Ocean Optics deuterium lamp was used to excite the luminescence, and a fiber-optic assembly transmitted the UV radiation to the diamond and the emitted fluorescence from the sample. A USB 2000 spectrometer recorded the fluorescence and phosphorescence spectra. In the fluorescence measurements, a series of filters were used to block the visible light of the lamp.

The fluorescence peak locations and shapes were segregated into three categories, which corresponded well with the diamonds' bodycolors. Fancy white, pink, and yellow diamonds

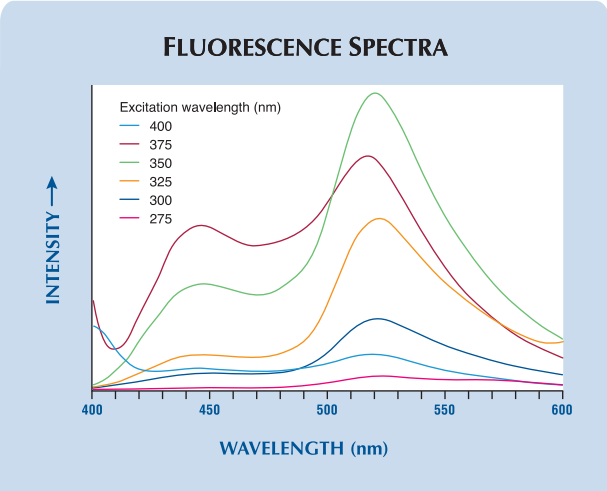

Emission spectra of the UV fluorescence are shown at various excitation wavelengths for Aurora Butterfly no. 213, a 0.46 ct yellow-green diamond.

showed two emission peaks centered at 450 and 490 nm that are possibly caused by the N3 defect or dislocations. Green and violet diamonds exhibited an asymmetric peak at 525 nm, likely due to H3 centers (see figure). Orange and "chameleon" diamonds showed a broad symmetric peak at 550 nm, and nitrogen platelets are tentatively assigned as the responsible center (Collins and Woods, 1982). Depending on the length of the "tail" of the emission band extending to 600 nm, the observed fluorescence could be either yellow or orange.

Since fluorescence is caused by certain defect centers in diamonds, different colored diamonds with similar fluorescence spectra likely have similar optically activated defects. Fluorescence spectroscopy could therefore be a useful technique for classifying colored diamonds.

Acknowledgments: We are grateful to Alan Bronstein for his time and for providing access to the Aurora collections, to Thomas Moses and Wuyi Wang of the GIA Laboratory in New York who loaned a DiamondView instrument for this project, and to Russell Feather, gem collection manager at the Smithsonian Institution, for his assistance.

REFERENCE
Collins A.T., Woods G.S. (1982) Cathodoluminescence from 'giant' platelets, and of the 2.526 eV vibronic system, in type Ia diamonds. *Philosophical Magazine*, Vol. 45, pp. 385–397.

The Bragança "Diamond" Discovered?

Rui Galopim de Carvalho (ruigalopim@labgem.org)
Labgem, Sintra, Portugal

The famous Bragança diamond (internationally spelled "Braganza") has been in the imagination of gem lovers since it was first mentioned in the early 19th century. Its reported 1,680 ct weight would make it second only to the Cullinan among the world's largest rough gem diamonds. The Bragança, named after the dynastic name of King D. João VI (1767–1826) of the House of Bragança, is reportedly a large pale-colored pebble that was found in Brazil. The fascination with the mysterious Bragança is based on the fact that the existence of this diamond has never been proven.

Modern authors have stated that this stone, if it ever existed, was not a diamond but a topaz. This is consistent with the fact that in 19th century Brazil, colorless topaz was being produced for Portuguese jewelry manufacturing. The negligible difference in specific gravity between diamond and topaz, and the fact that both can show perfect cleavage planes, may have contributed to a possible misidentification.

The ongoing study of Portuguese Royal Treasuries at the Royal Palace of Ajuda has made it possible to access rare documents, gems, and jewelry. In addition to the fabulous gem-set jewelry, a few Brazilian mineral specimens were once in the collection of King D. João VI. Among those was a very light greenish blue rounded pebble weighing 342 grams that was referred to as an aquamarine in the 19th century and later confirmed as beryl in the 1950s (see figure). A simple conversion from grams to metric carats yields 1,710 ct (i.e., 342 g × 5 ct/g), which is quite close to the reported 1,680 ct of the Bragança. However, this carat value referred to old carats, and not the post-1907 universally accepted 1 ct = 200 mg = 1/5 g. The 1,710 ct value may easily be converted to 1,680 old carats, assuming a conversion factor of 1 ct = 203.5 mg, an admissible figure around Europe in the 19th century.

The fact that a round gem pebble exists in the collections documented in the King D. João VI inventory, and that the

This 342 g (62 × 61 mm) Brazilian aquamarine has a history, weight, and general description that are consistent with those given for the Bragança diamond in the literature. Photo © Palácio Nacional da Ajuda, Lisbon; courtesy of IPPAR—Instituto Português do Património Arquitectónico.

description and weight are consistent with what is reported as the Bragança diamond, may not be enough to say that they are the same. The search for further documentation is continuing that may confirm or deny that the Bragança is neither a diamond or a topaz, but most probably an aquamarine in the actual inventory of the Portuguese Royal Treasuries.

The Evolution of the American Round Brilliant Diamond (aka American Cut), 1860–1955

Al Gilbertson (al.gilbertson@gia.edu)
GIA Research Department, Carlsbad, California

Today "American Cut" is synonymous with "Ideal Cut." This is a product of education that primarily came from GIA and the American Gem Society. The terms are equated with proportions espoused by Marcel Tolkowsky in 1919. Mr. Tolkowsky was Belgian, not American, and the terms *American Cut* and *Ideal Cut* were in use before 1919 with almost identical proportions. The trade has largely accepted this simplification of history and is unaware of why the term *American* is associated with this cutting style. Tracing the history of the American Cut, a term incorrectly associated with Mr. Tolkowsky and proportions espoused by him, also parallels the search to equate the value of a faceted diamond with its appearance. Quality of cutting is often judged by a diamond's appearance. This history follows a quest for cutting the most attractive diamonds that began before Henry Morse, but was revitalized by him in the 1860s. Prior to his involvement, David Jeffries (1750) and John Mawe (1823), as well as others, talked about cutting diamonds for their beauty. Until the late 1800s, diamonds were primarily cut to maximize weight and not beauty.

Mr. Morse revolutionized diamond cutting by using mechanized bruting and measuring angles with the first angle gauge. Prior to this, hand bruting made it very slow and difficult to make a diamond uniformly round in shape, and most were squarish. Other American innovations that followed were mechanical dops and sawing. Early ray tracing and mathematical calculations for best cutting angles performed by Americans such as Henry Whitlock and Frank Wade corresponded to the angles in use for the American Cut. Merchandising of the American Cut (see figure) became easier as Americans boasted that they could do things as well as or better than Europeans. The patriotic timbre of the American view of their contributions to diamond cutting can be a bit strong, yet it is a vital contribution to the evolution of the American Cut.

The early proportions gave way to very slight changes proposed by Mr. Tolkowsky. Advocates of early proportions for the American Cut, including Mr. Wade, embraced Mr. Tolkowsky's slightly different proportions. Mr. Wade's efforts and GIA's support (starting in 1931) of the American Cut's proportions solidified its position in the trade. The final validation that placed the American Cut firmly as a diamond with beauty and value came with the changes in GIA course material in 1953, which evaluated cut and associated its evaluation with current market prices.

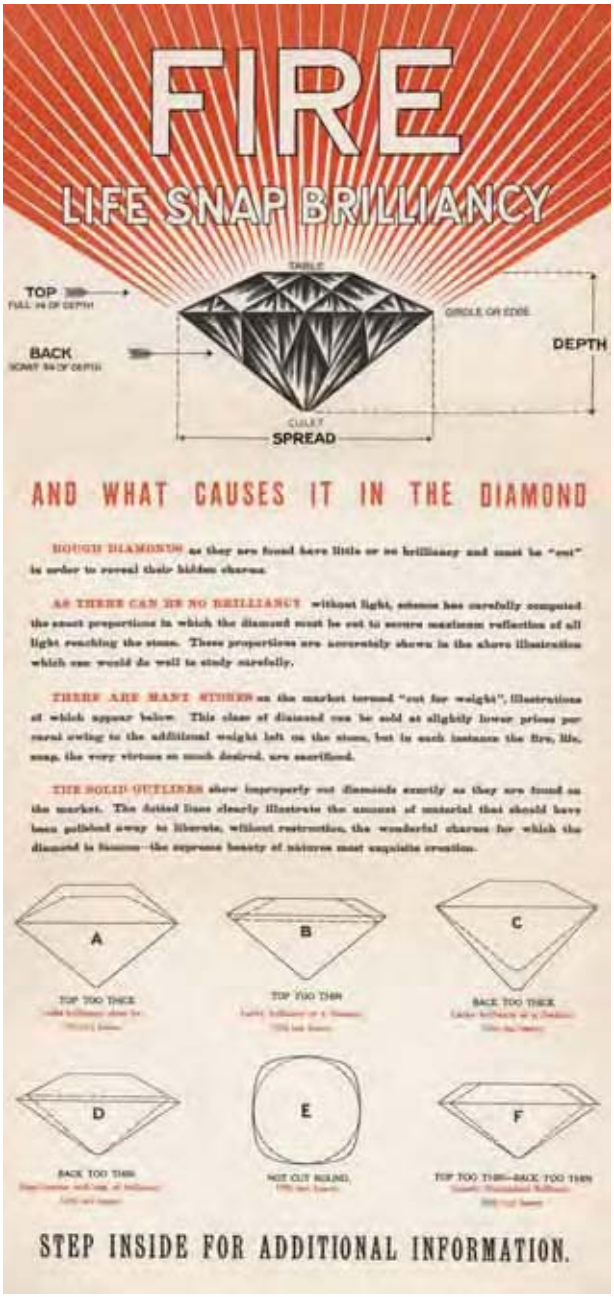

This poster was used in retail stores to discuss proportions for the American Cut as early as 1915. It was supplied to trade members by J. R. Wood and Sons.

Funding for Gemological Research: Ideas and Case Studies

Lee A. Groat (lgroat@eos.ubc.ca)
Department of Earth and Ocean Sciences, University of British Columbia, Vancouver, Canada

Research on gem materials and deposits ranges from basic to applied science, and has implications for a wide variety of topics from advanced materials to our understanding of geological processes. For example, gem deposits are rare because

the required geological conditions are exceptional, and thus are often worthy of scientific study. In turn, the more we know about gem deposits, the more successful we should be at finding new ones. The obvious model is diamonds and kimberlites, but surprisingly little is known about the origin of most colored stone deposits. This is especially important as traditional sources decline.

Of course, research costs money, for student stipends and salaries, instruments, analyses, transportation, journal page charges, conference fees, and a myriad of other expenses. Funding can come from a variety of sources, including governments and industry. Agencies such as the Natural Sciences and Engineering Research Council (NSERC) in Canada, and the National Science Foundation (NSF) in the United States, support research in mineralogy, materials science, and related fields through grants to individuals in academic institutions and museums in some cases. Proposals undergo a highly competitive peer-review process. NSERC has a number of Partnership Programs, including Collaborative Research and Development (CRD) grants, which support well-defined projects undertaken by university researchers and their private-sector partners. CRD awards cover up to half of the total eligible direct project costs, with the industrial partner(s) providing the balance in cash and in kind. Similar programs exist with granting agencies in other countries. Government geological surveys are another possible source of funding.

Mining companies may also support gem research, provided there is a clear plan with detailed budgets and timelines. It also helps to show a willingness to get one's hands dirty in the field. Sometimes numerous meetings are necessary before a company will commit to funding a project. Funding can be both monetary and in-kind (transportation, accommodation, data, etc.). Companies need to understand the regulations that the researcher must adhere to in any university-industry partnership. One of the best ways to cooperate is to have the company fund a graduate student. This creates good public relations and there is the possibility that the student will become an employee upon graduation. A major labor shortage is developing in the geosciences, and such collaboration is one way for a company to build a relationship with a potential employee.

Relationship between Texture and Crystallization Degree in Nephrite Jade from Hetian, Xinjiang, China

Mingyue He (hemy@cugb.edu.cn)
School of Gemmology, China University of Geosciences, Beijing

China is one of the most important countries of the world's ancient civilizations, with a history of mining and using jade that extends for thousands of years. Nephrite was and remains the most important jade in Chinese culture. This study used petrographic microscopy and powder X-ray diffraction to study the relationship between texture and "crystallization degree" in nephrite from Hetian in Xinjiang Province. The crystallization degree, which is also referred to as crystallinity, is the degree of structural order in a solid (often represented by a fraction or percentage) and provides a measure of how likely atoms or molecules are arranged in a regular pattern (i.e., into a crystal).

Microscopic observation of the jade revealed a crystalloblastic texture. Based on the spatial relationships among the constituent grains, this crystalloblastic texture could be subdivided into the following seven types: felt-fiber intertexture, rimmed fiber, leaf fiber, broom, radial fiber, replacement relic, and replacement metasomatic (pseudomorph). The overall fabric of the jade could be classified as either blocky or schistose. The former is the most important and popular for gem material, while the latter is subject to fracturing along foliation and, thus, is not commercially significant.

X-ray diffraction (XRD) analysis indicated that the jade is composed fundamentally of tremolite. In general, the XRD pattern for Ziyu material (an alluvial deposit) was consistent with that of tremolite, while there were weak diffraction peaks for accessory minerals such as serpentine in Shanliao material (a primary deposit). The higher-angle diffraction peaks indicate that the material is well crystallized. The indices of crystallization (calculated from the XRD patterns) of tremolite in Hetian jade were lower than that of standard coarse-grained tremolite. Within the Hetian jades, the indices of crystallization were relatively higher for the majority of Shanliao samples (which have a coarser grain size), which showed strong, sharp, and rather symmetric diffraction peaks. The indices of crystallization were lower for the Ziyu jade and a small amount of the Shanliao jade (in which the grain size was relatively fine), as shown by diffraction peaks that were weak, dispersed, and less symmetric. The crystallization degree was therefore consistent with the textural features seen with the microscope.

Integrating the Diamond Project Development Process

Karin O. Hoal (khoal@mines.edu)
Colorado School of Mines, Golden, Colorado

Diamond project development by producers affects the market because geologic source is tied to a geopolitical location, and mining methods may adversely affect sales. The diamond project development process refers to how diamond projects are developed to improve recovery, reduce environmental impact, and contribute to local communities (see table). The visibility of programs such as the Diamonds and Human Security Project (www.pacweb.org/e/images/stories/documents/sierraleone_e.pdf) the Diamond Development Initiative (www.casmsite.org/Documents/DDI_Accra_Oct05.pdf), and Diamonds for Development (www.diamondsfordevelopment.com) shows how project development affects producers through to retailers, as well as the public's perception of goodwill accompanying any mining-related activity, however far removed (i.e., jewelry). Diamond project development is particularly important to mineral-rich African countries that rely on mining revenues for infrastructure and development.

At the Colorado School of Mines, we are establishing the first interdepartmental geometallurgical research center with state-of-the-art QemScan instrumentation, that will be used for new applications in diamonds and gems (e.g., rapid indicator mineral assessment, stone source identification techniques, materials characterization) among other mineral studies. In association with the USGS, research in Liberia illustrates how diamond project development is enhanced by integrating geology, resource assessment, extraction and characterization techniques, and marketing initiatives in a revitalizing industry with a new government. Past export figures for Liberia from the 1950s to 1980s, including trafficked stones, averaged about 300,000–600,000 carats/year, declining to 3,700 carats in 2001 (Greenhalgh, 1985; Coakley, 2004). While production is on hold until UN sanctions are lifted (perhaps by December 2006), exploration efforts and some artisanal operations continue and there is considerable potential for new deposit discoveries.

Liberian geologic and mineral assessment includes identifying (1) the boundaries of the West African Craton, (2) potential lithospheric delamination by the Pan African orogeny and subsequent diabase dike swarms, (3) structural controls, (4) potential sites conducive to kimberlite emplacement, (5) erosional and weathering profiles for alluvials, (6) secondary reworking sites, and (7) the potential for paleodrainage and marine deposits. These geologic factors help determine elements of the project development process, such as extraction techniques, processing methods for difficult materials, laboratory facility methods, geometallurgical characterization, and a mining plan. Community development follows, through geological survey assistance, certification programs, GPS-database systems of mining sites and recovery values, and training-the-trainer programs. Recovery and sales of rough diamonds through cooperatives with government-appointed monitors are geared toward a sustainable system that benefits sellers with the best prices, brings income to communities, and develops branding initiatives for conflict-free, high-quality Liberian stones.

REFERENCE

Coakley G.J. (2004) *The Mineral Industry of Liberia*. U.S. Geological Survey Minerals Yearbook, pp. 24.1–24.4.

Greenhalgh P. (1985) *West African Diamonds 1919–1983: An Economic History*. Manchester University Press, Manchester, UK, 306 pp.

Melo "Pearls" from Myanmar

Han Htun[1], William Larson[2], and Jo Ellen Cole (jocole2@cox.net)[3]

[1]Stalwart Gem Laboratory, Yangon, Myanmar; [2]Pala International, Fallbrook, California; [3]Cole Appraisal Services, Carlsbad, California

Non-nacreous "pearls" produced by Melo volutes are found along coastal areas of Myanmar, as well as Indonesia, Thailand, Cambodia, and Vietnam. Occurring in a range of colors, the most prized is an intense orange hue. In Myanmar, the volutes are called *Ohn kayu* (coconut shell), and the orange pearls derived from them are called *Ohn pale*. The volutes are fished at a depth of 30–50 m from a muddy sea bottom. A non-nacreous pearl forms when an irritant enters the mollusk's mantle, and the size and color of the Melo pearl is determined by the size and lip color of the parent mollusk.

In addition to a strong orange coloration, the best-quality Melo pearls exhibit an attractive silky flame-like structure and a porcelaneous luster. The microscopic "flames" are actually thin lamellar-like structures composed of intercalated calcite and aragonite crystals that display different optical behaviors. The lamellae are almost parallel to one another, and when oriented perpendicular to the axis of the pearl they produce a pseudo-chatoyancy effect. Some Melo pearls show a regular pattern of parallel elongated striations that impart a silky sheen.

Melo pearls are generally round, but a near-spherical or true round shape is very rare. They may vary from a few millimeters to more than 32 mm in diameter. Fluorescence is

Some components of integrated diamond project development.

Geologic →	Resource →	Extraction →	Development →	Market
Regional mapping	Past production estimates	Survey methods, capabilities	Identify local pipeline, methods, politics	Government tax, concession structure
Craton architecture	Current production	Estimate losses due to methods	Government capabilities	Local participation, tribal, community
Lithosphere modifications	Estimation of potential	Local plant flow sheet, footprint	Geological survey facility, personnel	Establish working cooperatives
Structural controls	Estimation of preservation	Develop methods for difficult materials	Open-file set up and access	Monitoring system and personnel
Kimberlite emplacement	Regional synthesis	Basic equipment installation	Field worker training, mineral processing	Establish market price structure, centers
Secondary, alluvial deposits	Neighboring country capacity	Environmental local impact	Technical training, instrumentation	National marketing initiative
Accumulation sites and traps	GPS, GIS of sites, past/current	Nontoxic lab facilities	Train-the-trainer programs	Kimberley Process, development diamonds certificate
Marine diamond capability	Database of sites' value, volume	Sustainability of process	Beneficiation, cutting/polishing centers	International branding, advertising, sales

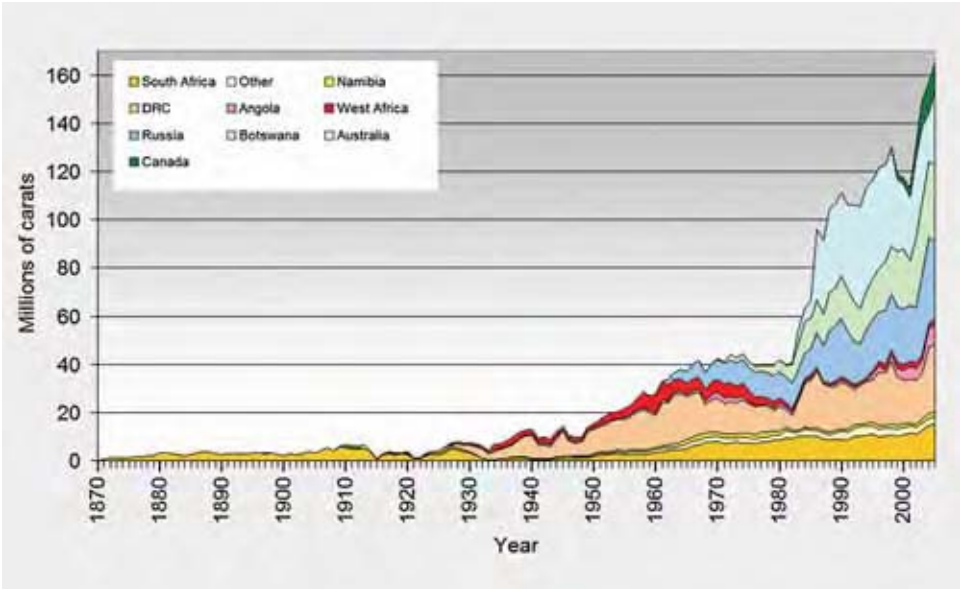

This graph shows the annual global rough diamond production from 1870 to 2005, subdivided according to the major sources.

variable, mostly chalky blue or orange. The refractive index typically ranges from 1.51 to 1.64, with lower values ranging from 1.50 to 1.53 and the higher values ranging from 1.65 to 1.67. Variations could be greater if a larger sample group were studied. With exposure to the UV radiation in sunlight, both the Melo shells and their pearls are known to fade in color.

The majority of Burmese Melo pearls are fished from the Mergui Archipelago and traded in the town of Myeik (or Mergui). The color, shape, size, and quality of the flame structure are considered in determining their price. Imitation Melo pearls have been created by polishing round pieces cut from the thickest portion of the volutes shell. They display a different flame structure pattern that consists of concentric radiating flames and parallel-banded layers displaying the pseudo-chatoyancy effect.

Melo pearls are among the rarest gems in the world. Myanmar coastal areas offer an ideal environment for the habitat of Melo gastropods, and it is certain that many more of these exotic orange pearls will be retrieved from Myanmar waters in the future.

Global Rough Diamond Production from 1870 to 2005

A. J. A. (Bram) Janse (archonexpl@iinet.net.au)
Archon Exploration Pty. Ltd., Perth, Western Australia

Data for annual global rough diamond production from 1870 to 2005 were compiled and analyzed. Assembling these data was an arduous and difficult task because the figures for several countries may vary as much as 10% between various publications. To maintain consistency, production figures were taken from sources that are believed to be reliable and were published in the U.S. These sources include *Minerals Yearbook* (published by the U.S. Bureau of Mines from 1934 to 1966 and thereafter by the U.S. Geological Survey). For the period from 1870 to 1934, the "Gemstones and Precious Stones" chapters in *The Mineral Industry* and *Mineral Resources of the United States*, as well as Wagner (1914), were consulted.

Global production, as indicated by carat weight, was divided into 10 major source countries or regions (see figure and a data table in the *G&G* Data Depository at http://www.gia.edu/gemsandgemology). The data show a spectacular increase in 1985 when the Argyle mine in Australia began production. Declines in South African production were caused by World War I in 1915, the sudden influx of diamond jewelry put on the market by Russian émigrés in 1921–22, and the global depression in the early 1930s. Starting in the 1930s, production from West Africa and the Congo increased greatly and peaked in the period of 1955–1975. Russian production began in 1960 and increased starting in 1985, during the same time as production in Botswana (beginning in 1971) and Australia (beginning in 1983) began to rise significantly. The latest entry is Canada, which began production in 1998.

Data and statistics for 27 diamond-producing countries have been tabulated (again, see table in the *G&G* Data Depository). South Africa ranks first in value (although fourth in volume), mainly because of its long history in production; Botswana ranks second in value and fifth in volume, although its production history dates only from 1970; Russia is third in value and third in volume; while Namibia, although ranking only eighth in volume, is fourth in value because of the high value of the diamonds from its beach deposits. Congo-Zaire is first in volume, but because of the low diamond value it ranks fifth in value, and likewise Australia ranks second in volume but is only eighth in value. The total global production up to 2005 is estimated at 4.5 billion carats, valued at $315 billion with an average value per carat of $70.

REFERENCE
Wagner P.A. (1914) *The Diamond Fields of Southern Africa*. The Transvaal Leader, Johannesburg, South Africa, 347 pp. (reprinted in 1971 by C. Struik, Cape Town, South Africa, 355 pp.).

Identification of Beryl Varieties: "Beryl Color Circle," "Color Memory," and a Proposed New Variety—Chromaquamarine

Arūnas Kleišmantas (arunas.kleismantas@gf.vu.lt)
Geology and Mineralogy Dept., Vilnius University, Lithuania

The goals of this study were to create a method to classify gem beryl varieties and identify indications of heated beryls. In addition, based on a study of material from Zambia and Australia, a new beryl variety is proposed.

With increasing heating temperature, the color of beryl containing Fe^{3+} changes as follows: yellowish brown → yellow → slightly yellow → slightly green → colorless with slightly green-blue → slightly blue. This observed sequence was calculated theoretically by using Goethe's Color Circle and Maxwell's Triangle (Agoston, 1982). When transferred to the CIE (1931) color space diagram, the color spectra for various beryl varieties show a consecutive sequence: golden beryl → heliodor → green beryl → goshenite → aquamarine. Golden beryl and heliodor clearly distinguish themselves as separate varieties in this CIE (1931) diagram, and their designation should be based on their hue—yellow for golden beryl, and greenish yellow for heliodor.

A new proposed variety—*chromaquamarine*—can be distinguished on this same color diagram. Chemical analysis with a JXA-50A scanning electron microscope of five chromaquamarines (four from Kafubu, Zambia, and one from Poona, Australia) and 26 emeralds from different localities showed that the chemical composition of chromaquamarine is close to that of emerald, but with a considerably larger amount of Fe^{N+} (0.475–1.11%) than either Cr^{3+} (0.081–0.146%) or V^{3+} (<0.018%). The hue of chromaquamarine varies from greenish blue to bluish green. However, because of the presence of chromium, this material cannot be considered to belong to the iron-bearing beryls, and must be closer to emerald.

Having made use of the Goethe Color Circle, a new diagram—a "Beryl Color Circle"—has been devised to reflect the diversity of beryl varieties (see figure), and shows the variety of stones with similar hues.

From the absorption spectra of heated beryl, it was found that after heating, beryl possesses a "color memory" because the color centers remain after the heat treatment. This could help indicate whether or not a beryl has been heated.

REFERENCE
Agoston G.A. (1982) *Color Theory and Its Application in Art and Design*. Mir Publishers, Moscow, pp. 62–113 (in Russian).

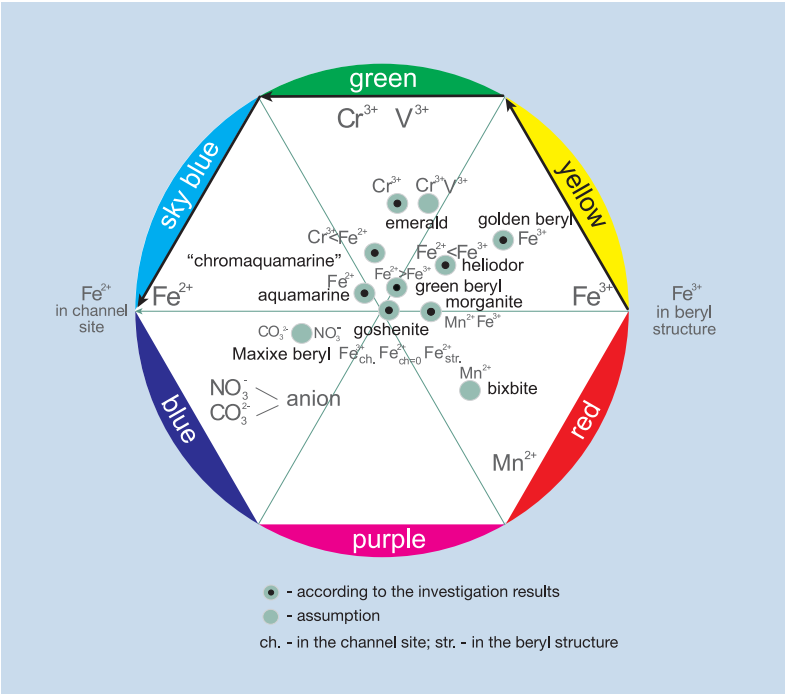

This "Beryl Color Circle" was compiled according to color-causing impurities elements and their position in the beryl crystal structure.

Gemological Properties of Colorless Hyalophane from Busovaca, Bosnia-Herzegovina

Goran Kniewald (kniewald@irb.hr)[1] and Vladimir Bermanec[2]
[1]Center for Marine and Environmental Research, Rudjer Boskovic Institute, Zagreb, Croatia; [2]Institute of Mineralogy and Petrology, University of Zagreb, Croatia

Hyalophane has the formula $K,Ba[Al(Al,Si)Si_2O_8]$, and is a mineral belonging to the solid-solution series of K-Ba feldspars with the end-members orthoclase $K[AlSi_3O_8]$ and celsian $Ba[Al_2Si_2O_8]$. Gem-quality hyalophane has been found in the Busovaca area in central Bosnia-Herzegovina, some 50 km northwest of Sarajevo. It occurs in stratabound hydrothermal veins associated with Paleozoic chlorite and amphibolite schists (Bermanec et al., 1999). This occurrence has been described previously in the literature, and data on crystal morphology, chemistry, and optical properties have been published (Baric, 1972; Bank and Kniewald, 1985). A colorless, transparent cut hyalophane was shown to be biaxial with refractive indices of n_x = 1.541, n_y = 1.546, and n_z = 1.549, giving a birefringence of 0.008; the hydrostatic specific gravity was 2.89 (Bank and Kniewald, 1985). The identity of the studied hyalophane was confirmed with powder X-ray diffraction.

Before the onset of war in Bosnia during the 1990s, some additional crystals of gem-quality hyalophane were found and several stones ranging from 0.5 to 1.5 ct were cut from this material. Attempting to identify hyalophane with standard gemological tables is difficult, since this mineral is not mentioned in the common gemological literature. To our knowledge, this is the only known occurrence of gem-quality hyalophane.

REFERENCES
Bank H., Kniewald G. (1985) Farbloser hyalophane von Busovača, Jugoslawien. *Zeitschrift der Deutschen Gemmologischen Gesellschaft*, Vol. 34, No. 3/4, pp. 169–170.

Baric L. (1972) Hyalophan aus Zagrlski (Zagradski) Potok unweit von Busovaca in Zentralbosnien. *Wissenschaftliche Mitteilungen des Bosnisch-Herzegovinischen Landesmuseums*, Band II, Heft C (Naturwissenschaften), pp. 5–37.

Bermanec V., Palinkas L., Balog K., Sijaric G., Melgarejo J.C., Canet C., Proenza J., Gervilla F. (1999) Stratabound hydrothermal metamorphogenic Ba-Cr-Fe-Cu-Zn deposit of Busovaca, central Bosnia. In C. Stanley et al., Eds., *Mineral Deposits: Processes to Processing*, Balkema, Rotterdam, pp. 927–930.

Some Dissolution Features Observed in Natural Diamonds

Taijin Lu (tlu@gia.edu)[1], Mary L. Johnson[2], and James E. Shigley[1]
[1]GIA Research, Carlsbad; [2]Mary Johnson Consulting, San Diego, California

Most natural diamonds have been subjected to at least one dissolution process since their nucleation and growth in the mantle (Orlov, 1977). This dissolution not only modifies the external morphology, but it also leaves various etch figures on the surfaces of the crystal. Besides the best-known feature—trigons (small triangular depressions seen on some octahedral crystal faces)—many other dissolution features can be observed. In this presentation, some less common etch figures are discussed: etch channels (Lu et al., 2001), etch figures at twin boundaries, discoid sculptures (Wang et al., 2004), and nested etch patterns.

Etch channels of various forms, from parallel lines to irregular ribbon- or worm-like shapes, can be seen in both type I and type II diamonds from various localities (see, e.g., Johnson et al., 1998). These channels have surface openings with rhombic or modified rhombic shapes and, internally, they often terminate at mineral inclusions. They appear to originate either from the outcrop of a bundle of dislocations perpendicular to {111} planes, or along dislocation dipoles elongated along the <110> direction in the diamond. The final internal morphology of the channels varies depending on the interaction with other defects during the dissolution processes (Lu et al., 2001).

Etch figures associated with twin boundaries (contact twins) usually display high symmetry (such as hexagonal or rhombic forms). Most etch figures can be removed by polishing, but they will appear at the same locations if the faceted stone is etched again because twin boundaries penetrate deep inside most diamonds. Dislocations at the kinks of zigzag-like twin boundaries are preferential sites for the formation of these etch figures during selective dissolution processes.

Discoid sculptures and nest-like etch patterns on diamond surfaces are much less common than the etch channels and etch figures associated with the twin boundaries. "Crater-like" depressions were seen randomly scattered on the surface of a 2.70 ct diamond crystal with a modified dodecahedral/octahedral form, and were probably due to selective dissolution under specific chemical conditions (Wang et al., 2004). An etch pattern with triangular nested steps was seen on an octagonal face of a thick plate-like diamond crystal from Argyle, Australia (see figure). This pattern may have been caused by a selective and slow layer-by-layer dissolution of a fractured surface.

REFERENCES
Johnson M.L., Schwartz E., Moses T.M. (1998) When a drill hole isn't. *Rapaport Diamond Report*, Vol. 21, No. 45, pp. 1, 19, 21, 23, 25, 26.

This 1.66 ct diamond crystal from the Argyle mine shows a large nested triangular etched pattern completely covering one surface. Photo by Taijin Lu.

Lu T., Shigley J.E., Koivula J.I., Reinitz I.M. (2001) Observation of etch channels in several natural diamonds. *Diamond and Related Materials*, Vol. 10, No. 1, pp. 68–75.

Orlov Y.L. (1977) *The Mineralogy of the Diamond*. John Wiley & Sons, New York.

Wang W., Lu T., Moses T.M. (2004) Lab Notes: Moon-like surface on a [diamond] crystal. *Gems & Gemology*, Vol. 40, No. 2, pp. 163–164.

The Role of Brillianteering Variations in the GIA Cut Grading System

Ilene Reinitz (ireinitz@gia.edu)[1], Al Gilbertson[2], and Ronnie Geurts[3]
[1]GIA Laboratory, New York, [2]GIA Research, Carlsbad; [3]GIA Antwerp, Belgium

The GIA cut grading system for round brilliant diamonds includes seven components addressing appearance, craftsmanship, and design. We related these components to the average proportions, descriptions of girdle thickness and culet size, and the polish and symmetry grades provided in the GIA Diamond Grading and Dossier reports. The grading system also includes evaluation of cutting variations applied during the brillianteering process—purposeful, symmetric displacement of the upper and/or lower girdle facets, known in the trade as *painting* and *digging out* (see figure).

Because these facets (often called "halves" by diamond cutters) cover about 40% of the surface of the round brilliant, and are part of so many light paths through it, these brillianteering techniques can affect the overall appearance of a round brilliant as much as or more than variations in the average proportions. In some cases, painting (movement of the halves toward the adjacent bezel or main) or digging out (movement of the halves toward each other) is done specifically to manipulate the face-up pattern; in other cases, these techniques allow greater weight recovery, or ease the removal of inclusions. The average proportions are fully established before the upper and lower halves are polished, so they cannot describe the extent to which either brillianteering technique was applied. Painting and digging out can be assessed in several ways, but the most direct visual estimate is made from the appearance of the diamond's

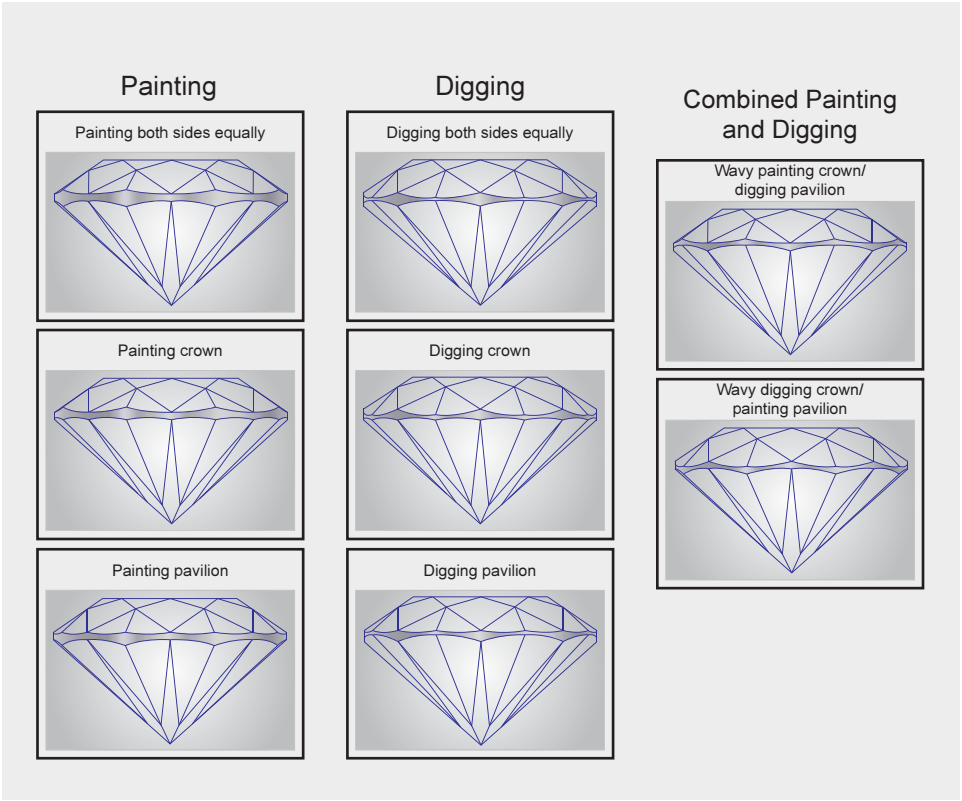

Variations in the placement of the upper and lower girdle facets (the "halves") can substantially impact the face-up appearance of a round brilliant diamond. Such variations can be applied independently to the crown and the pavilion. The most direct way to visually assess the degree of brillianteering is to examine the appearance of the girdle in profile view.

girdle in profile view. Asymmetries such as uneven crown height or wavy girdle can interfere with the assessment of brillianteering variations.

Like other appearance factors, we determined the impact of painting and digging out on overall appearance by analyzing human observations of round brilliant diamonds of common proportions, with and without various degrees of brillianteering variations. The many possibilities available to the diamond cutter for varying the half facets lead to a wide variety of visual effects. Brillianteering variations can reduce contrast, or increase it. They can enhance fire, sometimes at the expense of brightness, or they can enhance brightness, sometimes at the expense of fire. In general, moderate-to-significant brillianteering variations create differences in face-up appearance that may appeal to the taste of some diamond consumers, but severe variations cause defects in appearance that merit a low cut grade. Such variations are indicated with a comment on the grading report when it is the grade-setting factor. In conjunction with the overall grade, this comment alerts the report holder to look at the diamond's appearance and to make a personal judgment.

Preliminary Observations of a New Polishing Process for Colored Gems

Peter Richardson (peter@aurumplus.com)[1], Tom Stout[2], Carley McGee-Boehm[3], William Larson[4], and Edward Boehm[3]

[1]Aurum Plus, San Bernardino, California; [2]Veeco Instruments Inc., Tucson, Arizona; [3]JOEB Enterprises, Solana Beach, California; [4]Pala International, Fallbrook, California

A new process for polishing colored gems, diamonds, and finished jewelry—called PolishPlus—was introduced in 2003. Colored stones such as opal, amethyst, corundum, emerald, spinel, tanzanite, and tourmaline appear to show improvement in transparency, luster, brilliance, or phenomenon. Pearls, especially older worn pieces, show significant improvement in luster and surface quality. Mounted pieces of jewelry may be polished using this process, improving the appearance of the gems as well as providing brighter and smoother metal surfaces. This could prove useful to the antique and estate jewelry market, where removing a gemstone from its original setting for repolishing can sometimes compromise the value of the entire piece of jewelry.

The polishing process involves the use of various patent-pending and proprietary polishing mediums that employ special methods designed specifically for polishing gems and jewelry. PolishPlus employs a dry finishing medium ("MiracleMedia"), and special vibratory finishing machines with oscillatory motions of over 6,000 cycles per minute. The object being polished is bombarded from multiple directions with successive grits to sizes below 0.02 microns (which is about 1,000 times finer than the conventional industry standard grit). The polishing process can take from several hours to several days, depending on the material being polished. There are virtually no limitations on the size or shape of material that can be polished.

In an effort to scientifically substantiate the improvements in appearance, the authors have tested and photographed

numerous gem samples before and after the polishing. The experiments seem to indicate that the optical improvements are the result of a higher degree of polish than has previously been achieved on these gemstones. This results in more light entering the gem due to less hindrance from surface anomalies, and therefore a more beautiful gemstone. Using the Wyko optical profiling systems by Veeco Metrology Group, we measured the topography of the gemstones and metal surfaces at extremely high magnification. The instrument uses optical phase shifting and white light vertical scanning interferometry to produce detailed subnanometer measurements that are displayed on a computer monitor as three-dimensional color images. Samples with apparent visual improvements resulting from the PolishPlus process had improved polish to subangstrom levels.

Identification of Dyed Chrysocolla Chalcedony

Andy Shen (andy.shen@gia.edu), Eric Fritz, Dino DeGhionno, and Shane McClure
GIA Laboratory, Carlsbad

Chrysocolla chalcedony (marketed as "gem silica") is probably the most valuable variety of chalcedony. The material is colored by minute chrysocolla inclusions and usually ranges from an intense-to-vivid blue to blue-green. The diaphaneity of gem-grade material is semitransparent to semitranslucent. The color of this type of chalcedony is easily enhanced by soaking in water (Koivula et al., 1992; Johnson and Koivula, 1996). Furthermore, because colorless or milky chalcedony absorbs aqueous solutions readily, it can easily be dyed with inorganic cobalt or copper salts to simulate chrysocolla chalcedony.

Chrysocolla is a hydrous copper silicate mineral that forms from the weathering of copper minerals. Therefore, visible inclusions of chrysocolla together with other copper minerals (such as malachite) within the chalcedony provide the best evidence of natural origin. Visible absorption spectra and mineralogical associations are the main gemological criteria. If a chalcedony is dyed with cobalt, characteristic absorption lines (triplet at 620, 657, and 690 nm) may be seen with a hand-held spectroscope. However, for samples dyed by a copper solution with no clear mineral inclusions, we found that UV-Vis-NIR spectroscopy is necessary to identify them.

We recorded UV-Vis-NIR spectra of 29 untreated and 10 treated samples. A typical UV-Vis-NIR absorption spectrum (250–2500 nm) of natural chrysocolla chalcedony shows four distinct broad bands. A broad band covering 527–1176 nm (centered at ~721 nm) is due to the crystal-field effect of the Cu^{2+} ion in the chrysocolla lattice (Burns, 1993, p. 238). A band around 1300–1700 nm correlates to total OH content. The molecular water content is represented by a band at 1800–2100 nm. A band at 2128–2355 nm represents structurally bonded OH (Graetsch, 1994; Shen and Keppler, 1995). Furthermore, the concentrations associated with the four bands can be calculated if the path length and the absorption coefficient are known. We employed a simpler approach by looking at the ratio of the integrated areas under the Cu^{2+} (527–1176 nm) band and the structurally bonded OH (2128–2355 nm) band. All of the chalcedony colored by chrysocolla had a ratio between 7 and 44, whereas all of the samples dyed with copper solutions had a ratio from 0.5 to 3.

REFERENCES

Burns R.G. (1993) *Mineralogical Applications of Crystal Field Theory*, 2nd ed., Cambridge University Press, Cambridge, UK, 551 pp.

Graetsch H. (1994) Structural characteristics of opaline and microcrystalline silica minerals. *Reviews in Mineralogy and Geochemistry*, Vol. 29, No. 1, pp. 209–232.

Koivula J.I., Kammerling R.C., Fritsch E., Eds. (1992) Gem News: Chrysocolla-colored chalcedony from Mexico. *Gems & Gemology*, Vol. 28, No. 1, pp. 59–60.

Johnson M.L., Koivula J.I., Eds. (1996) Gem News: Update on porous chrysocolla-colored chalcedony. *Gems & Gemology*, Vol. 32, No. 2, pp. 129–130.

Shen A.S., Keppler H. (1995) Infrared spectroscopy of hydrous silicate melts to 1000°C and 10 kbar: Direct observation of H_2O speciation in a diamond-anvil cell. *American Mineralogist*, Vol. 80, No. 11/12, pp. 1335–1338.

Study of Interdependence: Fancy-Color Diamond Appearance, Cut, and Lighting Conditions

Sergey Sivovolenko (serg@next.msu.ru)[1] and Yuri Shelementiev[2]
[1]OctoNus Software, Moscow, Russia; [2]Diamond Design, Moscow

To optimize diamond cut proportions, we should consider three factors: illumination, the diamond, and human perception. These factors can be approximated by using computer modeling. During color grading, a diamond is compared against color master-stones in standard illumination and viewing conditions. However, diamonds are shown, sold, or worn in many different environments. Even if two of the above factors are fixed, a change in the third condition can dramatically change the overall perception of a diamond.

To study variations in a stone's appearance, we photographed yellow cubic zirconia in various faceted shapes using a symmetric ring-shaped, daylight-equivalent lamp and other illumination conditions. The same stones and lighting conditions were then modeled in DiamCalc software, and their three-dimensional models were obtained using a non-contact measuring device (Helium Polish scanner developed by OctoNus). The three-dimensional models contain information about each cut stone's shape, facet arrangement, real symmetry features, slope (angle), and index (azimuth) angles of each facet.

The DiamCalc software can closely model the appearance of polished colored stones in any lighting condition, and thus it is possible to model the appearance of any colored diamond in any cut, as represented in the figure. Even though these results were obtained for cubic zirconia, diamond appearance can be modeled with this software by using the appropriate refractive index in the calculations.

It is advisable to use several controlled lighting conditions when designing and optimizing new cuts because of diamond's variability in appearance under different lighting conditions. Diamond proportions with an inconsistent appearance under different types of lighting can be avoided. A good diamond cut should have an attractive appearance under all lighting conditions. One can use computer models of several common illuminations to predict a stone's appearance before it is cut.

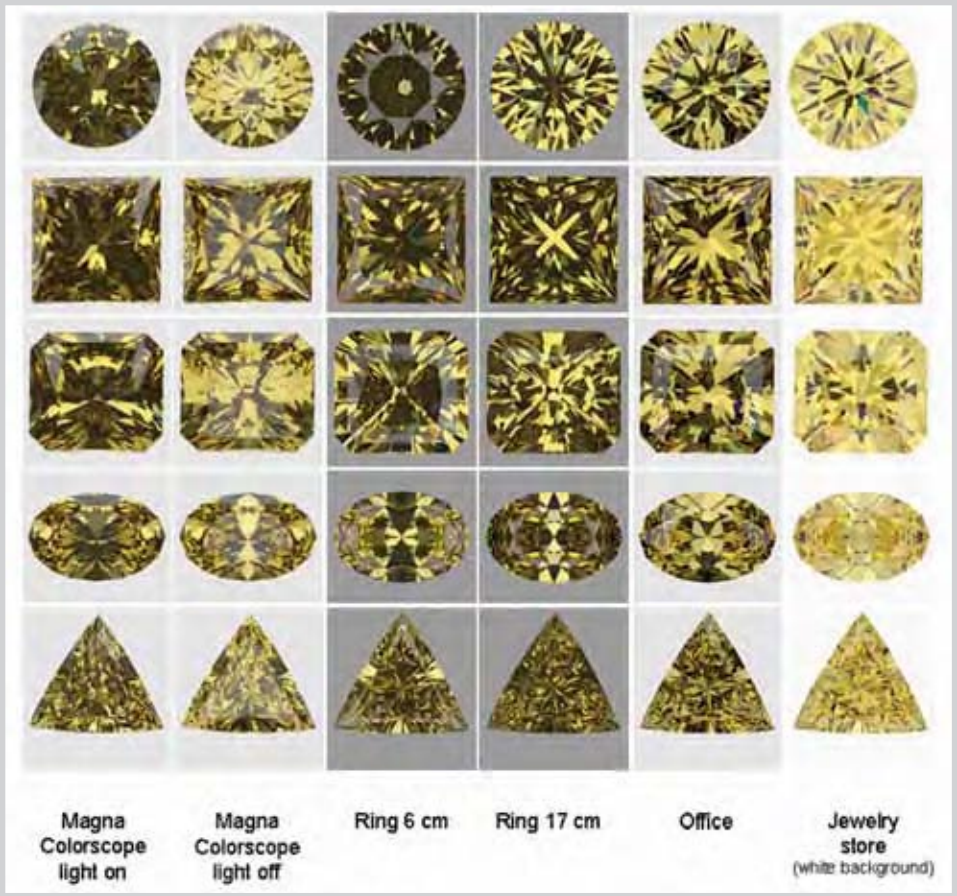

Various images of five cuts (round, princess, radiant, oval, and trilliant) were produced by modeling with DiamCalc software (here, for yellow cubic zirconia) under various illumination conditions. The round, princess, and radiant cuts are scanned models with real symmetry deviations, while the oval and the trilliant cuts are parametrical models. Each row contains images of the same cut modeled in different lighting conditions. "Magna Colorscope" lighting represents color grading illumination; these stones are tilted by 15° from the face-up position. The ring illuminations are symmetrical, while the office and jewelry store variations represent "real situation" lighting environments.

Comparative Investigation of Diamonds from Various Pipes in the Malaya-Botuobiya and Daldyn-Alakit Areas (Siberia)

Yulia P. Solodova (gigia@rol.ru)[1], Elena A. Sedova[1], Georgiy G. Samosorov[2], and Konstantin K. Kurbatov[3]

[1]GIA Russia, Moscow; [2]Russian State Geological Prospecting University, Moscow; [3]ALROSA Diamond Sorting Center, Mirny, Sakha, Yakutia, Russia

A selection of at least 2,000 diamond crystals from the Siberian craton, representing various size-weight groups, was examined from the following pipes: Dachnaya and Internationalaya in the Malaya-Botuobiya (M-B) area, and Udachnaya, Aikhal, and Jubileynaya in the Daldyn-Alakit (D-A) area. The mineralogical features and physical properties of diamonds within each area were quite similar, and they showed less variation than a comparison of diamonds from pipes from different areas.

According to Orlov's (1984) mineralogical classification, category I diamonds were prevalent (up to 98.8%) in the M-B area, and those remaining were category VIII. About two-thirds of the category I diamonds consisted of well-formed, flat-faced octahedrons. The proportion of category I diamonds was somewhat less (71–96%) from the D-A area. The balance of those diamonds were from a number of other categories (II, III, IV, V, VIII), consisting of flat-faced crystals, rounded crystals, and intermediate forms.

Category I diamonds from the M-B area were yellow and brown. Purple diamonds were also noted from both of those pipes. In crystals from the D-A area, browns dominated over yellows, or these colors were present in approximately equal amounts. Also present were gray diamonds and diamonds with a green skin. Intensely colored diamonds were rare from both areas.

Blue or pink fluorescence to long-wave UV radiation was noted in diamonds from both areas. Some diamonds from the D-A area showed yellow or green fluorescence.

IR absorption spectra showed that diamonds from the M-B area contained nitrogen, mostly as A centers. In D-A area diamonds from Udachnaya, the occurrence of nitrogen as B2 centers was higher than in those from the other pipes. Differences in B1 and H centers between diamonds from the two areas were not significant.

Diamonds from some of the pipes were studied using electron paramagnetic resonance (in collaboration with the Institute of Geology of Ore Deposits, Petrography, Mineralogy and Geochemistry of the Russian Academy of Sciences, Moscow). Paramagnetic centers containing Ni were found in diamonds from Jubileynaya, M2 centers were recorded in those from Internationalaya, and N1 centers were found in diamonds from Dachnaya.

Raman spectroscopy (in collaboration with the Institute of Element Organic Synthesis, Moscow) demonstrated that the average full width at half maximum (FWHM) values of the diamond Raman lines ranged from 2.4 to 3.4 cm^{-1}.

"Keshi" cultured pearls are observed in a variety of sizes, shapes, and colors.

In octahedral and dodecahedral crystals, the Raman FWHM was 2.4–3.0 cm^{-1}, and for the cuboid diamonds it was 3.2–4.0 cm^{-1}. Brown and gray diamonds had greater FWHM values than colorless and slightly yellow ones.

REFERENCE

Orlov Y.L. (1984) *Mineralogy of the Diamond*. Nauka Publishers, Moscow, 263 pp (in Russian).

The "Keshi" Pearl Issue

Nick Sturman (nick@commerce.gov.bh) and Ali Al-Attawi

Directorate of Precious Metals and Gemstone Testing, Ministry of Industry and Commerce, Manama, Kingdom of Bahrain

The word *Keshi* has traditionally been used to describe small natural saltwater pearls ("seed" pearls) as well as similarly sized pearls that resulted as a byproduct of the Japanese cultured pearl industry. Nowadays, the term is predominantly used to describe cultured pearls with sizes well above those that would be considered seed-like. Hence, *Keshi* is now used generically to describe any pearl byproduct without a bead nucleus that is produced by the culturing process (e.g., see figure), regardless of the ocean in which the pearl farm is located.

The contentious aspect of Keshi cultured pearls revolves around the following question: Can gemological laboratories differentiate between all Keshi cultured pearls and natural pearls? In our opinion and experience, the answer to this question is no. Some Keshi cultured pearls are instantly recognizable by their overall visual appearance, and their cultured origin can be further validated by their internal structural features, as revealed by X-radiography. In other cases, laboratories are faced with an identification issue that may be either straightforward (i.e., the X-radiographic structures are quite distinct, classifying them as tissue-nucleated cultured pearls) or difficult (i.e., they exhibit natural-appearing structures).

Quantity testing of Keshi cultured pearls (i.e., in rows, necklaces, or parcels) may be thought of as less complicated because the test results are based on those samples that show the most evident structures. However, this is not always true, and we often have to issue mixture, majority/minority, or even natural reports on parcels of what appear to be Keshi cultured pearls. When individual pearls are submitted (i.e., for a full test as opposed to batch testing), the situation may be trickier since only the structure of a single sample, and not a group of pearls, is available to the gemologist. If the structure appears natural by X-radiography, then a natural report can be issued. In our experience, individual pearls with internal structures that are undoubtedly natural will pass as such in most, if not all, laboratories.

We do not have a solution to the differences in opinion that exist in the trade regarding what constitutes a "Keshi pearl," and believe that a good deal of research still needs to be carried out on the subject.

A System to Describe the Face-up Color Appearance of White and Off-white Polished Diamonds

Thomas E. Tashey Jr. (ttashey@sbcglobal.net)[1,2] and Myriam C. Tashey[2]

[1]ID Gemological Laboratory, Ramat Gan, Israel; [2]Professional Gem Sciences, Chicago, Illinois

The traditional color grading of polished diamonds in the D-to-Z range is performed by observing them table-down in a standardized viewing environment, and comparing them to master stones of known bodycolor, also in the table-down position. Observing the diamonds table-down facilitates discerning subtle differences in the amount of color or of shades or tonal differences between them. There is generally a good correlation between the bodycolor observed table-down and the face-up color appearance of similarly sized and proportioned round brilliants. However, fancy-cut diamonds can show significantly more color face-up than round brilliants of the same color grade. Conversely, diamonds with strong blue fluorescence can appear to have less color face-up than non-fluorescent stones of the same color grade.

We propose a system to describe and classify the face-up color appearance of colorless and near-colorless polished diamonds. Face-up color appearance standards can be made from certain master comparison diamonds, and the color of polished diamonds can then be compared face-up to these standards. These standards should be nonfluorescent, very well made, round brilliant-cut diamonds that range from 6.0 to 7.0 mm in diameter. The colors of these master diamonds should be G, J, L, N, S, and W. The stones should be slowly rocked (tilted back and forth through an angle of ±30° from the table normal) while placed next to one another for comparison. Using this technique for fancy-cut diamonds, it should be noted that more yellow color will be observed in the table area than in their outer crown facets. Conversely, the round brilliants will show the most yellow color in their crown facets outside of the table area as they are rocked back and forth.

To describe color, we propose the standardized descriptions of Top White, White, Near White, Yellowish White,

Pale Yellow, and Very Light Yellow, as well as additional classifications for the fancy color range (see figure). This proposed system is based on standardized color nomenclature, and is also supported by Munsell color system standards.

Diamonds that have moderate or stronger blue UV luminescence should first be observed table-down with a UV filter to screen out the fluorescence. However, the face-up color appearance of these fluorescent diamonds should be observed without the UV filter, and any color enhancement due to the fluorescence should be allowed to upgrade their face-up appearance classification.

These standardized descriptions are suggested in addition to the traditional color grade listed on a diamond report.

Digital Color Communication for Gemstones, with an Exploration of Applications within Our Industry

Thom Underwood (thomu@cox.net)[1], Menahem Sevdermish[2], and Liat Sevdermish[2]

[1]Quantum Leap, San Diego, California; [2]Advanced Quality A.C.C. Ltd., Ramat Gan, Israel

The continuing maturation of the computer graphic interface has provided an environment suitable for effective gemstone color display and communication. Gem*e*wizard is a suite of digital tools providing a variety of solutions for gem color communication for students, gemologists, gemstone brokers, appraisers, and web-based jewelry companies.

Current applications include the Gem*e*square, one tool within the Gem*e*wizard suite that is used by GIA for the instruction of gemstone color science in their classrooms. Quantum Leap Appraisal Software has seamlessly integrated with Gem*e*square to virtually communicate gemstone color in the jewelry appraisal process. The Stuller Company uses aspects of Gem*e*wizard to improve communications within their gemstone ordering process.

Empirical measurement of gemstone color has proven elusive and impractical, as well as too expensive for common gem industry applications such as appraising and gem brokerage. Consequently, previous and currently available systems such as Gem Dialogue, GemSet, Color Scan, and the ColorMaster have relied on the human eye to compare the color(s) in a gemstone with the similar color(s) presented by the given system. Gem*e*square falls in this "comparative" category, but it uses a flat-screen LCD computer monitor to present the color palette to the user. While each color system may analyze and present the color palette differently, the common thread is the attempt to consistently "place" a gemstone within a reasonably small portion of color space, thereby effectively communicating the gemstone's color.

The digital environment used by Gem*e*square has many positive aspects as well as some weaknesses. Its strengths reside in its digital roots, making it convenient to calibrate the virtual color space, easy to integrate into commercial and professional applications, and simple to propagate the system and results to a potentially universal user base. Its weaknesses also reside in its digital roots, raising questions of monitor calibration (both comparative and over time), a monitor's inability to display very highly saturated colors, and questions regarding gem-viewing environments.

This chart shows the boundaries of the proposed color nomenclature on the D-to-Z scale and continuing into the fancy-color range; it applies for round brilliant–cut diamonds that are well made, 6.0–7.0 mm, and nonfluorescent. © Professional Gem Sciences 2006.

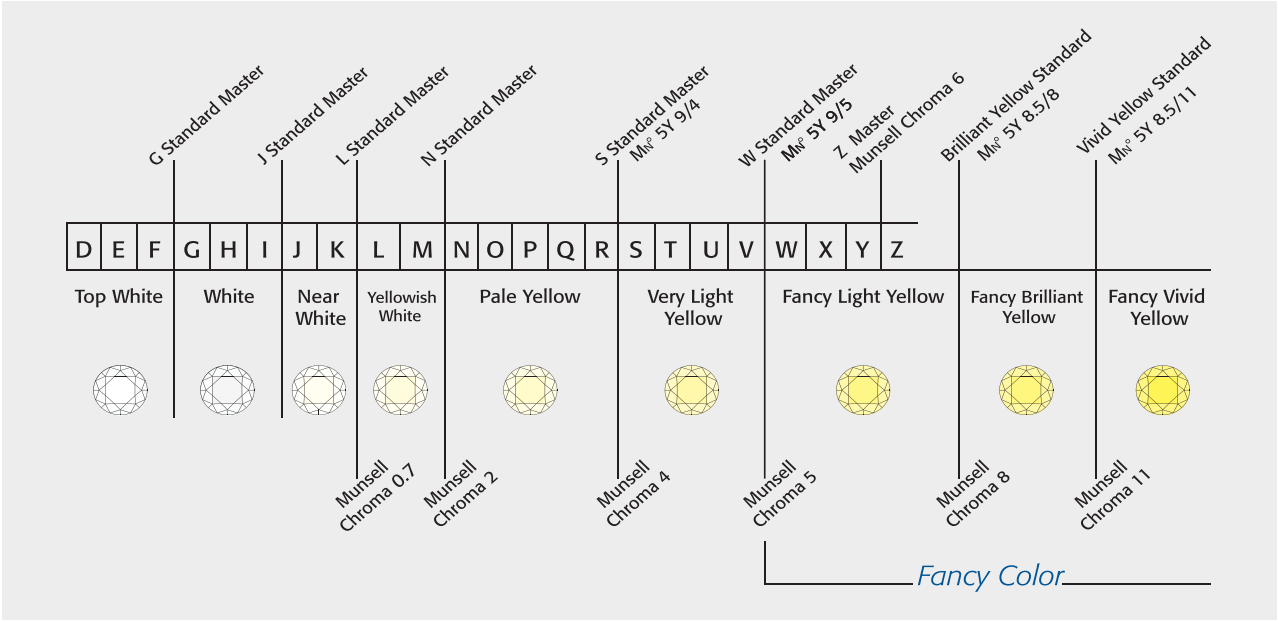

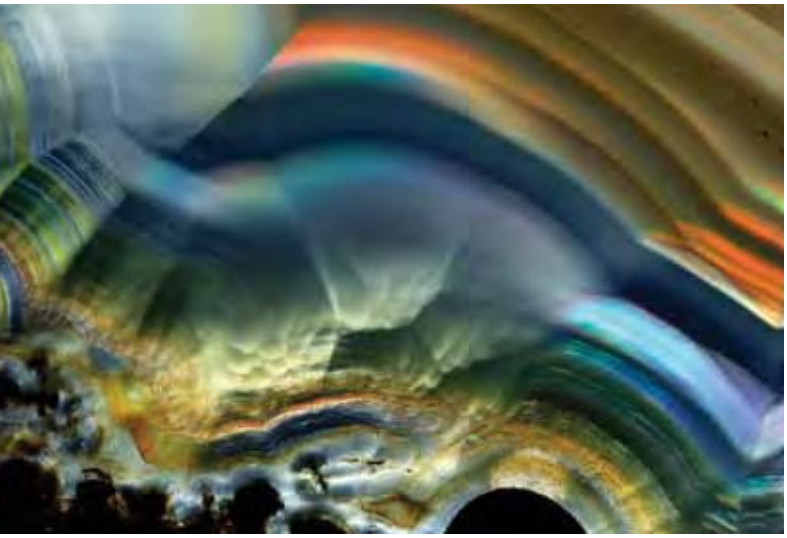

This thin slice of iris agate from Mexico was backlit using pinpoint fiber-optic illumination to reveal the iridescence in the agate bands. The field of view is approximately 2.5 cm wide; photo by R. Weldon.

Photographing Phenomenal Gemstones

Robert Weldon (robert.weldon@gia.edu)
Richard T. Liddicoat Gemological Library & Information Center, GIA, Carlsbad

Phenomenal gemstones pose unique challenges to gemologists. Chief among them is how to best light the gems to reveal their optical characteristics, such as chatoyancy, asterism, play-of-color, color change, iridescence (see figure), schiller effect, and labradorescence. Lighting the gem for photography parallels the actions taken by a gemologist to observe such phenomena.

Lighting is the most important aspect to consider when photographing phenomenal gems. With chatoyancy or asterism, the direction and intensity of the light source are crucial. Whether a light source is diffuse, or pinpointed and direct, also plays a role. A traditional three-point lighting system (in which gems are back- and side-lit) is not used for chatoyant or asteriated gems because the various light sources may cause phenomenal effects to appear in unintended parts of the gem. Even if side lighting is diffused, distracting reflections appear in cabochon-cut gemstones. Photographers prefer to rely on a single light source, aimed perpendicular to the convex top of the cabochon, to bring out asterism and chatoyancy.

A light source's color temperature is also important to render the correct color balance in photographs of gems and minerals. With digital photography, this adjustment can be corrected "in-camera." Color-change phenomena in gems are observed under specific lighting color temperatures. However, in both digital and film photography, capturing accurate color change under various lighting conditions is not as straightforward; in many cases "corrections" are made with direct observation and photo-editing software.

Not all phenomenal gemstones of a particular type require similar lighting. To observe play-of-color in opal, direct, pinpoint lighting is often thought to be ideal, but that is not always true. Some opals are successfully lit, and their play-of-color displayed, with diffused light—or with a combination of direct and diffused light.

Phenomenal feldspars, such as moonstone, sunstone and labradorite, require diffused illumination to exhibit the phenomena. In moonstones, diffused lighting, as well as the physical orientation of the gem, allows the photographer to judge where the gem's adularescence appears strongest (i.e., its photogenic angle). Adularescence is most obvious when a moonstone is photographed against a dark background. Copper platelet inclusions in American sunstones, which cause the schiller effect, may reflect too strongly with direct lighting, creating hot spots. In such cases, the gem may need to be tilted, or the camera angle changed, so that a plane of inclusions is softly illuminated. The goal is to illuminate the inclusions to show moderate-to-strong relief and sharp detail.

Recent Trends in World Gem Production

Thomas R. Yager (tyager@usgs.gov)
U.S. Geological Survey (USGS), Reston, Virginia

Estimates of world colored gemstone production are inherently difficult because of the fragmentary nature of the industry, the lack of governmental oversight in many countries where colored gemstones are mined, and the wide variation in quality of the production. Therefore, global production figures for colored gemstones have not been published previously by the USGS, although data are available for some individual countries.

Based on government data, company reports, and a review of the colored gemstone mining literature, the overall emerald, ruby, sapphire, and tanzanite production from 1995 to 2004 have been estimated. Amethyst and garnet production figures for selected countries also have been compiled.

Global emerald production increased from about 3,600 kg in 1995 to 5,900 kg in 2004; output rose in Colombia, Brazil, Madagascar, and Zambia. Colombia's status as the world's leading emerald producer was challenged by Brazil and Zambia. Brazil's emerald production increased sharply because of the development of large-scale mechanized mines.

World ruby production is also estimated to have increased, from about 4,400 kg in 1995 to 9,100 kg 2004. This increase was primarily attributable to greater production in Kenya, which tends to mine cabochon-grade ruby. Production declines in Myanmar and Tanzania were reversed in 2001 and 2004, respectively. Madagascar's ruby output increased because of the discovery of the Andilamena and Vatomandry mining areas.

Global sapphire production is estimated to have declined from about 26,200 kg in 1995 to 22,600 kg in 2004 as production increases in Madagascar and Sri Lanka were more than offset by decreases in Australia and Tanzania. In Australia, large-scale mining operations shut down or reduced output because of high production costs. Tanzania's production fell because of the depletion of near-surface deposits by artisanal and small-scale miners. In Madagascar, the discovery of sapphire at Ilakaka

and Sakaraha led to substantial increases in production from 1998–2000, but output has declined in 2003–04. Sri Lanka's production of geuda increased in 2003–04.

Tanzanite production declined from about 6,500 kg in 2002 to 3,100 kg in 2004 because of a lack of new deposits being discovered and higher costs associated with the increasing depths of small-scale mines in Blocks B and D at Merelani; cutbacks in production have not been offset by mechanized mining in Block C.

Gem production has shifted rapidly between countries and within countries in recent years. With the depletion of near-surface alluvial deposits, colored gemstone mining is likely to shift from small-scale to large-scale operations.

Geology of Gem Deposits

The Importance of Surface Features and Adhering Material in Deciphering the Geologic History of Alluvial Sapphires—An Example from Western Montana

Richard B. Berg (dberg@mtech.edu)[1] and Christopher F. Cooney[2]
[1]Montana Bureau of Mines and Geology, Butte, Montana; [2]Gem Mountain, Philipsburg, Montana

Western Montana hosts three large alluvial sapphire districts: terraces along the Missouri River east of Helena, placers along Dry Cottonwood Creek 25 km northwest of Butte, and placers in the Gem Mountain (Rock Creek) area 90 km northwest of Butte. Though the Gem Mountain district is the largest, the geologic processes leading to its formation are poorly understood. A detailed study of Gem Mountain sapphires and their adhering material by optical microscopy, scanning electron microscopy, energy-dispersive X-ray spectroscopy, and X-ray diffraction analysis has proven useful in deciphering their geologic history.

In the Gem Mountain district, metasedimentary rocks of the Proterozoic Belt Supergroup are overlain by Tertiary felsic volcanic rocks (both lava flows and tuffs). Sapphires recovered adjacent to weathered volcanics exhibit two types of adhering material. The most abundant is fine-grained kaolinitic clay that includes small glass shards. The surfaces of some of these sapphires, as revealed by removal of the kaolinitic coating, are almost completely covered by conchoidal fractures. Internal conchoidal fractures are also coated with a very thin layer of kaolinite. We interpret these features to indicate that these sapphires were brought to the surface by violent volcanic eruption, and the accompanying volcanic ash was weathered into kaolinite. Small remnants of adhering felsite on other samples are evidence that some of the sapphires in this district weathered from a volcanic rock. Careful removal of the felsite reveals a highly irregular surface, characterized by small flat depressions surrounded by mesa-like features that either formed during growth of the sapphire or by resorption during magmatic transport.

Whereas the bedrock sources for many well-documented alluvial sapphire deposits are basalt, we conclude that the sapphires in the Gem Mountain sapphire district were derived from Tertiary volcanic rocks of felsic composition. This interpretation is based on adhering felsic volcanic rock and associated volcanic ash. Abrasion during fluvial transport produced microscopic chips that are typically concentrated on projections on the surface of the sapphires.

Mining of Pegmatite-related Primary Gem Deposits

Jim Clanin (jclanin54@aol.com)
JC Mining Inc., Hebron, Maine

Mining gems from pegmatites requires a variety of techniques to remove the gem material without destroying it, and each deposit presents its own set of challenges. For nearly 30 years the author has mined several types of pegmatites around the world, and has developed mining techniques for various situations based on the geology and the available resources.

Granitic pegmatites with miarolitic cavities—such as those at the Cryo-Genie mine, San Diego County, California, and the Mt. Mica mine, Oxford County, Maine—should be mined with the utmost care to avoid drilling into or blasting near a gem "pocket." Mining at the Cryo-Genie usually consisted of drilling and blasting the individual blocks of pegmatite (i.e., between naturally occurring joints), while at Mt. Mica this was performed in two stages. First, the area above the core zone was removed to produce a bench, and then the bench was carefully blasted in search of pockets.

The John Saul ruby mine, Mangare, Kenya, is a metasomatic deposit where a desilication process resulted in a syenitic pegmatite called a plumasite. The pegmatite averages about 1 m thick and is the host for the ruby. There are no pockets associated with this pegmatite, but some areas have contained 40 vol.% of ruby. Since the mine is located within the boundaries of the Tsavo National Park, blasting was not permitted, so jackhammers and numerous workers were employed to remove the rock.

The Landaban Rhodolite group of mines is located near Mt. Kilimanjaro, Tanzania. The garnet is hosted by a near-vertical granitic pegmatite, within a 10-m-thick zone that is quartz-poor and feldspar-rich. Local miners traditionally utilized a hammer and chisel to move the rock and a gunnysack to remove the tailings. By using air-powered jackhammers and a chute system to remove the tailings, the removal of pegmatite rock was increased from about 1.4 to 52 tonnes per day.

The Ambodiakatra emerald mine in eastern Madagascar is similar to the emerald deposits of Zambia. In these deposits, the pegmatite–hydrothermal vein system is not the host for the gem material, but is the source of the Be needed for emerald crystallization. Open-pit mining was used to exploit this deposit and was conducted 24 hours per day, six days per week until the rainy season began. Holes to be loaded with explosives were bored with sinker drills during the night, blasting occurred in the morning, and the remaining time was spent removing the blasted rock with large excavators.

What Determines the Morphology of a Resorbed Diamond?

Yana Fedortchouk (yana@uvic.ca) and Dante Canil
School of Earth and Ocean Sciences, University of Victoria, British Columbia, Canada

Diamond resorption in kimberlite melts produces a variety of surface features. The most common are trigons, square etch pits, and the substitution of primary octahedral morphology with the hexoctahedron. The mechanism of diamond resorption in kimberlite magmas is not well understood, and therefore the causes of certain resorption features are unknown. Our experiments demonstrate that the fluid phase of kimberlite magma oxidizes diamonds. The composition of this fluid determines the shape of the diamond and the intensity of the surface resorption. Understanding the processes that lead to various natural diamond shapes will help to predict the quality of diamonds in a kimberlite pipe, to understand how these features can be imitated, to provide information on their mantle source, and to possibly distinguish diamonds from various localities.

We studied diamond oxidation at 100 kPa in a CO_2-CO gas-mixing furnace with controlled oxygen fugacity at 1000–1100°C. The diamonds were cut into cubes so that etch features on {100} surfaces could be studied. The square etch pits produced on {100} surfaces in the oxidized runs (high CO_2/CO ratio) differed in orientation, size, and shape from those produced at reducing conditions (low CO_2/CO ratio). The crystal edges were more rounded after the oxidized runs.

High-pressure experiments also were conducted, in a piston-cylinder apparatus at 1 GPa and 1350°C, in H_2O and CO_2 fluids. The oxidation was studied on {111} faces (octahedrons) and {100} surfaces (cut cubes). The primary octahedral morphology was much better preserved in CO_2 than in H_2O. Oxidation in H_2O produced a few large flat-bottom trigon etch pits on the {111} faces, and square etch pits on the {100} surfaces. In CO_2 the whole diamond surface became covered with numerous small trigons and some hexagonal etch pits on {111} faces, and square etch pits on the {100} surfaces.

The diamond lattice has different positions of open bonds in the three primary crystal planes: {111}, {110}, and {100}. We propose that the configuration of the molecules present in the fluid determines how fast they react with certain faces of a diamond. Differences in activity of the volatiles will (1) determine the diamond oxidation rate in the three crystal planes, (2) result in faster or slower disappearance of the primary octahedral morphology, and (3) determine the shape and number of etch pits on the diamond surface. Further experiments using fluid compositions relevant to natural kimberlite, and a better understanding of the chemistry of the reaction of volatiles with diamond, will help to explain the variety of natural diamond forms.

Jadeite Jade from Guatemala: Distinctions among Multiple Deposits

George E. Harlow (gharlow@amnh.org)[1], Sorena S. Sorensen[2], Virginia B. Sisson[3], and John Cleary[4]
[1]Department of Earth and Planetary Sciences, American Museum of Natural History, New York; [2]National Museum of Natural History, Smithsonian Institution, Washington, DC; [3]American Museum of Natural History, New York; [4]Ventana Mining Co., Reno, Nevada

The New World jade of Middle America came from deposits of jadeitite (jadeite rock) in serpentinite mélanges straddling the Motagua fault zone in central Guatemala. Sources north of the fault are now known to extend 100 km from east to west; to the south there are three distinct jadeite sources within a 15 km diameter zone.

Jadeitites north of the fault are associated with high pressure–low temperature metamorphic rocks (eclogites and garnet amphibolites) in serpentinites from Pachalum (Baja Verapaz Department) to Río Hondo (Zacapa Department). These jadeitites are all similar: whitish to gray-green with rare streaks of Imperial green (see figure), generally coarse grained (millimeter-to-centimeter scale), with albite, white mica, omphacite, and late analcime and *no* quartz. Darker green jadeitite is more common away from the fault. Other rocks used as "jade" and found with jadeitite include deep-green omphacitite (*Jaguar*) and omphacite-taramite rock (*Jade Negro*), a metasomatised mafic rock. Albitites are associated with jadeitite, and the assemblage indicates formation at 6–10 kbar and 300–400°C.

The jadeitites south of the Motagua fault zone (again, see figure) are sourced from three areas in the mountains of Jalapa and Zacapa Departments, and are individually distinctive:

1. Near Carrizal Grande, jadeitites coexist with lawsonite eclogites and blueschists. Colors vary from medium to dark green to blue-green (when light—*Olmec Imperial*; when dark—*New Blue*) with veins of dark green and/or blue omphacite; the translucency surpasses most northern jade. Phengitic muscovite is common, followed by titanite, lawsonite, omphacite, minor quartz, garnet, and rare analcime. Jadeite grain size is medium to fine (submillimeter), and alteration is minor. Assemblages indicate formation at 12–20 kbar and 300–400°C.
2. La Ceiba jadeitites are generally moderate-to-intense dark green, with occasional white, lavender, and dark Imperial color, and coexist with omphacite-glaucophane blueschists. Grain size is fine, translucency is good, but intense fracturing on the millimeter-to-centimeter scale makes this material difficult to work. Inclusions and veins consist of quartz, omphacite, diopside, cymrite, actinolite, titanite, and vesuvianite. Formation conditions are 10–14 kbar and 300–400°C.
3. La Ensenada jadeitite (marketed as *Lila* or *Rainbow jade*) is whitish and opaque with green, blue, orange, and "mauve" streaks and spots. It is a fine-grained jadeite-pumpellyite rock, veined with grossular (the source of orange color), omphacite, and albite, and contains minor titanite but no quartz. This rock is essentially iron-free and coexists with an iron-free-chlorite rock and lawsonite blueschists that formed at 6–9 kbar and from <200°C to ~300°C.

Some representative colors and textures of jadeite jade from Guatemala are shown here for samples recovered from either side of the Motagua fault zone: north side—Carrizal Grande, La Ceiba, and La Ensenada; south side—El Chol and Río Hondo(?). Photos by G. Harlow.

Mineral Assemblages and the Origin of Ruby in the Mogok Stone Tract, Myanmar

George E. Harlow (gharlow@amnh.org)[1], Ayla Pamukcu[2], Saw Naung U[3], and U Kyaw Thu[4]

[1]Department of Earth and Planetary Sciences, American Museum of Natural History, New York; [2]University of Chicago, Illinois; [3]Mogok, Myanmar; [4]Macle Gem Trade Lab, Yangon, Myanmar

The Mogok Stone Tract of Myanmar (Burma) is legendary for producing the finest rubies and spinels; however, the geology of the marble-hosted assemblages is complex. In particular, rubies have been ascribed to metamorphism of aluminous sediments, but Iyer (1953) argued that the association of ruby-bearing marble with pneumatolytic veins emanating from nearby intrusives was critical. In spite of difficulties in gaining access to mines and samples, progress has been made recently in understanding the characteristics and origins of gem minerals from the Tract.

Mineral assemblages involving corundum have been studied utilizing collections at the American Museum of Natural History (~300 specimens from more than 30 mines) and those of the Burmese authors (~900 specimens from ~20 additional localities). The hosting Mogok Metamorphic Belt of marbles and schists was formed from Proterozoic sediments (>750 million years ago [Ma]) that were metamorphosed and intruded by syenitic-to-granitic magmas during collision with a Gondwana fragment (Burma Block) in Cretaceous time (~150 Ma), and later with the Indian Block commencing in Eocene time (~50 Ma), with metamorphism continuing to ~20 Ma and intrusions to ~15 Ma. This complex geologic record helps explain the diverse mineral assemblages in the Mogok marbles.

The assemblage of ruby + calcite + graphite ± muscovite ± pyrite is most common, but colorless minerals adjacent to ruby may have been overlooked. Dattaw produces ruby in marble with conspicuous blue cancrinite/davyne and less obvious scapolite + colorless sodalite ± nepheline as well as phlogopite ± spinel ± pargasite ± tourmaline. Similar assemblages with scapolite, sodalite, nepheline, datolite, or moonstone are found elsewhere in the Mogok Tract at Kolan, Lay Oo, Ongaing, Pyant Gyi, Sakan Gyi, and the sources between Kabaing and Sinkwa: Wet Loo, Kyakpyatthart, and Thurein Taung. The silicates are typical of skarns, and they provide support for a likely interaction between magmas (or their fluids) and marble. The fact that rubies are surrounded by or connected to skarn-silicate veins may indicate ruby crystallization is affected or even produced by the skarn reactions.

Recent work on painite ($CaZrBAl_9O_{18}$; see Rossman et al., 2005 and http://minerals.caltech.edu) from mines in the Kabaing–Sinkwa area suggests growth during a skarn-forming event between leucogranite and marble. Associated minerals support this interpretation: scapolite, tourmaline, and margarite (as well as ruby). A conspicuous textural feature of these specimens is ruby crystallized on painite, demonstrating corundum growth during skarn formation.

References

Iyer L.A.N. (1953) *The Geology and Gem-Stones of the Mogok Stone Tract, Burma.* Memoirs of the Geological Survey of India, No. 82, 100 pp., 2 maps.

Rossman G.R., Naung S., Harlow G.E., Hunt J. (2005) Painite ($CaZrBAl_9O_{18}$): A second source in Myanmar and metasomatic origins. *Goldschmidt Conference Abstracts 2005*, A278.

Major Diamond Mines of the World: Tectonic Location, Production, and Value

A.J.A. (Bram) Janse (archonexpl@iinet.net.au)
Archon Exploration Pty. Ltd., Perth, Western Australia

The spatial distribution of the world's major diamond mines is intimately related to the age of the earth's crust (see figure). According to Clifford-Janse terminology, the three age-defined tectonic crustal elements are archons, protons, and tectons. At present, all diamond mines developed on kimberlite pipes are located within the boundaries of an archon, while those developed on lamproite pipes are located on a proton. Even though only one major diamond mine is underlain by a lamproite pipe (the Argyle mine in Australia), several small diamond mines on lamproite pipes and other occurrences of diamond-bearing lamproites support this view. The figure also shows that major diamond mines largely cluster into three regions of the world: southern Africa, Siberia, and western Canada.

The tabulated data (see table in the *G&G* Data Depository at www.gia.edu/gemsandgemology) show that Jwaneng in Botswana has the greatest current value and very high current production, followed by Udachnaya in Siberia, Orapa in Botswana, Ekati and Diavik in Canada, and Venetia in South Africa. The Argyle mine in Australia has a high production, but a low value. The most important producers for the next decade are likely to be Jwaneng, Orapa, Venetia, and Diavik, with Jubileynaya, Nyurba (Russia), Catoca (Angola), and Murowa (Zimbabwe) having slightly less importance. Argyle will continue to produce large quantities of near-gem material. The monetary values for the top six mines are in the same league as a major gold mine or a medium-sized oil field.

Data were also tabulated for seven advanced projects for which production is planned in the near future (although Jericho already commenced production in the first quarter of 2006, it is a small mine compared to Snap Lake). Victor is also small, but it has an extraordinary high value. Gahcho Kué is currently only a resource, not yet a proven reserve and only indicated reserves are available. Camafuca is an elongated pipe or the fusion of five pipes in a line underneath the bed of the

Most of the world's major diamond mines are located in Archean-age portions of the earth's crust. Also shown are several projects that are expected to begin producing diamonds in the near future.

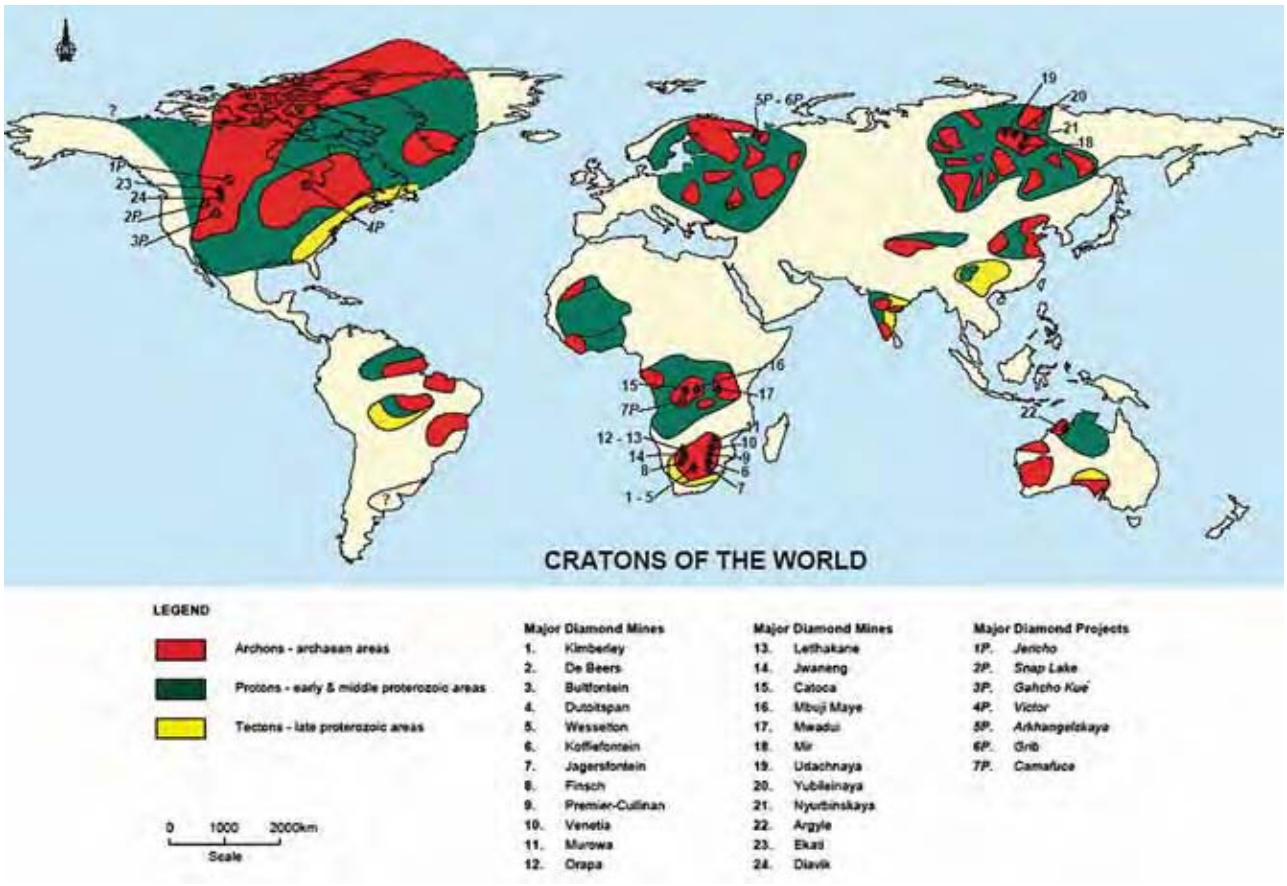

Chicapa River, and it will be first operated by a five-year dredging program.

The major mines of the future are Arkhangelskaya and Grib (both in Russia), but Grib's opening is hampered by litigation. The Arkhangelskaya pipe will be the first of the Lomonosov cluster of five pipes to open in 2007.

Geology of Placer Gem Deposits

James M. Prudden (jpruddenpgsgems@yahoo.com)
Prudden Geoscience Services, Elko, Nevada

Placer gem depositional environments consist of colluvial, fluvial, and beach deposits. The weathering of primary gem-bearing deposits forms overlying eluvial deposits, and the down-slope migration of the residual gems by both gravity and water creates colluvial deposits. Fluvial systems range from youthful through mature and old-age sedimentological regimes with associated channel geometries that determine the hydraulic energy and therefore the locations of gem deposition. Fluvial systems commence with straight steep-channel gradients, with low depth-to-width ratios containing unsorted clasts and larger gems. This evolves into to the downstream, low-energy, old-age fluvial systems with low channel gradients that host bedded, well-sorted smaller clasts deposited in a meandering fashion within a broad flood plane. Gems in this environment are smaller and more rounded. At the point where the river enters a marine or lacustrine environment, the resulting abrupt gradient change is very favorable for gem deposition. Wave energy and long-shore currents further winnow and transport gems in beach environments. Alpine and continental glaciers are nature's "bulldozers," and the braded fluvial streams that are fed from their melt water effectively concentrate the contained gems from the glacial rubble.

Gem characteristics such as specific gravity, hardness, shape, and durability will influence their related depositional environments and survivability, thus favoring the economic concentration of certain gems in the fluvial "milling" environment.

Select case histories of a variety of placer deposits illustrate the practicality of applying detailed geology and sedimentology to placer gem exploration: (1) Australian Tertiary modified paleo-colluvial type sapphire deposits, derived from the weathering of alkaline basalts, have been a major global source of sapphires. (2) Namibian long-shore diamond distribution along the Atlantic Ocean coast constitutes the world's most valuable diamond deposit, extending westward 100 km to the continental shelf edge and 200 km northward. The diamonds were originally liberated from South African kimberlites (and possibly more distant sources) by post-Gondwana erosion of the southern African craton, which commenced in the humid Middle Cretaceous with the formation of the ancient Karoo and Kalahari Rivers. Subsequent erosion of these diamondiferous placers was accomplished by the Orange River in the Miocene. Prolonged winnowing of the diamonds increased their value by about 500%. (3) Fluvial reworking of glacial sediments in British Columbia, Canada, concentrated sapphires and garnets from several cubic kilometers of glacial material. (4) A fluvial diamond deposit in China's Hunan Province was deposited on complexly weathered karst bedrock, which presents challenges to sampling and mining.

Three Parageneses of Ruby and Pink Sapphire Discovered at Fiskenæsset, Greenland

William Rohtert (william.rohtert@gte.net)[1] and Meghan Ritchie[2]
[1]True North Gems Inc., Vancouver, British Columbia, Canada; [2]Department of Earth Sciences, University of Cambridge, United Kingdom

In the Fiskenæsset district of southwest Greenland, gem-quality corundum mineralization is widespread, well developed, and locally abundant. Corundum mineralization is observed in three paragenetic styles: metamorphic, metasomatic, and hydrothermal. There are 18 corundum showings, including nine principal ruby occurrences, recognized across a geographic domain measuring 20 × 60 km. Ruby mineralization typically occurs at the hanging-wall contact of the Archean-age, cumulate-layered, Fiskenæsset anorthosite complex. The same intrusive contact with an overlying amphibolite covering a discontinuous basal package of metasedimentary rocks is also an environment known for chromite and platinum mineralization.

The metasomatic deposits contain ruby, pink sapphire, sapphirine, kornerupine, pargasite-tschermakite, phlogopite, and red spinel in matrix association with plagioclase, hornblende, enstatite, gedrite, sillimanite, and anthophyllite. The hydrothermal deposits contain ruby, dolomite-magnesite, and kyanite with fuchsite. The metamorphic deposits consist mainly of ruby, hornblende, biotite, and anorthite. Individually, the ruby-bearing zones measure up to 20 m thick and up to 200 m long. They occur as single showings, but also as multiple showings in alignment, collectively up to 2 km in strike length.

In 2004, True North Gems collected and processed 3 tonnes from the Siggartartulik (metasomatic) occurrence, historically the best-known ruby location in the district. This sample returned 9.73 kg/tonne total corundum, which was divided into 1.5% gem, 33.5% near-gem, and 65.0% non-gem (where *gem* is transparent to semitransparent, *near-gem* is translucent to semitranslucent, and *non-gem* is opaque). Typically, the gem-grade material is faceted, while near-gem is made into cabochons and non-gem produces beads. In 2005, the same company collected five 3-tonne, mini-bulk samples, one from each of the following showings: Lower Annertussoq, Upper Annertussoq, Kigutilik, Ruby Island (Tasiusarsuaq), and Qaqqatsiaq. These samples were processed by standard mineral extraction techniques routine to the modern diamond industry, including dense-media separation and optic sorting, at the laboratory of SGS Lakefield Research Ltd. in Peterborough, Ontario, Canada. A total of 889.1 kg of corundum-rich concentrate was obtained, along with 29.8 kg

of nonliberated hand-picked corundum on matrix, and another 9.6 kg of hand-picked liberated ruby and pink sapphire. Preliminary results are encouraging for the Kigutilik (metasomatic) and Upper Annertussoq (hydrothermal) showings. Optic-sorting results indicate that the hydrothermal-type deposit shows the highest percentage of gem-quality ruby. Fiskenæsset is an advanced exploration project on trajectory for production feasibility in 2008.

Controls on Mineralization in Block D′ of the Merelani Tanzanite Deposit, Tanzania

Reyno Scheepers (admin@searchmin.com)
Unit for Gemstone Geology, University of the Free State, Bloemfontein, South Africa

Tanzanite is found at only one location on Earth, the western slopes of the Lelatema mountain range ~60 km south-southeast of Mount Kilimanjaro in northeastern Tanzania. The Lelatema Mountains form part of the Eastern Granulite Complex of the Mozambique Orogenic Belt. Tanzanite mineralization resulted from a prolonged geologic history, and it shows the delicate interrelationship between primary deposition, diagenesis, metamorphism, structural geology, and geochemistry to create one of nature's most remarkable gems. The geology of Block D′ is an example of the typical mineralization style of a tanzanite deposit. Three mining shafts have been sunk at Block D′, which borders Block D to the north side.

The deposit is flanked to the west and east by 040° striking dolomitic marble units that dip ~45° northwest. Sillimanite-kyanite-garnet gneiss occurs parallel to the dolomitic marbles. Within and parallel to the sillimanite-kyanite-garnet gneisses are zones of graphite-kyanite gneiss. The graphite-kyanite gneiss hosts several subparallel layers of metasomatic rocks consisting of calcic plagioclase, grossular, diopside, and zoisite. These layers are also wrapped around boudins (sausage-shaped structures) with relict skarn cores, in which quartz-diopside layers acted as competent units during metamorphism and boudin formation.

The boudin zones are repeated throughout the succession by tight isoclinal folds, verging northwest with fold axes plunging 20° from horizontal in a north-northeasterly direction. Further deformation of the stratigraphic sequence took place during folding associated with Pan-African metamorphism (620–500 million years ago).

The stratigraphic succession is typical for a sequence developed in a shallow marine shelf environment with intermittent addition of volcano-sedimentary material. Vanadium was introduced into the succession by the volcanic component, and organically enriched and further concentrated during early diagenesis by adsorption on clay minerals. The volcanic component is further evident by the abnormally high enrichment of Zn in specific layers of the sequence.

Quartz-diopside skarn layers developed during prograde metamorphism (850°C and 13 kbar). These layers were boudinaged and folded during two-dimensional shortening. V-bearing grossular garnet (tsavorite) crystallized in trap sites associated with boudinage. During an extended period of isobaric cooling, dewatering, and retrograde reaction, tsavorite reacted to form quartz, calcite, and tanzanite (V-bearing zoisite; Scheepers and Olivier, 2003). The ore body was further complicated by a series of shearing events that created secondary boudins and renewed tanzanite crystallization.

REFERENCE
Scheepers R., Olivier B. (2003) Geology and geochemistry of the Merelani tanzanite deposit. *Geoforum 2003*, Johannesburg, South Africa, June 25–27, p. 11.

Texture and Composition of Kosmochlor and Chromian Jadeite Aggregates from Myanmar: Implications for the Formation of Green Jadeite

Guang-Hai Shi (shigh@cugb.edu.cn)[1], Bernhard Stöckhert[2], and Wen-Yuan Cui[3]
[1]School of Gemology, China University of Geosciences, Beijing; [2]Institut für Geologie, Mineralogie und Geophysik, Ruhr-Universität Bochum, Germany; [3]School of Earth and Space Sciences, Peking University, Beijing

The jadeite mines of Myanmar (Burma) are the principal source of top-grade jade, including Imperial jadeite. Petrologically, Imperial jadeite is a fine-grained, Cr-bearing jadeitite. However, it is unclear how Cr^{3+} from chromite impurities became incorporated into the jadeite. We have studied the textures and compositions of kosmochlor and chromian jadeite aggregates (including maw-sit-sit) collected from the Myanmar jadeitite area to explore how the best-quality jadeite formed.

There are four distinct textures of kosmochlor and chromian jadeite: (1) spheroidal or ellipsoidal aggregates surrounding relict chromite; (2) spheroidal or ellipsoidal aggregates with a core of low-Cr jadeite; (3) granoblastic textures in undeformed coarse-grained clinopyroxene rocks, and (4) recrystallized fine-grained aggregates of deformed low-Cr jadeitite (see figure).

Electron-microprobe analysis revealed four compositional pairs of coexisting kosmochlor (Ko) and chromian jadeite (Jd) along the Ko–Jd join. Sharp compositional boundaries between them suggest the possibility of miscibility gaps or different stages of replacement of kosmochlor by jadeite. However, replaced textures of kosmochlor by jadeite exclude the possibility of miscibility gaps. The correlation between the textures and compositions of kosmochlor and jadeite is more likely associated with replacement at different stages of formation or spatial differences in the chemical environment. The presence of relict chromite in spheroidal or ellipsoidal aggregates with kosmochlor indicates a metasomatic origin of the jadeitites from original peridotites that reacted with an aqueous solution rich in Na, Al, and Si at a minimum pressure of 1.0 GPa and temperatures of 250–370°C (Shi et al., 2005). Recrystallization during later ductile deformation of the clinopyroxene rocks formed fine-grained aggregates of chromian jadeite, including the Imperial jadeite.

The textural and compositional features of the studied samples suggest that the chromium in the jadeite came from

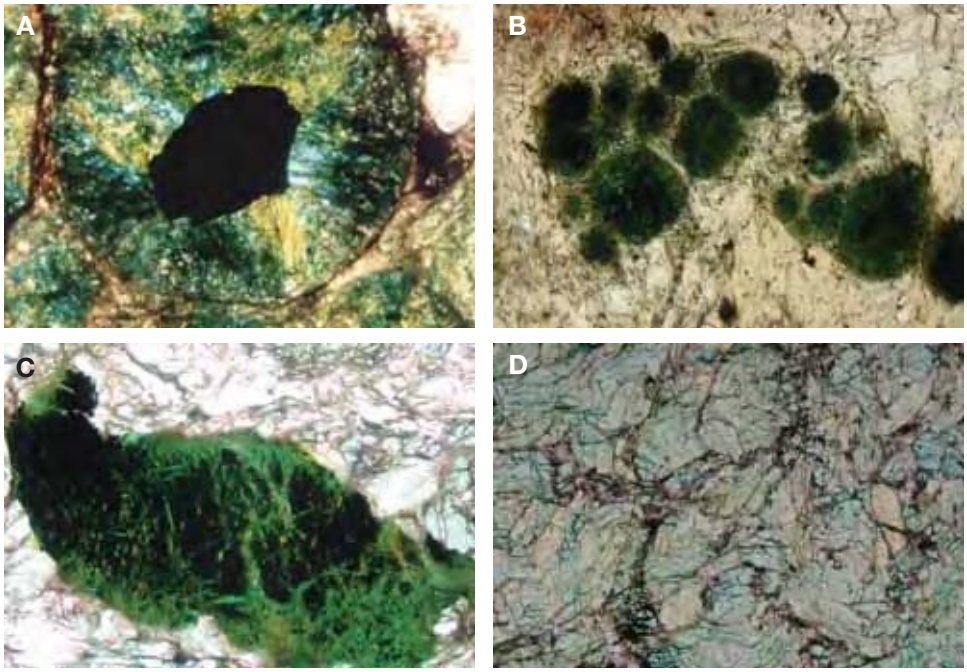

The four types of textures exhibited by kosmochlor and chromian jadeite aggregates in Myanmar jadeite are: (A) spheroidal or ellipsoidal aggregates with a residual chromite core; (B) spheroidal or ellipsoidal aggregates with a core of low-Cr clinopyroxene; (C) granoblastic textures consisting of relict chromite surrounded by kosmochlor and chromian jadeite; and (D) deformed and partially recrystallized chromian jadeite. Photomicrographs by Guang-Hai Shi; plane polarized light.

chromite in the adjacent host serpentinite. The chromium was incorporated into the jadeite via the following sequence: (1) metasomatic reactions of chromite to kosmochlor, forming spheroidal textures or granoblastic textures; (2) replacement reactions of kosmochlor to chromian jadeite, accompanied by metasomatism; and (3) replacement reactions of chromian jadeite to Cr-bearing jadeite (about 0.3 wt.% Cr_2O_3 in Imperial jadeite), accompanied by recrystallization induced by deformation. Further evolution of the final sequence led to the formation of light green jadeite with lower Cr contents. These processes were influenced by the local mineral assemblage, the characteristics of deformation/metamorphism induced by shearing, the pressure-temperature conditions, and local fluid compositions.

REFERENCE
Shi G.H., Stöckhert B., Cui W.Y. (2005) Kosmochlor and chromian jadeite aggregates from the Myanmar jadeitite area. *Mineralogical Magazine*, Vol. 69, No. 6, pp. 1059–1075.

Pegmatite Genesis—Complex or Simple Emplacement? Revisiting Southern California Pegmatites

Lawrence W. Snee (lsnee@usgs.gov)[1], Eugene E. Foord[1,*], Douglas M. Morton[1], Gary P. Landis[1], Robert O. Rye[1], and J. Blue Sheppard[2]
[1]U.S. Geological Survey, Denver, Colorado; [2]Millennium Inc., Pala, California

* Eugene E. Foord is deceased.

Are complex zoned pegmatites the product of a single injection event and the subsequent rapid cooling of late magmatic volatile-rich residual silicate melt? Some field and mineral paragenesis relationships suggest that some pegmatites were not the result of a single emplacement event. Pegmatite conductive cooling models (e.g., Webber et al., 1999) predict that crystallization and cooling of the magma occurred rapidly, on the order of days or years, at the most. The conductive cooling models also assume single-stage emplacement.

Snee and Foord (1991) used argon thermochronology to define the emplacement age and cooling history of gem- and specimen-producing granitic pegmatites and their host rocks in the Pala, Ramona, and Mesa Grande districts of San Diego County, California. The results showed that the pegmatites were emplaced into cool (<150°C) country rocks that are several million years older than the individual pegmatites. The apparent ages of white mica from the pegmatites ranged from 100 to about 93 million years. Surprisingly, the muscovite cores of several zoned-mica samples of the Little Three pegmatite were up to 1.3 million years older than their corresponding rims of similar composition. More recent work at other mines in southern California also document anomalous differences in the apparent ages—within single pegmatites. These mica age differences are due either to differential cooling rates, to different argon closure temperatures, or to different times of crystallization (e.g., a complex multi-event pegmatite emplacement). Field, mineral paragenesis, and fluid inclusion evidence (Cook, 1979) suggest that the classic zoned Harding pegmatite in New Mexico may also be a product of complex emplacement processes.

We have begun a more comprehensive study of these pegmatites to better understand observed mica age differences and pegmatite genesis, emplacement, and evolution processes. Along with revised mineral paragenesis and recognized complex cross-cutting field relationships, new argon and U-Pb geochronology, fluid inclusion microthermometry and gas-solute chemistry, noble gas and stable isotope compositions, and field relationships should provide insights into the magma-volatile processes, sources of components, and pegmatite emplacement rates and processes. Additional studies, such as

that of Smith et al. (2005), which showed that incorporation of Li, F, Rb, and Cs in the mica structure resulted in lower argon closure temperatures in lepidolite, will be done to evaluate the effects of chemical zonation in white mica on argon retention.

REFERENCES

Cook C.W. (1979) Fluid Inclusions and Petrogenesis of the Harding pegmatite, Taos County, New Mexico. Masters Thesis, University of New Mexico, Albuquerque, 143 pp.

Smith S.R., Kelley S.P., Tindle A.G., Breaks F.W. (2005) Compositional controls on $^{40}Ar/^{39}Ar$ ages of zoned mica from rare-element pegmatites. *Contributions to Mineralogy and Petrology*, Vol. 149, pp. 613–626.

Snee L.W., Foord E.E. (1991) $^{40}Ar/^{39}Ar$ thermochronology of granitic pegmatites and host rocks San Diego County, California. *Geological Survey of America Abstracts with Programs*, Vol. 23, No. 5, p. A479.

Webber K.L., Simmons W.B., Falster A.U., Foord E.E. (1999) Cooling rates and crystallization dynamics of shallow level pegmatite-aplite dikes, San Diego County, California. *American Mineralogist*, Vol. 84, pp. 708–717.

Geology of "True" Hiddenite Deposits

Michael A. Wise (wisem@si.edu)

National Museum of Natural History, Smithsonian Institution, Washington, DC

Spodumene ($LiAlSi_2O_6$) is a relatively common mineral that is found predominantly in lithium-rich granitic pegmatites. Transparent, facetable spodumene may crystallize in miarolitic cavities or "pockets" that develop within some pegmatites that are emplaced at shallow crustal levels. Gem-quality spodumene may display lilac-to-pink colors (kunzite), pale yellow hues, or various shades of green. Gemmy gray to gray-blue spodumene may also occur, but these colors are not stable in sunlight and rapidly fade to pink hues. The color of chromium-bearing spodumene (hiddenite) varies from yellowish green to light green, bluish green, "grass" green, and to bright "emerald" green, the rarest and most desired color. Although "emerald" green spodumene, which was originally found near the town of Hiddenite, North Carolina, is considered to be the standard, the name *hiddenite* has also been misleadingly applied to ordinary pale green spodumene. The distinction between "true" hiddenite and other green varieties is significant and is based on differences in coloring agents, mode of formation, intrinsic properties (e.g., luminescence), and geologic setting.

The Hiddenite area of western North Carolina constitutes the most significant emerald-producing region in North America, and is the world's only confirmed locality for "true" hiddenite, which occurs in cavities hosted by steeply dipping quartz veins that crosscut highly deformed migmatitic schists and quartz-biotite gneiss. Associated minerals that line the cavity walls include: albite, calcite, chabazite, clinochlore, graphite, muscovite, pyrite, quartz, and rutile. Emerald, which occurs in similar quartz veins in the area, is never found together with "true" hiddenite. The crystal morphology of calcite, quartz, rutile, and pyrite can be used to differentiate between hiddenite-bearing and emerald-bearing veins.

Electron-microprobe analyses of "true" hiddenite showed fairly uniform major-element chemistry; only iron concentration varied within narrow limits (0.68–1.63 wt.%, as Fe_2O_3). The chromium content was low (typically less than 0.2 wt.% Cr_2O_3), but significantly higher than that of green spodumene from granitic pegmatites, which typically do not contain chromium. Vanadium was generally below the detection limit of the microprobe (<0.1 wt.% V_2O_3).

The crystallization temperature and pressure of "true" hiddenite as determined by fluid inclusion studies were well below the experimentally determined P-T stability field for spodumene from pegmatites. Stabilization of spodumene to low pressures (<1 kbar) and low temperatures (<250°C) may be related to the presence of relatively high concentrations of Fe and Cr, the source of which is currently unknown. The paragenesis of the open fissures at Hiddenite is typical of Alpine-type veins and represents the first documented occurrence of spodumene formed under hydrothermal conditions.

Laboratory Growth of Gem Materials

Optical Characterization of CVD Synthetic Diamond Plates Grown at LIMHP-CNRS, France

Ans Anthonis (anan@hrd.be)[1], Olivier De Gryse[1], Katrien De Corte[1], Filip De Weerdt[1], Alexandre Tallaire[2], and Jocelyn Achard[2]

[1]Hoge Raad voor Diamant (HRD) Research, Lier, Belgium; [2]Laboratoire d'Ingénierie des Matériaux et des Hautes Pressions–Centre National de la Recherche Scientifique (LIMHP-CNRS), Université Paris 13, France

In this study, eight monocrystalline CVD synthetic diamond plates, grown in 2004 by the diamond group at LIMHP-CNRS, were investigated for the first time. The nitrogen content intentionally added to the gas phase ranged between 0 and 6 ppm. The samples were studied by optical microscopy, surface luminescence imaging (DiamondView), and FTIR, laser-induced photoluminescence (PL), and UV-Vis spectroscopy. Seven of the plates received a Gran color grade of "E" or better (i.e., colorless), and the eighth plate was brown. All the samples were type IIa and had a thickness between 175 and 785 μm and horizontal dimensions between 3.8 and 5.7 mm. They showed typical orange or blue fluorescence in the DiamondView, depending on the amount of nitrogen (more nitrogen caused a more orange fluorescence). When viewed with crossed polarizers and diffuse illumination, each sample showed cross-shaped birefringence patterns. These patterns have never been observed in natural diamonds. The patterns were more distinct in specimens with a higher amount of nitrogen added to the gas phase during growth.

Spectroscopic analysis revealed the presence of a feature at 737 nm (related to Si-V defects) in absorption and/or PL (see figure, left spectrum). In addition, the PL spectra of most of the samples showed N-V centers (575 nm peak), and some showed a doublet at 596.5/597.5 nm and/or a peak at 533 nm. The FTIR spectra of some samples showed H-related peaks at 3323 and 3123 cm^{-1}. All these characteristics are in agreement with the results of Martineau et al. (2004).

HPHT treatment of the brown sample in a BARS press (2300°C for 15 minutes) caused the brown color to decrease. The fluorescence in the DiamondView changed from orange

in the as-grown sample to green in the treated sample. An additional FTIR peak at 3027 cm^{-1} appeared, and the H-related peaks at 3323 and 3123 cm^{-1} disappeared. PL spectroscopy (see figure, right spectrum) revealed the annealing of the N-V centers. The peak at 737 nm was still clearly visible and had broadened. The 596.5/597.5 nm doublet was not observed, and new features at 451–459 nm were recorded after treatment.

All the samples (as-grown and HPHT treated) could clearly be identified as CVD synthetic diamond through a combination of microscopic observation and spectroscopic analysis.

REFERENCE

Martineau P.M., Lawson S.C., Taylor A.J., Quinn S.J., Evans D.J.F., Crowder M.J. (2004) Identification of synthetic diamond grown using chemical vapor deposition (CVD). *Gems & Gemology*, Vol. 40, No. 1, pp. 2–25.

New Data for Distinguishing between Hydrothermal Synthetic, Flux Synthetic, and Natural Corundum

Alexei S. Bidny (bidny@mail.ru), Olga S. Dolgova, Ivan A. Baksheev, and Irina A. Ekimenkova

Division of Mineralogy, Department of Geology, Lomonosov University, Moscow, Russia

The synthesis of colored corundum became widespread long ago. The most common growth techniques are Verneuil (flame fusion), flux, and hydrothermal. Each of these methods may be used to grow large crystals of various colors, thereby making synthetic corundum readily available and inexpensive. Differentiating natural and synthetic corundum is not challenging. Microscopy, FTIR, UV-Vis, and EDXRF data are sufficient in all cases to make this distinction.

For this study, 34 rough samples consisting of natural corundum from various deposits, and synthetic corundum grown by the flux and hydrothermal methods, were studied by spectroscopic techniques and oxygen isotopic analysis.

The IR spectra of the hydrothermal synthetic samples showed strong absorption bands related to OH complexes at 3600–3100 cm^{-1}. These "water" bands were much less evident in the spectra of the natural stones, and were absent from the flux synthetic corundum.

Photoluminescence spectra were also collected to distinguish between natural and flux synthetic corundum. The excitation spectra for red photoluminescence caused by chromium impurities displayed a pair of broad bands with maxima at 410 and 550 nm in all samples. However, the synthetic corundum (both flux-grown and hydrothermal) also displayed an excitation band at 290 nm (see figure, left spectrum). (*Editor's note*: An excitation spectrum plots the intensity of radiation emitted by a sample as the wavelength of excitation is varied.) The emission region for that electron transition lies between 380 and 490 nm, and therefore may excite red chromium fluorescence, so identifying the center responsible for the 290 nm band is difficult.

Distinctive features were revealed in the UV absorption spectra of the samples. In addition to common chromium and iron absorptions there was a band at 342 nm in the spectra of the flux synthetic corundum (see figure, right spectrum).

Oxygen isotopic composition was studied by a MAT-250 mass spectrometer at GEOCHI RAS (Institute of Geochemistry and Analytical Chemistry, Russian Academy of Sciences), Moscow, Russia. The isotopic composition of the natural samples and flux synthetic corundum were quite different from those of the hydrothermal synthetics. The $\delta^{18}O$ value for most of the natural samples ranged from +2.0 to +9.1‰, although

These photoluminescence spectra (514 nm excitation) were taken of CVD synthetic diamonds before (left) and after (right) HPHT treatment.

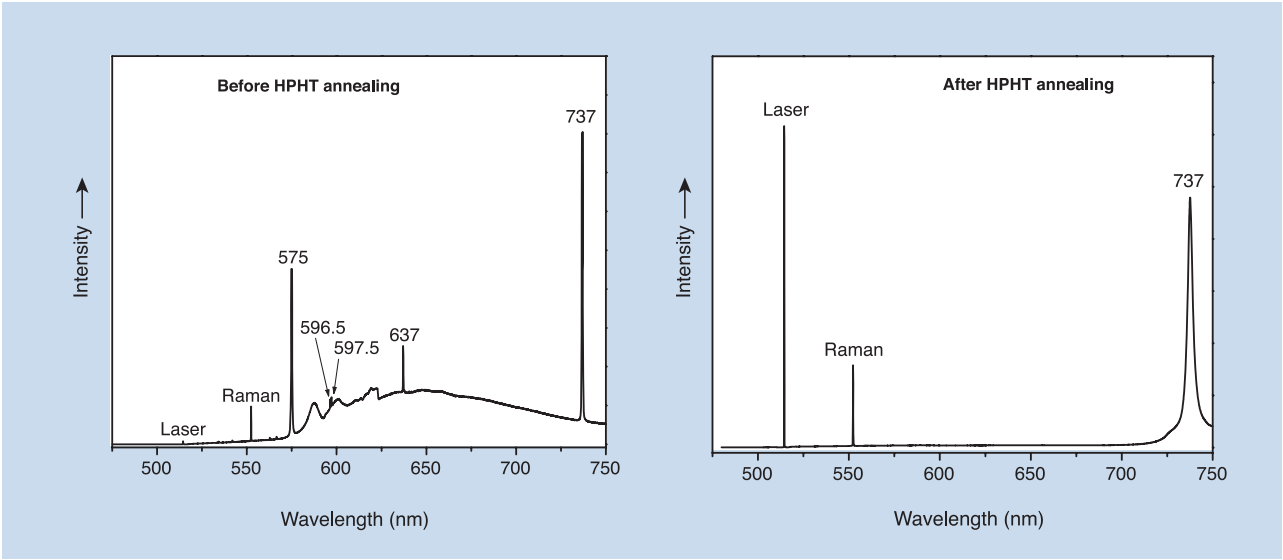

values up to +23.0‰ have been reported for natural corundum (Giuliani et al., 2005). The $\delta^{18}O$ value for the flux synthetic corundum ranged from +4.8 to +14.8‰, and for the hydrothermal synthetic samples it ranged from −5.8 to −0.7‰.

In combination with standard gemological observations, isotopic analysis can help distinguish natural and hydrothermal synthetic corundum. Since isotopic analysis is a destructive technique, it may best be used for rough corundum.

Acknowledgments: The isotopic study was financially supported by the Gemological Centre of Lomonosov Moscow State University.

REFERENCE
Giuliani G., Fallick A.E., Garnier V., France-Lanord C., Ohnensteter D., Schwarz D. (2005) Oxygen isotope composition as a tracer for the origins of rubies and sapphires. *Geology*, Vol. 33, No. 4, pp. 249–252.

Study of Fancy-Color and Near-Colorless HPHT-grown Synthetic Diamonds from Advanced Optical Technology Co., Canada

Branko Deljanin (brankod@eglcanada.ca)[1], Dusan Simic[2], Marina Epelboym[2], and Alexander M. Zaitsev[3]
[1]EGL Gem Lab, Vancouver, British Columbia, Canada; [2]EGL USA, New York; [3]College of Staten Island, City University, New York

Laboratory-created diamonds now on the market are grown under high-pressure, high-temperature (HPHT) conditions, and in the last few years, they have become more available in the jewelry trade. EGL USA has studied yellow-to-orange synthetic diamonds from Chatham Created Gems and the Gemesis Corporation (Woodring and Deljanin, 2004), and as a result of this research is offering a laboratory service of testing and certifying synthetic diamonds.

This is the first study of synthetic diamonds created by Advanced Optical Technologies Corp. (AOTC), based in Ottawa, Canada. They are producing as-grown yellow-to-orange, blue, and near-colorless synthetic diamonds, as well as pink-to-purple ones that are produced by the irradiation and annealing of as-grown yellows. Produced in Europe using Russian BARS-type presses, the crystals typically weigh 1–4 ct, and the polished samples are 0.50–2 ct. Recently AOTC has started commercially selling their synthetic diamonds for jewelry purposes in North America under the name "Adia Created Diamonds." All of the faceted stones are certified and laser inscribed as "AOTC-created" at EGL in Vancouver, Canada. Since the color of AOTC-created diamonds is stable, EGL is grading them with the same terminology that is used for natural diamonds.

We examined the following AOTC synthetic diamonds: 247 yellow to orange (Fancy Light to Fancy Vivid), 68 blue (light to Fancy Vivid), eight pink to purple (Fancy Intense to Fancy Deep), and five near colorless (D to I). Some contained gray metallic inclusions that were irregular in shape and very different from crystals seen in natural diamonds. Their clarity grades ranged from VVS to I, with the majority (59%) in the VVS to VS categories.

Most synthetic diamonds from other producers can be identified by a characteristic cross-shaped UV luminescence pattern that is stronger in short-wave than in long-wave UV radiation. The majority of the AOTC-created diamonds did not show characteristic color zoning nor any fluorescence pattern when illuminated with a standard UV lamp, so we used UV sources with higher intensity such as the DiamondView and a custom-made EGL instrument

Natural and synthetic corundum can be differentiated by their excitation spectra (left) and UV absorption spectra (right).

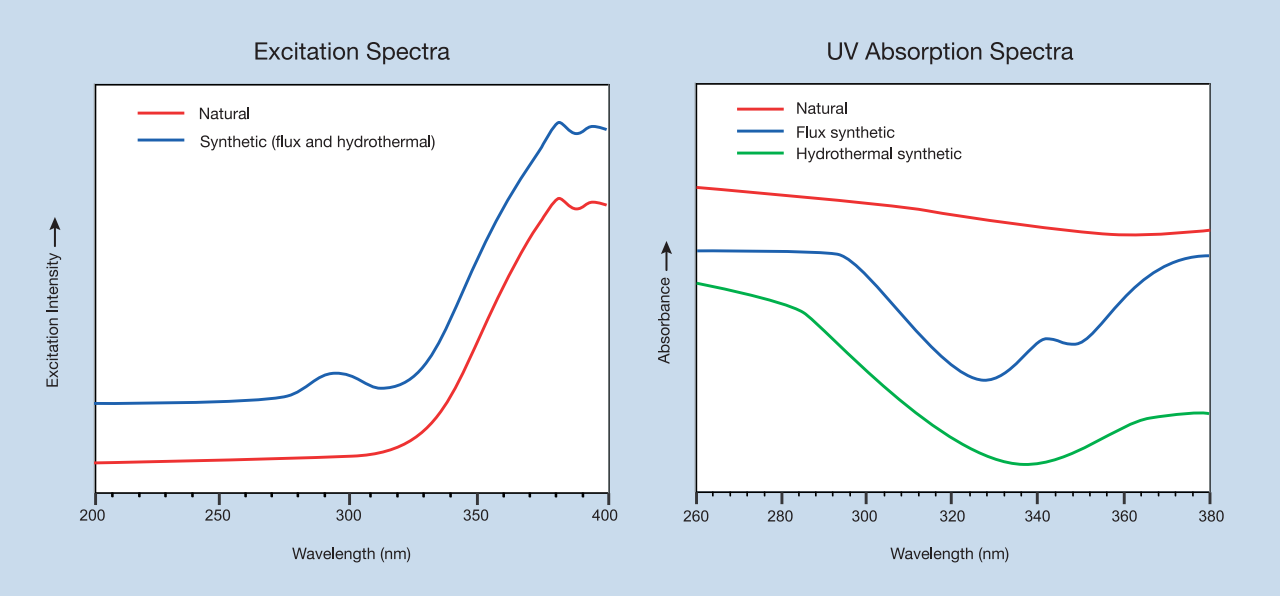

(at wavelengths of 220, 254, and 365 nm). With this UV illumination, we could observe the cubo-octahedral color zoning that is typical of HPHT-grown synthetic diamonds.

These new AOTC-created synthetic diamonds can be separated from their natural counterparts based on careful observation with the microscope, and through the use of crossed polarizers, the DiamondView, and advanced spectroscopy.

REFERENCE

Woodring S., Deljanin B. (2004) Laboratory Created Diamonds. EGL USA, New York.

A Refined Infrared-Based Criterion for Successfully Separating Natural from Synthetic Amethyst

Stefanos Karampelas (steka@physics.auth.gr)[1,2], Emmanuel Fritsch[2], Triantafyllia Zorba[3], Konstantinos M. Paraskevopoulos[3], and Spyros Sklavounos[3]

[1]Department of Geology, Aristotle University of Thessaloniki, Greece; [2]Institut des Matériaux Jean Rouxel, Nantes University, France; [3]Department of Physics, Aristotle University of Thessaloniki, Greece

Since the first commercial manufacture of synthetic amethyst about 30 years ago, the separation from natural material has been difficult for gemologists. Even today, significant quantities of synthetic material are mixed into parcels of natural amethyst. This has had a negative effect on consumer confidence, and has prompted further research into identifying the material.

Synthetic amethyst crystals are grown in either a near-neutral NH_4F solution or an alkaline K_2CO_3 solution. The identification of material grown in the NH_4F solution is straightforward using standard microscopy (i.e., diagnostic twinning and color zoning) or by recording specific IR absorption bands at 3684, 3664, and 3630 cm^{-1}. However, the vast majority of synthetic amethyst in the market today was grown in the K_2CO_3 solution, and it is sometimes difficult to identify this material using standard gemological techniques. This problem is particularly noteworthy for larger gems of good color that do not contain inclusions or diagnostic twinning.

IR absorption spectra of amethyst in the region of R-OH stretching (particularly from 3900 to 3000 cm^{-1}) reveal several bands that have been used for the separation of natural from synthetic amethyst. The presence or absence of certain features in this region (i.e., the 3595 or 3540 cm^{-1} bands) are helpful for making the separation. However, some rare exceptions to such criteria have been found.

The current study is based on the measurement of the intensity and shape of these IR spectral bands in 33 natural and nine synthetic amethysts at various resolutions. IR absorption spectra were recorded on oriented samples (cut parallel and perpendicular to the c-axis), randomly orientated samples (parallel-polished plates), and faceted stones. Most of the IR spectra were obtained using a diffuse reflectance accessory as a beam condenser. Using a resolution of 0.5 cm^{-1} (significantly higher than the standard 4 cm^{-1} resolution), the 3595 cm^{-1} band was documented in all of the natural samples and rarely in the synthetics (see figure). In the synthetic amethyst containing this band, its full width at half maximum (FWHM) was about 7 cm^{-1} (±1 cm^{-1}), which was approximately twice that measured for the natural amethyst (3.3 cm^{-1} ± 0.6 cm^{-1}). This new, refined criterion worked for all of our samples, and it provides an additional means of recognizing synthetic amethyst grown from alkaline K_2CO_3 solutions.

New Gem Localities

Ultraviolet Mineral Prospecting for Sapphire on Baffin Island, Nunavut, Canada

Luc Lepage[1] and William Rohtert (william.rohtert@gte.net)[2]

[1]Department of Geological Sciences and Geological Engineering, Queens University, Kingston, Ontario, Canada; [2]True North Gems Inc., Vancouver, British Columbia, Canada

The Beluga sapphire occurrence on Baffin Island, Nunavut, Canada, is a metamorphic-type deposit with a hydrothermal overprint. Sapphire mineralization occurs as a late metamorphic and hydrothermal replacement within a coarse-grained, calc-silicate gangue consisting principally of anorthite, calcite, diopside, dolomite, phlogopite, potassic feldspar, and scapolite with lesser amounts of apatite, graphite, muscovite, pyrrhotite, spinel, and zircon. Rare phases include nepheline, rutile, dravite tourmaline, sanbornite, thomsonite, and zirconolite.

To date, 12 gem corundum occurrences, including blue,

IR absorption spectra are shown at resolutions of 4 cm^{-1} and 0.5 cm^{-1} for a randomly oriented faceted synthetic amethyst (0.6 ct) grown in K_2CO_3 solution (produced in the U.S. by Sawyer) and for natural amethyst from Namibia (taken parallel to the c-axis). The 3595 cm^{-1} band is rarely recorded in synthetic amethyst; when it is present, the FWHM of this band (at 0.5 cm^{-1} resolution) can be used to conclusively identify this material. The spectra are offset vertically for clarity.

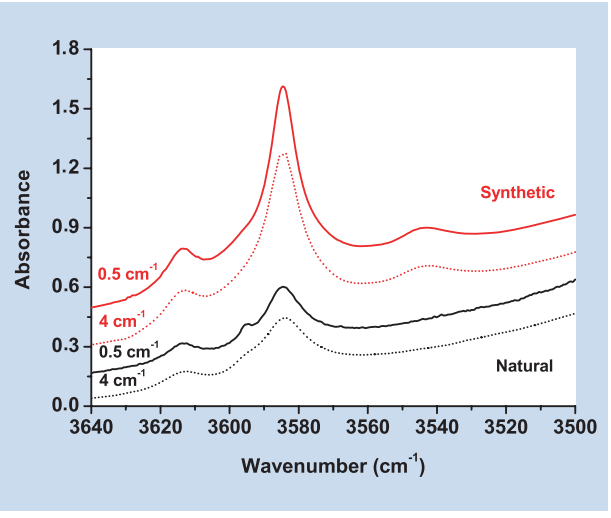

colorless, pink, and yellow sapphires, have been discovered over a lateral distance of 2,700 m and across an elevation range of 50 m. These occurrences lie within four geographic clusters, measuring from 220 × 100 m to 600 × 200 m, each comprising multiple showings of gem corundum in close association with abundant, coarse-grained, fluorescent scapolite. The latter mineral association triggered the development of a scapolite surveying technique that greatly increased the effectiveness of sapphire prospecting on the Beluga property. The very strong yellow fluorescence of scapolite to long-wave UV radiation is due to trace amounts of sulfur, a known activator element, within its crystal structure. The origin of the sulfur is unclear, but it appears to be closely related to the hydrothermal event that produced the sapphires.

Scapolite is one of the brightest fluorescent minerals known, and its yellow luminescence could easily be distinguished from the cyan-greens of the fluorescent calcite precipitates and the pale whites of the lichen-covered rocks. However, under Arctic twilight conditions, a classic UV lamp can only produce scapolite fluorescence from a short distance (<1 m), while the light emitting diode (LED) UV lamp can increase this distance to well over 5 m. The modern LED technology also produces UV radiation that does not require further filtering, saving considerable battery power while producing the same UV output. Fluorescence was further enhanced by using special long-pass filters to block the shorter wavelength colors (violets and blues), and carefully selecting the LED wavelength that is closer to the optimum excitation wavelength of scapolite (i.e., a slightly longer wavelength than conventional long-wave UV).

From drift prospecting to the interpretation of hydrothermal contacts within the mineralized zones, scapolite fluorescence was a powerful tool at all stages of sapphire exploration at this locality.

These tourmaline crystals (~2 kg total weight) were recently mined in the Camp Robin area of central Madagascar. Photo by Roberto Appiani.

Gemological Investigation of Multicolored Tourmalines from New Localities in Madagascar

Margherita Superchi (superchi@mi.camcom.it)[1], Federico Pezzotta[2], and Elena Gambini[1]

[1]CISGEM of the Milan Chamber of Commerce, Milan, Italy; [2]Natural History Museum, Milan, Italy

The Proterozoic crystalline basement of central Madagascar is characterized by the presence of one of the most important concentrations of rare-element, gem-bearing pegmatites in the world. Although gems have been actively mined in this area for more than a century, new discoveries are occasionally made by local miners in wild and relatively unexplored areas. Over the past few years, a series of new mining areas have been established, mainly for multicolored tourmaline.

Several gem tourmaline samples from these new localities, consisting of crystal fragments, slices, and cut gemstones and cabochons, were selected for chemical analysis and spectroscopic studies. They originated from the following deposits:

1. Manapa area (southwest of Antsirabe): pegmatites at Ampanodiana (red-purple), Ambatomigaby ("ruby" red to purple), Ambesabora (purplish red, purple, azure blue, and vivid blue), and Antsikoza (purple).
2. Camp Robin area (between Ambositra and Fianarantsoa): Anjomanandihizana and Fiadanana-Valozoro deposits and the Ankitsikitsika and Antsengy pegmatites. The samples from these localities were multicolored, mainly in pink, purple, red, "olive" green, yellow-brown, and yellow. Homogeneous red crystals also have been produced from the Camp Robin area (see, e.g., the figure).

In addition, a selection of rough and cut tourmaline (red-purple to bright blue) was characterized from the Anjahamiary pegmatite, located close to Tranomaro village, in the Fort Dauphin area of southern Madagascar. These samples were collected in 1999–2000.

The tourmalines were studied with UV-Vis and FTIR absorption spectroscopy, Raman spectroscopy, and electron-microprobe analysis using an energy-dispersive system. The preliminary data indicate that regardless of their color, the tourmalines range in composition from Ca-rich elbaite to liddicoatite. No traces of Cu have been found in the azure blue and vivid blue samples from the Ambesabora and Anjahamiary deposits. Significant amounts of the trace elements Bi and Pb have been found in multicolored tourmalines from the Antsengy pegmatite. Traces of Pb, but not of Bi, have been found in multicolored tourmalines of the Anjahamiary pegmatite.